Pharmacokinetics/Pharmacodynamics and Analysis of the Effect of β-Amyloid Peptide on Acetylcholine Neurocycle and Alzheimer's Disease Medications

by

Asmaa Abdallah Awad

A thesis
presented to the University of Waterloo
in fulfillment of the
thesis requirement for the degree of
Master of Science
in
Chemical Engineering

Waterloo, Ontario, Canada, 2013

Author's Declaration

I hereby declare that I am the sole author of this thesis. This is a true copy of the thesis, including any required final revisions, as accepted by my examiners.

I understand that my thesis may be made electronically available to the public.

Abstract

The brain of Alzheimer's disease (AD) is characterized by accumulations of β-amyloid peptide aggregates which promote neurodegentartive dysfunction. Comprehensive understanding of the interaction between β-amyloid aggregates and acetylcholine (ACh) neurocycle is required to uncover the physiological processes related to AD and might result in improving therapeutic approaches for AD. Pharmacokinetics (PK) and pharmacodynamics (PD) techniques were applied to allow predicting the extent of the interaction of certain doses of AD drugs and β-amyloid inhibitors and levels of ACh as well. Although many researchers focused on the β-amyloid interactions, the mechanisms by which β-amyloid affects cholinergic neurons and reduction of ACh are still unclear. The prediction of ACh and drug concentrations in the tissues and body needs an understanding of the physiology and mechanisms of β-amyloid aggregates processes and their compilation into a mechanistic model

In this work, two hypotheses are proposed to investigate the dynamic behavior of the interaction between β-amyloid peptide aggregates and cholinergic neurocycle and the possible therapeutic approaches through proposing pharmacokinetic/pharmacodynamics (PK/PD) models to represent the impact of β-amyloid aggregates in AD. The effect of β-amyloid peptide aggregates is formulated through incorporating β- amyloid aggregates into non-linear model for the neurocycle of ACh where the presynaptic neuron is considered as compartment 1 and both synaptic cleft and postsynaptic neurons are considered as compartment 2. In the first hypothesis which is choline leakage hypothesis, β-amyloid peptide aggregates are considered to be located in the membrane of the presynaptic neuron and create pathways inside the membrane to allow for the intracellular choline to leak outside the cholinergic system. It is observed that β-amyloid aggregates via the choline leakage hypothesis could cause significant reductions of ACh and choline levels in both compartments. Furthermore, the process rates of ACh synthesis and hydrolysis have been affected negatively by a wide range of β-amyloid aggregate concentrations. It is found that as the input rate of β-amyloid aggregates to compartment 1 increases, the loss of choline from compartment 1 increases leading to an increase in the intracellular concentration of β-amyloid.

In the second hypothesis, β-amyloid peptide aggregates are proposed to interact with the enzyme ChAT which is responsible for the synthesis of ACh in compartment 1; three different kinetic mechanisms are suggested to account for the interaction between β-amyloid aggregates and ChAT activity. In the first and second kinetic mechanisms, β-amyloid aggregate is supposed to attack different species in the enzyme. It is found that there is a significant decrease in the rate of ACh synthesis in compartment 1 and ACh concentrations in both compartments. However, it is observed that there is no effect on choline levels in both compartments, the rate of ACh hydrolysis in compartment 2, pH, and ACh levels in compartment 2. In the third kinetic mechanism, all species in ChAT are attacked by β-amyloid aggregates; it is observed that at very high input rates of β-amyloid aggregates, the oscillatory behavior dominates all components of the neurocycle of ACh. The disturbance observed in ACh levels in both compartments explains the harmful effect of the full attack of β-amyloid aggregates to all species of ChAT. It is found that to contribute significantly in ACh neurocycle, choline leakage hypothesis needs concentration of β-amyloid aggregates lower than that needed in ChAT activity hypothesis which is in agreement with experimental observations. The significant decrease in ACh levels observed in both choline leakage and loss of ChAT activity hypotheses leads to cognitive loss and memory impairment which were observed in individuals with AD.

A one-compartment drug PK/PD model is proposed to investigate a therapeutic approach for inhibiting β-amyloid aggregation via choline leakage hypothesis where the maximum feed rate of β-amyloid (K_{L2} = 1) is considered. The drug is assumed to interact with the tissues of the presynaptic neurons where β-amyloid aggregates are located. The PK/PD model is built based on the effect of β-amyloid aggregates via choline leakage hypothesis where the maximum feed rate of β-amyloid aggregates is considered. The dynamic behavior of all concentrations of β-amyloid aggregates, choline, ACh, acetate, and pH in both compartments in addition to the rate of ACh synthesis in compartment 1 and ACh hydrolysis are investigated by monitoring the impacts of the drug on β-amyloid aggregates and cholinergic neurocycle over a wide range of the input drug dosage. The PK/PD model is able to predict the reduction in levels of β-amyloid aggregates and the increase in choline and ACh, in both compartments as well as both rates of ACh synthesis and hydrolysis catalyzed.

The parameters of the PK/PD model such as maximum concentration (C_{max}), maximum time (T_{max}), area under the curve (AUC), and maximum effect (E_{max}) were investigated. It was found that it takes a longer time (T_{max}) (3-5 h) to reach E_{max} as the drug dose increases. Furthermore, AUC was found to increase with increasing drug dosage. The results of the current work show that drugs / therapeutic agents inhibiting β- amyloid aggregation in the brain represent a likely successful therapeutic approach to give systematic highlights to develop future trials, new diagnostic techniques, and medications for AD. This study is helpful in designing PK and PD and developing experimental animal models to support AD drug development and therapy in the future.

Acknowledgements

I would like to extend my thanks and appreciation to my supervisor Prof Elkamel for helping me during the course of this project. He provided a motivating, enthusiastic, and critical atmosphere during the discussions we had. It is a great pleasure for me to conduct this project under his supervision. I would like to express my thanks and gratitude to Dr Ibrahim for his valuable advice, guidance and encouragement throughout the project. I also would like to express my thanks to the School of Graduate Studies and the Department of Chemical Engineering at the University of Waterloo. Finally, I hope to extend my heartfelt gratitude to my husband, my parents, my sons: Muhammad, Amr, and Khaled, brothers and my sisters.

Table of Contents

List of Figures

List of Tables

Notations

$[H^+]$	Hydrogen ions concentration (kmol/m^3
$[OH^-]$	hydroxyle ions coGncentration (kmol/m^3)
$[S_1]$ = ACh	acetylcholine concentration (kmol/m^3)
$[S_2]$= Ch	choline concentration (kmol/m^3)
$[S_3]$=AC	acetyl CoA concentration (kmol/m^3)
bA	β-amyloid concentrations
U	Drug concentrations
S_N	substrate N (catalyzed by enzyme N)
$\lfloor a \rfloor$	acetate concentration (kmol/m^3)
$\overline{AChE}$	concentration of acetylcholinesterase enzyme in compartment 2 (kg enzyme/m^3)
$\overline{CoA}$	concentration of coenzyme A in compartment 1 (kg enzyme/m^3)
$\overline{ChAT}$	concentration of cholineacetyltransferase in compartment 1 (kg enzyme/m^3)
K_{s1}, K_{h1}	kinetic constants for the choline acetyltransferase catalyzed reaction (kmol/m^3)
$K_{bA1}, K_{bA2}, K_{bA3}$	kinetic constants for the β-amyloid aggregates (kmol/m^3)
K_{L2}	β-amyloid input rates
K_{L3}, K_{L4}	kinetic constants for the β-amyloid aggregates
K_{U11}, K_e, K_{CL}	kinetic constants for the drug
K_{UU}	Drug efficacy
K_{U2}	Drug input rates
X_S	β-amyloid removal ratio
K_{s2}, K_h	kinetic constants for the coenzyme A catalyzed reaction (kmol/m^3)
K_{s3}, K_{i3}, K_{hh3}	kinetic constants for the acetylcholinesterase catalyzed reaction (kmol/m^3)
α'_{H^+}	membrane permeability for hydrogen ions (m/s)
α'_{OH^-}	membrane permeability for hydroxyl ions (m/s)
α'_{S_1}	membrane permeability for acetylcholine (m/s)

α'_{S_2}	membrane permeability for choline (m/s)
α'_{S_3}	membrane permeability for acetyl CoA (m/s)
α'_{A}	membrane permeability for acetate (m/s)
α'_{AC}	membrane permeability for acetic acid (m/s)
A_M	area of membrane separating compartments 1 and 2 (m^2)
q	volumetric flow rate (m^3/s)
R	recycle flow rate ratio
$V_{(j)}$	volume of compartment j (m^3)
E_N	enzyme N
P_N	reaction product N (produced by S_N catalyzed by (E_N)
V_R	V_1/V_2

List of Abbreviations

AChE	Acetylcholinesterase
ChAT	Cholineacetyltransferase
CoA	Coenzyme A
ACh	Acetylcholine
CSTR	continuous stirred tank reactor
Aβ	β-amyloid peptides
AD	Alzheimer's disease
Ch	Choline
AC	Acetate
ODEs	Ordinary differential equations
AUC	Area Under Curve
U	Drug
C_{max}	Maximum drug concentrations
E_{max}	Maximum drug effect
t_{max}	Time required to reach the peak
bA	β-amyloid aggregates concentrations
BBB	Blood-brain barrier
ROS	Reactive oxygen species
NFTs	Neurofibrillary tangles
MTs	Microtubules
MAO-B	Monoamine oxidase-B
THC	Tetrahydrcannabinol
DHA	Docosahexaenoic Acid
GSAP	Gamma-secretase activating protein`
PC	Phaeochromocytoma cells

GPR3	G-protein coupled receptor 3

Subscripts

1	Compartment 1
2	Compartment 2
f	Feed condition

Chapter 1
Introduction

1.1 Background

Alzheimer's disease (AD) is a progressive neurodegenerative disease. The irreversible declining of cognitive functions is considered the major characterizations of AD which has many symptoms of AD such as memory loss, neurons dysfunction, confusion, and thinking disabilities. AD is the most common neurodegenerative disease in industrialized countries where China, Western Europe, and USA have the largest number of effected persons. The statistics show that there are 25 million people worldwide who have related dementia diseases, most of them are thought to have AD where 26.6 million persons worldwide had AD in 2006, and half a million Canadians have AD about 71,000 of them are under age 65. Also, by 2050 it is expected that one in every 85 persons worldwide will have AD. Therefore, AD is considered one of the main public health troubles that attracted researchers interests in the last decade (Lancet et al., 2011). There are several factors that promote the development of AD such as advancing age, head injury, and environmental factors like exposure to lead and aluminum which are neurotoxins. Furthermore, exposure to some chemicals such as toluene or benzene could increases the risk of AD. Genetics or family history is another serious risk factor that increases the odd of incidence AD three to fourfold in first- degree relative (sibling or parent) (Khachaturian and Radebaugh, 1996). The most common lifestyle factors causing AD are obesity, alcohol intake, and smoking. Chronic diseases increase the risk of occurring AD, including stroke, type-2 diabetes, hypertension, and hypercholesterolemia. There is information from many independent resources of Swedish epidemiological studies that suggest that social activities and social work could reduce the incidence of AD. Promotion health living conditions, with a strong exercise are considered the most promising approach for reducing the incidence of AD. The educational and occupational attainments are important factors that decrease the risk of AD. Since education improves the brain's reserve capability, it is observed that only people

who achieve low education levels have a double probability of developing AD in comparison with the those who accomplished 8 or more years of being at school (Khachaturian and Radebaugh,1996). There are four stages of AD with progressive features of cognitive and functional impairments and can be explained as follows:

Stage 1- Pre-dementia: it is characterized by forgetting recently happened events and losing ability to acquire new learning issues or data.

Stage 2- Early stage: it is characterized by increasing impairment of memory and remembering capability. The effected person may forget how to use things, and may need supervision with the most cognitively demanding activities. Moreover, the patient at this stage suffers from difficulties in speaking and has shrinking vocabularies.

Stage 3- Moderate stage: it is characterized by memory difficulties where patients could not remember close relatives such as persons of his or her family or performs daily activities. He also has speech difficulty due to inability to remember vocabularies and forgetting the suitable words for speech.

Stage 4- Advanced stage: In this stage the persons with AD are completely dependent on caregivers. Also the patients are not able to perform the simplest activities like feeding themselves and they lose the control of urine feeling.

1.2 Interaction between β- amyloid peptide aggregates and AD

The brain of Alzheimer's disease (AD) is characterized by accumulations of β-amyloid peptide aggregates which promote neurodegenerative dysfunction. Amyloid plaque is aggregates of β-amyloid peptides that deposit in the brain. β-amyloid is formed by cleavage of a transmembrane protein known as amyloid precursor protein (APP) by ɣ-β secratase enzymes (Goldager et al., 1987). In addition, β-amyloid aggregates induce formation of neurofibrillary Tangles (NTF) in the form of accumulations of hyper phosphorylated tau protein inside nerve cell bodies. Tau protein is a protein responsible for stabilizing microtubules which represent the cytoskeleton of the cells. Hyper phosphorylation of tau proteins leads to destabilizing and disintegration of microtubules, and hence collapsing the neurons and impairing axonal transport. β-amyloid peptide aggregates affecting cholinergic neurocycle leading to low levels of acetylcholine (ACh)

and disturbances in cognition, memory, language and muscle movements. Therefore, cholinergic dysfunction in communication between neurons and cell death are produced. In AD, brain atrophy is characterized by loss of brain tissue and neuron cells that cause cognitive disorders, damage the connections between cells and decline in brain functions as indicated in Figure 1.1.

The reasons of AD are still unknown; there are several hypotheses that try to explain reasons of AD:

1- Amyloid hypothesis in amyloid cascade proposes that aggregation of β-amyloid which generates up on cleavage of amyloid precursor protein (APP) by ɣ-β secratase enzymes. These toxic aggregates of β-amyloid accumulate in the brain and on the surface receptors of neuron cells causing disturbance in neural communication by changing in the neuron components particularly choline and ChAT.

2- Cholinergic hypothesis: the idea of this hypothesis is based on decrease in synthesis of ACh neurotransmitter which causes AD. Cholinergic hypothesis is not strong enough because medications that cure ACh deficiency did not prove to be effective.

3- Tau hypothesis: this hypothesis supposes that tau abnormality causes AD. In this hypothesis the hyper phosphorylated of tau protein initiates the formation of neurofibrillary tangles in neuron cells (NFT). Presence of NFT means disintegration and collapse of microtubule where dysfunction in communication between neuron and cell death occurs.

4. Other hypotheses: There are several other hypotheses. One is based on the breaking down of myelin in brains of elder people which initiates brain damage by iron release. Homeostatic myelin repair causes deposits formation called proteinaceous such as β-amyloid deposits. Another hypothesis is degeneration of locus coeruleus cells that provide norepinephrine neurotransmitter. Norepinephrine has anti-inflammatory effect in area around glia cells, neuron, and blood vessels in hippocampus and neocortex. In an experiment carried out on mice showed that norepinephrine stimulates microglia cells for β- amyloid phagocytosis and suppresses production of cytokine by β- amyloid. Other example such as oxidative stress.

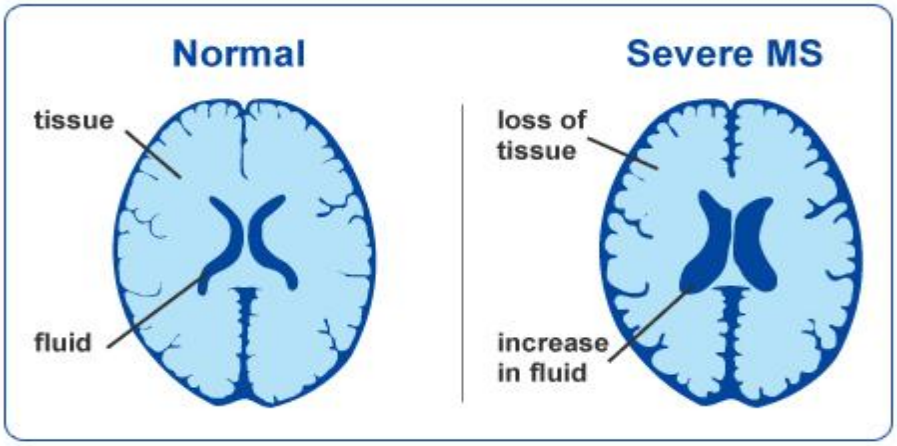

Figure 1.1 the difference between normal brain and brain affected by AD (http://www.my-ms.org/symptoms_atrophy.htm)

1.3 Research objectives

In this work we investigate the nature of interaction between β-amyloid aggregates and cholinergic neurons to understand the pathological pathways that β-amyloid aggregates take into ACh neurocycle to induce AD. Then, based on this study, a therapeutic approach can be determined through building a pharmacokinetics/pharmacodynamics (PK/PD) model based on a cholinergic two-enzyme/two-compartment model where the presynaptic neuron is considered as compartment 1 and both synaptic cleft and postsynaptic neuron are considered as compartment 2. The main objectives of the thesis are:

1) Describe the interaction between β-amyloid peptides and ACh neurocycle through incorporating the effect of β-amyloid aggregates into two-enzyme/two-compartment model via proposing the following two hypotheses:

   i) The first one is choline leakage hypothesis. It is proposed that β-amyloid aggregates existing in the membrane of the presynaptic neuron create channels leading to loss of choline (which is required for synthesizing ACh) outside the cholinergic system.

   ii) The other hypothesis is that β-amyloid aggregates interact with the enzyme ChAT which catalyzes the synthesis of ACh. In this hypothesis, three different kinetic

mechanisms are proposed to account for the interaction between β-amyloid aggregates and certain species in ChAT.

2) Investigate the effect of β-amyloid aggregates on the dynamic behavior of ACh neurocycle in each hypothesis. The dynamics of ACh, choline, acetate, pH in both compartments are monitored at different concentrations of inlet β-amyloid aggregates to determine which state variables are affected negatively.
3) Compare the effect of each kinetic mechanism proposed in ChAT hypothesis to identify which targeted species in ChAT have the most inhibiting effect.
4) Determine if β-amyloid aggregates cause harmful effects in ACh neurocycle by observing concentrations of ACh, choline, acetate, rate of ACh synthesis and hydrolysis in each compartments by comparing the consequences of each hypothesis.
5) Perform sensitivity analysis on the model parameters in order to choose the most appropriate values for kinetic constants that give results compatible with the experimental observations.
6) Build a pharmacokinetics/pharmacodynamics (PK/PD) drug model to investigate the dynamic effects of drug on the inhibiting effect of β-amyloid aggregates and investigate the dynamics of the system state variables at different doses of the drug.
7) Determine the PK/PD parameters of the drug model such as AUC, C_{max}, t_{max}, and E_{max} in order to determine the maximum concentration of each dose giving the maximum effect and the time taken to reach it.

1.4 Thesis outlines

This thesis comprises of six chapters: Chapter one is an introduction for AD features and factors, β-amyloid aggregates, and the objective of the research. Chapter two includes a comprehensive literature review for the effects of β-amyloid aggregates as a major risk factor for AD with reference to choline leakage hypothesis, ChAT inhibition mechanism, and AD medications. Chapter three explains the choline leakage theory of β-amyloid aggregates. Chapter four presents the ChAT inhibition by β-amyloid aggregates and the consequences of this effect on declining ACh level. Chapter five introduces a PK/PD drug model and the dynamic effects of drug on the inhibition effect of β-amyloid aggregates and the dynamics of the system state variables at

different doses of the drug. Chapter six provides the conclusions of the study and some recommendations for future work.

Chapter 2

Background and Literature Review

(Introduction for the physiological processes in the neuron cell and their relation to Alzheimer's disease)

This chapter focuses on the necessary function of Acetylcholine (ACh) as a neurotransmitter in the process of signal transmission between neuron cells. The processes of ACh synthesis and release are covered before highlighting the role that β-amyloid peptides role and how they are formed and released and the effects of β-amyloid as a neuron defective agent on cholinergic neurons. In addition, pharmacokinetic and pharmacodynamics of drugs dealing with Alzheimer's disease (AD) are focused.

2.1) Acetylcholine (ACh) neurocycle

ACh is a neurotransmitter in both peripheral nervous system (PNS) and central nervous system (CNS) which facilitates cholinergic transmission and regulates cognition, memory, language and muscle movements. ACh probably has been developed long before the appearance of a nervous system, since the machinery to synthesize and degrade ACh is present in microorganisms such as bacteria, fungi, protozoa and plants [Kazue S. (2004)]. Even in so-called higher organisms, ACh is present in non-neural tissues such as the placenta, suggesting that ACh has cellular functions other than neurotransmission [Kazue S. (2004)].

2.1.1) Functions of ACh

ACh is a neuromodulator which plays necessary functions in PNS and CNS. In PNS, ACh activates muscle movements. As soon as ACh binds to cholinergic receptors (nicotinic and muscarinic receptors) on skeletal muscle, the ligand-gated sodium channels on the cell membrane open to permit sodium ions to go inside the muscle cell. Then, entrance of sodium ions triggers frequent steps that generate muscle contraction. In CNS, ACh acts as a

neuromodulator where ACh has a vital role for improving of sensory recognition during wake up and sustaining attention. Damaging ACh cholinergic system in brain leads to memory dysfunction which leads to AD.

2.1.2 Synthesis of ACh

ACh is produced in the presynaptic neurons by interaction of choline and acetate in the presence of choline acetyltransferase enzyme (ChAT) (Eckenstein and Baughman, 1984) as shown below:

$$\text{Choline} + \text{Acetyl-CoA} \xrightarrow{ChAT} \text{ACh} + \text{CoA} \qquad (2.1)$$

Then, ACh is stored in presynaptic vesicles by the vesicular ACh transporter (VAChT) (Boucetta and Jones, 2009; Guyton and Hall, 2000; Tucek, 19780; Bussiere et al, 2001; Ballivet et al., 1996]. When the presynaptic neuron is depolarized by the action potential, the calcium channels open to facilitate entering of calcium ions. Influx of calcium ions triggers the fusion of synaptic vesicle to membrane to release ACh in the synaptic cleft. ACh diffuses in the synaptic gab and reacts with the cholinergic receptors protein (Nicotinic and muscarinic ACh receptors) in the postsynaptic membrane [Ballivet et al., (1996)]. This binding with the receptors causes excitation or inhibition of postganglionic cell [Quinn et al, 1995; Llinas, 1999; Tucek, 1978; Ballivet et al., 1996; Rand, J.B, 2007]. After ACh sets action on postsynaptic neuron receptors, it is hydrolyzed by acetyl cholinesterase (AChE) into choline and acetate. Choline is recycled to the presynaptic neuron for further ACh synthesis (Yael et al., 2011). The sources for the precursors required for ACh synthesis like acetyl-CoA and choline are as follows:

A) Sources of acetyl groups for the synthesis of ACh

Acetyl-CoA is a necessary cofactor in metabolism of glucose, fatty acids, and certain amino acids. It is synthesized within mitochondria matrix during pyruvate decarboxylation reaction. This reaction is the key process for metabolism of glucose where pyruvate coming from glucose metabolism is converted by pyruvate dehydrogenase complex into acetyl-CoA. The latter one carries carbon atoms inside acetyl group to Krebs's cycle (TCA cycle) for energy generation by oxidation. Also, Acetyl-CoA can be generated by β-oxidation of long chain fatty

acids or during oxidative degradation for some amino acids. The immediate precursor of the acetyl groups of ACh in living cells is acetyl-CoA. Acetyl-CoA is transported out of the mitochondria to participate in ACh synthesis. It is not clear how the acetyl groups of acetyl-CoA which is formed in the mitochondrial matrix from pyruvate pass into the extra mitochondrial space, where the synthesis of ACh occurs. The inner mitochondrial membrane is generally considered to be impermeable to acetyl-CoA. A number of substances (citrate, glutamate, acetylcanitine, acetate, acetoacetate, acetylated amino acids) have been proposed to act as carriers of acetyl groups from the mitochondria for metabolic reactions proceedings extra mitochondria [Tucek, (1978); Vera Yip (1991)]. A probable carrier for acetyl-CoA is citrate, which can diffuse into the cytosol and produce acetyl CoA via citrate lyase; a possible carrier is acetyl carnitine, and another possibility is Ca^{2+} induced leakage of acetyl-CoA from mitochondria [Cooper et al., (2003)].

B) Sources of choline for the synthesis of ACh

Strecker is the first one who discovered choline (Ch) in 1862; then choline has got an important interest because of the essential role it plays in body function. For example, choline is one of cell membrane structures (phosphatidyl choline), and it is a precursor for ACh neurotransmitter. Even human body has ability for choline synthesis de novo, choline rich food is the most effective source for Choline. Food containing choline is necessary for prenatal memory growth and liver function (Lockman and Allen, 2002). Since choline is an important component for ACh, any shortage in choline supply sources can lead to reduction of ACh formation in the body, and hence AD. Lockman and Allen (2002) showed that the concentration of choline in plasma varies around 10 µM. Food saturated with choline or food deficient choline can either increase or decrease plasma choline concentration. Stabilization of choline levels in plasma occurs by its synthesis from catabolism of phosphatidylcholine (cell membrane component). In presynaptic of the neurons ACh synthesis process occurs by choline reactions with acetyl-CoA via ChAT enzyme to generate ACh. As soon as presynaptic is excited by action potential, ACh is released in synaptic cleft to bind to post synaptic neurons receptors for transmission of action potential. Then ACh is hydrolyzed by AChE into choline and acetyl-coA. Choline is recovered

back into presynaptic neuron for further ACh synthesis. Choline recycle is a rate limiting step for ACh formation within the neuron (Lock man and Allen, 2002; Mustafa et al., 2012).

C) Choline Transport

Choline transmission is a necessary process for physiological body operations. Because choline has a hydrophilic charged cation at physiological pH, it has difficulties to cross the cellular membrane. There are many mechanisms for choline transport (Lockman and Allen, 2002) shown as follow:

1- Low–affinity choline transport mechanism: In this mechanism choline transport occurs via passive diffusion, and depends on choline concentrations and independent on sodium ions levels. Low – affinity transporter is carrier-mediated. For instance, in rat cortical synaptosom choline transport has exhibited a sodium-independent carrier-mediated process. Another example is in basolateral plasma membrane of the rat liver where choline transport has been shown to be sodium-independence and carrier mediated. Low–affinity choline transporter occurs in hepatocytes, placenta, synaptosomes, and mitochondria tissue. Choline transport by this mechanism provides choline for phosphatidyl choline and Phospholipids synthesis for cell membrane (Lock man and Allen, 2002).

2- High-affinity choline transport: Lockman and Allen (2002) defined the high-affinity choline uptake mechanism as a carrier-mediated, sodium and chloride dependent. Further, this transport system provides choline for ACh synthesis in presynaptic nerve ending. High affinity sites for this system are interpeduncular nucleus, olfactory tubercle, and caudate putamen. According to Yamamura and Snyder (1973) replacement of sodium with lithium decreased choline uptake by 95% in synaptosomes. According to Simon and Kuhar (1976) who showed that high-affinity mechanism of choline transport is chloride and energy dependent. Further, replacement of sodium with potassium or lithium lowered choline aggregations in human erythrocyte by approximately 60%. High-affinity choline uptake system is carrier-mediated sodium dependent mechanism in presynaptic cholinergic of the neuron.

3- Unique choline transport mechanism: This mechanism occurs at blood-brain barrier as a basic amine transport (Lockman and Allen, 2002). Choline needs to cross blood-brain barrier because brain has a high need for choline to maintain physiological role in CNS. In addition, the ability of brain to synthesize choline de novo is low in comparison to what is needed by cholinergic nerve terminals to set its physiological function (Lockman and Allen, (2002; Ansell, G.B. et al., 1971). Choline has low permeability across blood brain barrier because of its cationic charged at physiological pH where brain barrier allows lipid-soluble molecules to diffuse cross the membrane, but the hydrophilic compounds such as choline have low permeation at the blood brain barrier (BBB) (Lockman and Allen, 2002; Schuberth, J et al., 1969 and 1970). Therefore, BBB regulates the transport of choline between plasma and CNS. In addition, BBB is composed of endothelial cells that are joined to each other by tight connections at brain capillaries, and these junctions are tighter than other capillary endothelium junctions. The unique choline transport is a carrier mediated mechanism, and has the categories from both regular mechanisms and is similar to high-affinity system in affinity of choline, but it is sodium-independent as low-affinity mechanism. It has been shown that removal of sodium did not alter choline transport across capillary endothelial cells in mouse brain.

2.1.3) Degradation of ACh

Once ACh has completed its activation duty; it becomes susceptible to degradation process. The main reaction is described by equation (2.2) where ACh is degraded by the acetyl cholinesterase (AChE) into choline and acetic acid [Tucek (1978) and (1985); Bussiere et al, (2001)].

$R_{(2)}$: $\quad ACh + Water \xrightarrow{AChE} Choline + CH_3COOH \qquad (2.2)$

Choline is recycled to presynaptic by the high affinity choline transprter-1(CHT-1) for further synthesis of ACh (Kim et al., 2004).

Figure 2.1 shows that there are two main enzymes involve in ACh producing system can be explained as follow:

i) Choline Acetyltransferase enzyme (ChAT)

It is a single-strand globular protein, its synthesis process occurs in the body of the neurons (perikaryon of cholinergic neurons) and then it transported to the nerve terminals via axoplasmic flows. ChAT is responsible for the biosynthesis of ACh and it represents the most specific indicator for monitoring the functional state of cholinergic neurons in the central and peripheral nervous systems (Yoshio Oda, 1999). Inhibition of ChAT activity causes AD and abnormalities of ChAT in the brain could lead to schizophrenia (Yoshio Oda, 1999). Studying molecular and genetic nature of ChAT will help to understand the pathological nature of cholinergic neurons because ChAT plays a vital role in activation cholinergic neurons functions, such as learning, memory, sleep and muscle movement. The specific loss of ChAT activity was detected in AD

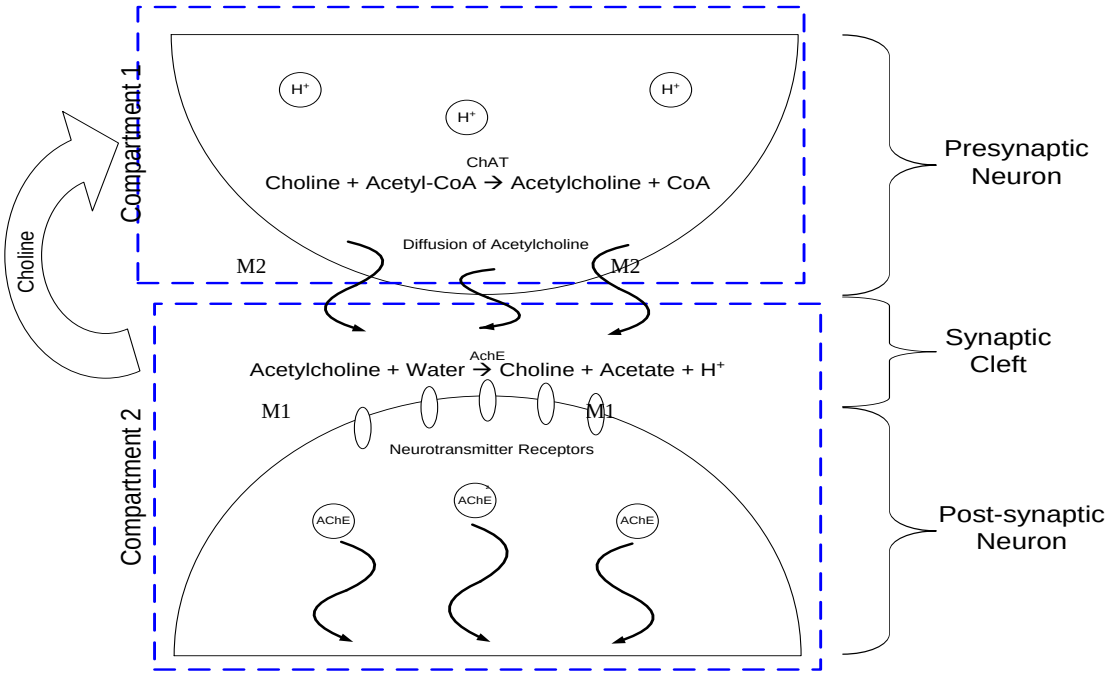

Figure (2.1) Schematic of synaptic neurons and cleft (Mustafa et al., 2009)

(Yoshio Oda, 1999). Although ChAT activity can be measured from the rate of utilization of either its substrates or the synthesis of its products, the most convenient method of its assay is based on the measurement of ACh [Rand, J.B. et al., (1984); Marco et al., (2002)]. This is done using [^{14}C] acetyl-CoA as substrate and measuring the radioactivity in ACh. Labeled ACh is the

most conveniently separated from labeled acetyl-CoA by extraction with tetraphenyloborn in 3-heptane [Tucek (985); Rand, J.B. et al., (1984); Bussiere et al., (2001); Marco et al., (2002)].

ii) Acetylcholinesterase [AChE]

AChE is an enzyme that hydrolyzes ACh into choline and acetate. All cholinesterases will hydrolyze not only ACh but other esters as well. Conversely, hydrolytic enzymes such as arylesterases, trypsin, and chymotrypsin will not hydrolyze choline esters. The problem in determining the number of cholinesterases is that different species and organs sometimes exhibit maximal activity with different substrates. The enzymes are divided into two rigidly defined classes: AChE (also called "true" or specific cholinesterase) and butyrylcholinesterase (also called "pseudo" or nonspecific cholinesterase; the term propionylcholinesterase is sometimes used since in some tissues propionylcholine is hydrolyzed more rapidly than butyrylcholine). Both of the two enzymes have similar molecular forms, but they have different entities, encoded by distinct genes. Current evidence suggests that in lower forms butyrylcholinesterase predominates, gradually giving way to AChE with evolution. When distinguishing between the two types of cholinesterase, at least two criteria should be used because of the aforementioned species or organ variation.

2.1.4) Axonal Transport of ChAT, AChE and ACh

Most of ACh which is used for synaptic transmission is synthesized in the immediate vicinity of the synapses, i.e. in terminal parts of cholinergic axons [Frederick et al, (1980); Rand et al, (1984)]. ChAT is produced in the bodies of the neurons and is transferred to the presynaptic nerve endings by the mechanism of axonal transport [Marco et al., (2002)]. Axonal transport also delivers to the nerve endings some, most or perhaps all of ACh which is produced in the perikarya and neuritis of cholinergic neurons [Marco et al., (2002) and Tucek, 1985].

To date, the only major through studies of ACh turnover in nervous tissue were done originally by Macintosh and colleagues and subsequently by Collier (2003) using the superior cervical ganglion of the cat [Cooper et al., (2003)]. Using one ganglion to assay the resting level of ACh and perfusing the contralateral organ, Cooper et al, (2003) determined the amount of transmitter synthesized and released under a variety of experimental conditions, including

electrical stimulation, addition of an anticholinesterase to the perfusion fluid, and perfusion media of varying ionic composition [Cooper et al, (2003)]. Their results may be summarized as depicted by Cooper et al, (2003) as follows:

1. During stimulation, ACh turns over at a rate of 8-10% of its resting content every minute (i.e., about 24-30 ng/minute). At rest, the turnover rate is about 0.5 ng/minute. Since there is no change in ACh content of the ganglion during stimulation at physiological frequencies, it is evident that electrical stimulation not only releases the transmitter but also stimulates its synthesis.
2. Choline is the rate-limiting factor in the synthesis of ACh.
3. In the perfused ganglion, Na^+ is necessary for optimum synthesis and storage and Ca^{2+} is necessary for release of the neurotransmitter.
4. Newly synthesized ACh appears to be more readily released upon nerve stimulation than depot or stored ACh.
5. More than half of choline produced by cholinesterase activity is reutilized to make new ACh.
6. At least three separate stores of ACh in the ganglion are inferred from these studies: *surplus* ACh, considered to be intracellular, which accumulates only in an eserine-treated ganglion and is not released by nerve stimulation but is released by K depolarization; *depot* ACh, which is released by nerve impulses and accounts for about 85% of the original store; and *stationary* ACh, which constitutes the remaining 15% that is non releasable.
7. Choline analogs, such as triethylcholine, homocholine, and pyrrolcholine, are released by nerve stimulation only after they are acetylated in the ganglia.
8. Increasing choline supply in the plasma during perfusion of the ganglion only transiently increases the amount of ACh that is releasable with electrical stimulation, despite accumulation of the transmitter in the ganglion.

ChAT appears to be transported slowly in mammalian nerves, at a rate of 1-6 mm/day. Its transport probably involves the entire enzyme in the axons and proceeds in the proximo-distal direction only; the transported enzyme is not associated with axonal organelles [Tucek (1987), Krishanu et al., (1999)]. There is, however, an alternative hypothesis which assumes that the transport concerns only a small part of ChAT in the axons but it proceeds at a high rate

[Krishanu et al., (1999)]. Contradictions on this point are difficult to resolve, since there is no way for determining the size of the mobile fraction of ChAT in the axons. Axonal transport of ChAT continues in the axons separated from nerve cell bodies, but its intensity is diminished. It is blocked by ischaemia.

ACh is also transported proximo- distally in cholinergic axons. The rate of its transport is estimated at 120 mm/day in mammalian nerves. The transport probably involves only the bound ACh in the axons, i.e. ACh contained in some unidentified axonal organelles, about 20% of the total ACh content. ACh supplied to the nerve endings via axonal transport represents a very small portion of the whole amount of ACh which is necessary for synaptic transmission [Tucek, (1987), Krishanu et al, (1999); Jesus et al, (2003)]. Most of ACh is synthesized in the nerve terminals, i.e. in the immediate vicinity of the synapse [Tucek, (1987) and (1985), Krishanu et al, (1999); Jesus et al, (2003)]. Axonal transport of AChE proceeds at a high rate in both directions [Krishanu et al, (1999)]. The transported enzyme is associated with axonal organelles and represents a small part of the total AChE content in the axons [O'Brien R A, (1978)]. The transport of AChE in the axons does not depend on the connection between the axons and the bodies of the nerve cells [O'Brien R. A. (1978)].

2.1.5) Organization and Control of the Synthesis of ACh in Presynaptic Nerve Endings

Although some ACh is synthesized in all parts of a cholinergic neuron, most of it is produced in close proximity to the sites from which it is released by nerve impulses, i.e. in the terminal parts of the axon and, in some neurons, probably in the *boutons en passant* and in the axonal varicosities as well **[**Shawn et al, (2004)]. The enzyme is responsible for the synthesis, ChAT, is mainly dissolved in the cytoplasm of the nerve endings, but a proportion of it is probably adsorbed by the cytoplasmic side of the surface membrane and by other membranes in the nerve endings, including the membranes of the synaptic vesicles [Tucek (1978); Shawn et al, (2004)]. ACh is localized in the cytoplasm and in the synaptic vesicles. It is not clear how the transmitter is synthesized in the cytoplasmic compartment, is transferred to the vesicles. What proportion of the total ACh in the tissue is present in the vesicles is also not [Tucek (1978), Shawn et al., (2004)]. It is possible that much of ACh originally present in the vesicles is

released or diffuses from them during the homogenization and fractionation of the tissue [Tucek (1978); Shawn et al, (2004)].

Most features of the release of ACh at the synapses are best explained by the vesicular hypothesis where nerve impulses are assumed to cause the release of ACh from the synaptic vesicles [Tucek, (1978); Shawn et al., (2004]. This hypothesis, providing an easy explanation for the fact that ACh is released in discrete quanta, is mainly supported by observations that the amount of vesicular ACh can be altered by stimulations, that the release of old ACh is accompanied by the appearance of newly synthesized ACh in those vesicles which had apparently undergone exocytosis, and that synaptic activity is accompanied by ultra-structural changes indicating exocytosis and recycling of vesicles [Tucek (1978); Shawn et al., 2004]. Objections to the vesicular hypothesis, ACh release are mainly based on observations of the nerve impulses which more easily produce changes of the so-called free ACh with comparison to the bound ACh; at least some, if not all free ACh is freely dissolved in the cytoplasm, where the bound ACh (stable- bound ACh in mammalian preparations) is contained in the synaptic vesicles [Tucek (1978), Shawn et al., (2004)].

Continuous slow synthesis of ACh proceeds in the cholinergic neurons even under conditions of 'rest' [Ballivet et al., (1996)] when the rate of ACh release is increased by nerve impulses. This rate of synthesis is also increased [Shawn et al., (2004)]. Recently it has been found that synthesized ACh is released preferentially during synaptic activity. Several hypotheses have been proposed to explain the mechanism of the control of the synthesis rest [Ballivet et al., (1996)]. The control of ACh synthesis is most probably based on the law of mass action, and the resting level of ACh in the compartment of synthesis corresponds to the concentration of ACh to be expected when the synthetic reaction is at equilibrium, lowering the concentration of ACh in the compartment of synthesis automatically leads to the synthesis of new ACh [Shawn et al., (2004)]. According to this hypothesis, the rate of synthesis and the equilibrium concentration of ACh are influenced by changes in the concentration of substrates, i.e. acetyl-CoA and choline at the site of synthesis [Shawn et al., (2004)]. The high affinity uptake of choline may represent an additional factor in the mechanism controlling ACh synthesis. Experimental observations indicate that the uptake of choline by the nerve endings is

augmented when the concentration of ACh in them is diminished. External (and perhaps also internal) ACh has an inhibitory action on the high affinity carrier of choline [Tucek (1978), Jian (2005)]. Further investigations are necessary to establish whether the supply of acetyl-CoA for ACh synthesis is influenced by the influx of Ca^{+} ions in the nerve terminals as a result of nerve impulses; Ca^{+} ions might act by causing the activation of pyruvate dehydrogenase phosphate phosphatase and by increasing the permeability of the inner mitochondrial membrane for acetyl-CoA [Tucek (1985), Jian (2005)]. It has been suggested that the control of ACh synthesis in the nerve endings depends on the inhibitory action of ACh and CoA on ChAT or on the effect of changing ionic concentrations on the activity of ChAT, but these mechanisms do not appear to be physiologically importance [Tucek (1978) and (1985); Shawn et al., (2004)]. In contrast to adrenergic synapses, re-uptake of the released transmitters into the presynaptic nerve endings and its re-utilization for synaptic transmission don not play any role on cholinergic synapses [Tucek (1978) and (1985); Shawn et al., (2004)].

2.1.6) Changes in ChAT Activity during the Lifetime of an Individual

It is very likely that measurements of ChAT activity in various organs and tissues removed from animals of the same species at different ages provide reasonably good information about long term changes of ACh synthesis in theses organs or tissues during the lifetime of individuals of the species.

Tucek (1978) and Shawn et al., (2004) showed that prenatal and early postnatal development of the central nervous system and of peripheral organs receiving a cholinergic innervations is accompanied by a marked increase in their ChAT activity. This increase is based not only on the growth of cholinergic neurons, but also on the elevation of the concentration of ChAT in them. Transient decrease of ChAT activity observed in some tissues during development may be caused by the fact that during certain periods the non-cholinergic components of theses tissues are developed faster than the cholinergic ones. In old age the activity of ChAT in cholinergic neurons generally diminishes [Nakamura et al, (1996)].

The activity of ChAT in neurons is very probably influenced by their functional activity. This is suggested by observations in salivary glands, adrenal glands and skeletal muscles, but the

relation between functional activity of neurons and ChAT synthesis in them requires more investigations. Changes of ChAT activity depending on hormonal influences have been well demonstrated in brain during hypothyroidism (a decrease) and after the administration of nor adrenaline into the brain ventricles (an increase); a sex- dependent difference in ChAT activity has been found in the preoptic suprachiasmatic area of the hypothalamus [Tucek (1978) and Nakamura et al., (1996)]. Androgenic hormones influence the activity of ChAT (and general development) of the levator and muscle [Tucek, (1978); Nakamura et al, (1996)].

A large decrease of ChAT activity leading to almost complete disappearance of its influence is observed during degeneration of peripheral nerves in homoeothermic animals generation of the axons is accompanied by the formation of ChAT in Schwann cells [Steven et al., (2002)]. The activity of ChAT in the axon is diminished during regeneration and for a long time after the regeneration has been completed [Steven et al., (2002), Tucek (1978) and Shawn et al., (2004)]. ChAT activity in cholinergic neurons and their axonal terminals is greatly influenced by the formation of synaptic contacts with postsynaptic cells [Steven et al., (2002)]. Experiments on hormonally induced changes in the levator indicate that ChAT activity in cholinergic nerve terminals is also dependent on the functional state of postsynaptic cells. The mechanism of retrograde transsynaptic effect of the postsynaptic on the presynaptic cell has not been clarified [Tucek (1978) and (1985); Steven et al, (2002)].

2.2) β-amyloid (Aβ) peptides

β-amyloid is a peptide of 36-43 amino acids that is produced from Amyloid precursor protein (APP) via proteolytic cleavage. β-amyloid peptides are considered to be the main toxic species in the pathogenesis of AD (Randall et al., 2010). The self-assembly of β-amyloid first forms clusters known as oligomers, then oligomers chains form fibrils, the latter accumulates into insoluble forms of aggregates that deposit in the brain causing AD (Verdier et al., 2004).

2.2.1) Amyloid precursor protein (APP)

APP is a transmembrane glycoprotein with C- terminal cytoplasmic part and a long N-terminal extracellular region. APP is located in synapses of the neurons cells and other tissue. The soluble

monomer form of β-amyloid peptide is generated by proteolysis effect of β-and ɣ-secretase to around 110 kDa transmembrane of APP. These soluble β-amyloid peptides accumulate to insoluble form of β-amyloid peptides called senile plaque (sp) in the brain (Walter et al, 2008). There are some genetic risk factors that could lead to AD generation via increasing β-amyloid peptides levels in the brain. When lab experiments were carried on a genetically engineered mice that has been developed by Walter et al, 2008, the genetically engineered mice was carrying a human gene, a gene that is responsible for a rare kind of inherited AD, Walter et al, (2008) observed that the generation of β-amyloid in the mice and memory dysfunction as well (Walter et al, (2008)). All mutation in APP genes, presenilin1 (PS1) gene, and presenilin 2 (PS2) contribute to early-onset AD. These three gene defects lead to imbalance between β-amyloid formation and its clearance. Consequently, complex intra-and extracellular accumulations of β-amyloid are formed leading to inflammation of neurons, synaptic changes, generation of neurofibrillary tangles, and loss of transmission (Verdier et al, 2004).

Whereas, mutation the ε4 allele of the apolipoprotein E gene, on chromosome 19 lead to late-onset AD, but expression of ε2 allele prevents AD developing (Kar et al., 2004; Holmes C, et al, 2002, Poirier t at al., 1993). Moreover, It is observed that changes on presenilin1 (PS1) gene on chromosome 14 and Presenilin 2 (PS2) on chromosome 1 initiate early onset familial cases of AD (under 65 years) (Kar et al, 2004).

2.2.2) Formation of β -amyloid

β-amyloid is produced by cleavage of amyloid precursor protein (APP). APP has the following two pathways for cleavage as indicated in Figure 2.2:

1- The first is non-amyloidogenic pathway by α-secretase between Lys 16 and Leu 17 amino acids residue to produce N-terminal soluble APPα (sAPPα) and C-terminal APP fragment. This pathway inhibits the formation of a complete-length β-amyloid peptide as shown in Figure 2.2. This pathway is not toxic and does not cause AD because of generation of more neurotrophic sαAPP protein (Kar et al., 2004). The sαAPP has abilities to regenerate brain cell particularly after sever brain injury that happens follow stroke and cerebral ischemia, and also sαAPP regulates excitation of neuron cells and synaptic plasticity. Additionally the

sαAPP has neurogenic, growth- promoting, and neuroprotective characterizations (Walter et al., 2008).

2- The second pathway for proteolysis is first processed by β-secretase to yield soluble APP and a membrane bound β-amyloid containing C-terminal. The Second cleavage to membrane bound β-amyloid containing C-terminal by ɣ-secretase to produce complete $A\beta_{1\text{-}40/42}$ peptide as shown in Figure 2.2 (Kar et al., 2004). $A\beta_{40}$ peptide is more neurotoxic and linked to vascular endothelium. $A\beta_{42}$ peptides aggregate to form the basic nucleus of senile plaque (SP) and then $A\beta_{40}$ peptides deposit later. The catalytic ɣ-secretase is considered the rate limiting step for formation of β-amyloid peptides (Walter et al, 2008). The two isoforms of $A\beta_{40/42}$ peptides are toxic because they can cause oxidative stress, neuron dysfunction, cell apoptosis and brain death (Walter et al., 2008). In normal cases approximately 90% of generated β-amyloid peptides are $A\beta_{1\text{-}40}$ which are soluble but convert to β-sheet that can be eliminated from the brain. On the other hand, 10% of secreted β-amyloids are $A\beta_{1\text{-}42}$ that self-assembled to amyloid plaques are deposited in the brain to generate AD (Kar et al, 2004).

Recent studies showed that there is a receptor SorLA/LA11 which is a transmembrane lipoprotein and regulates the endocytic pathways of APP (Walter et al., 2008). SorLA/LA11 plays an important role in determining which form of App is neurotoxic or neurotrophic up on proteolysis. Genetic mutations in sorting receptor result in late-onset AD. Currently, it is clear that α, β, and ɣ-sectrtases-SORL1 of APP have become pharmaceutical targets strategies to convert neurotoxic of APP pathway to neurotrophic one (Walter et al, 2008).

2.2.3) Aggregation of β-amyloid peptide

Accumulation of β-amyloid peptide is a multistep process. First it starts with misfolded β-amyloid to form β-Sheet, and then β-Sheet aggregates into oligomers (dimmers, trimmers, and dodekamers). This step of formation of oligomer is the rate limiting step called nucleation step (Verdier et al., 2004). After that protofibril generates until the aggregation of β-amyloid is insoluble form. Finally, protofibril elongated rapidly into insoluble fibril (Silva et al., 2010; Verdier et al., 2004).

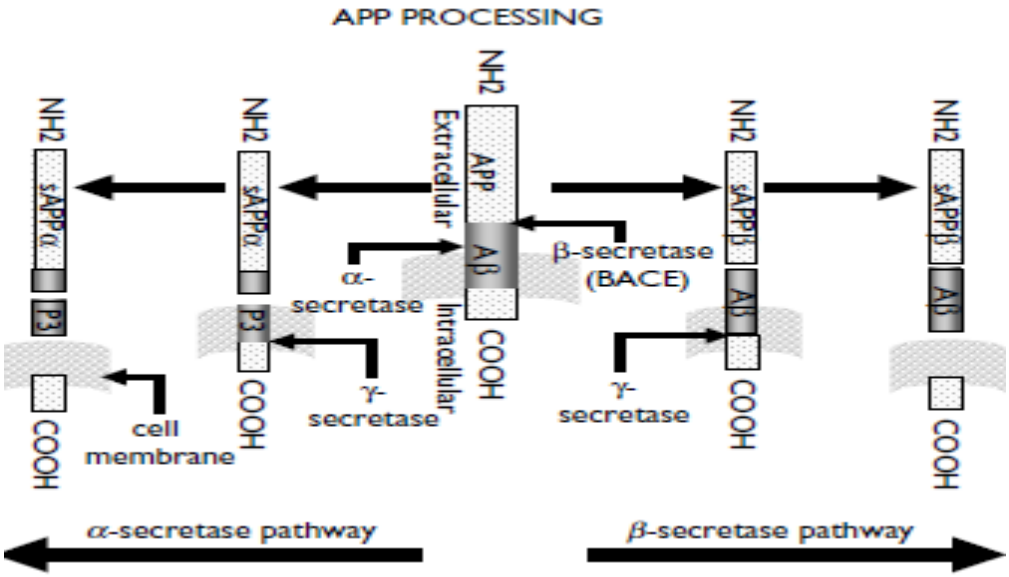

Figure 2.2: a schematic represents the two catalytic pathways for Amyloid precursor protein (APP) cleavage (Kar et al., 2004)

2.2.4) Toxic effect of β-amyloid

Randall et al, (2010) showed that the appearance of insoluble β-amyloid peptides in the brain is considered a hallmark of AD. These insoluble plaques of β-amyloid are the key toxic risk factor in pathology of AD where injection of β-amyloid oligomer into rodent CNS leads to disturbance in cognition functions (Clearly et al, 2005; Poling et al, 2008). Also, as shown in Figure 2.3 the aggregations of amyloid peptides in the brain cause shrinkage of neuron cells and decrease their ability to synthesize and release ACh neurotransmitter through depletion of ACh precursors like choline, and making complex with ChAT; exposure SN56 cholinergic cell lines to $A\beta_{1-40}$ caused shrinkage and cell death for these cells (Kar at al., 2004). Verdier et al 2004 indicated that the toxicity of β-amyloid peptides is due to their interaction with cholinergic cell membrane and cellular organelles as well. This causes an impairment of cellular physiological processes. For example, β-amyloid peptides make leakage in cell membrane of neurons leading to choline leakage, and hence decreasing in ACh level (Kar et al, 2004). Moreover, β-amyloid peptides bind to ChAT making a complex which hiders ChAT activity process for ACh synthesis (Cheng and Prusoff, 1973). Also, β-amyloid peptides interact with glial cells. This stimulates production of

toxic mediators from glial cells and causing neurotoxicity. The toxic effects of β-amyloid peptides can be explained as follows:

1- Changes of cholinergic functions

β-amyloid peptides at small concentrations (picomolar- nanomolar) can affect various steps of ACh synthesis and can be released as Figure 2.4 indicates. For instance, β-amyloid peptides cause inactivation of pyruvate dehydrogenase enzyme which is responsible for production acetyl coenzyme A (acetyl-CoA) from pyruvate (Kar et al., 2004). This effect of β-amyloid peptides is consistent with lab experiment observations where an exposure of nanomolar concentration of $A\beta_{1-42}$ peptides to rat septal neurons reduced ACh formation and decreased activity of acetyl-CoA production by decreasing activity of pyruvate dehydrogenase enzyme (PDH) (Kar et al, 2004; Pedersen, 1997)). Also, β-amyloid peptides could reduce high-affinity uptake of choline; incubation of hippocampal synaptosomes with nanomolar β-amyloid which stopped the depolarization that stimulates high-affinity choline uptake (Kar et al, 2004 and 1998). Moreover, high-dose exposure to β-amyloid peptides reduces activity of ChAT. β-amyloid peptides have an effect on reducing ACh release from synaptic vesicles (SV). When β-amyloid peptides were injected into rat, ACh release from hippocampus was decreased (Kar et al., 2004; Harkany et al., 1995). The inhibition effect of β-amyloid peptides on ACh release was regenerated by ginseng saponins (Lee et al., 2001; Kar et al., 2004). Furthermore, Kar et al., (2004) reported that β-amyloid peptides have the ability to impair muscarinic M_1 like signaling; incubation of nM-mM concentrations of $A\beta_{1-40}$ with rat cortical cultured neurons decreased the carbachol produced GTPase activation effect (Kar et al., 2004; Kelly, 1996). Moreover, increasing choline conductance from PC12 cells after long exposure to micromolar $A\beta_{1-40\ is}$ due to choline depletion by decreasing choline uptake and increasing choline leakage from the neurons (Kar et al., 2004).

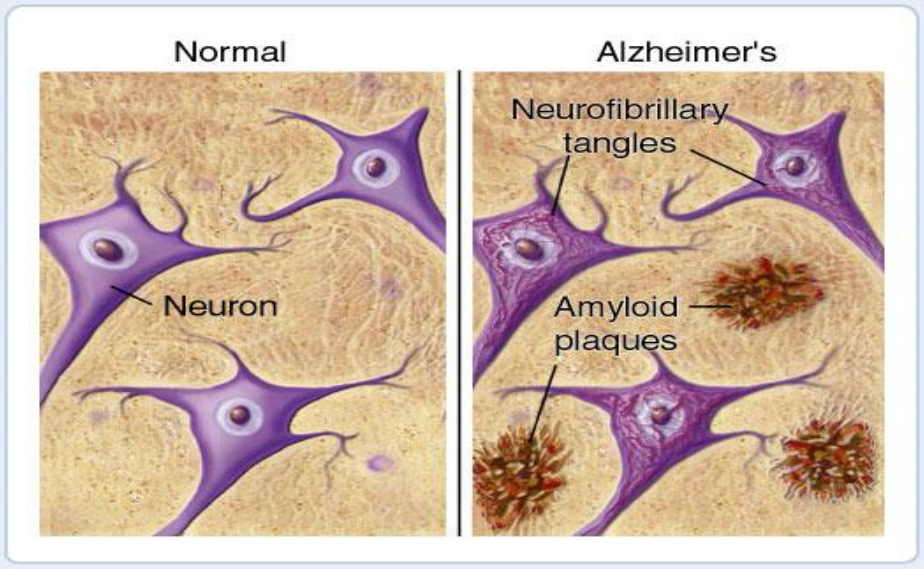

Figure 2.3: β-amyloid induced toxic effect through different mechanisms (http://www.sharpbrains.com/wp-content/uploads/2012/01/plaques_and_tangles_border.jpg)

2- Neurofibrillary Tangles (NFTs) Formation

β-amyloid peptides aggregations in the brain generate neurofibrillary tangles (NFTs): neurofibrillar tangles (NFTs**)** are paired of helical filaments that include hyper phosphorylated tau protein. Tau is a protein that is responsible for stabilizing microtubules (the cytoskeleton of the cells) via reversible enzymatic mechanisms including phosphorylated and dephosphorylated reactions. When phosphorylated tau is not able to undergo dephosphorylated by action of β-amyloid peptides, as a result hyper phosphorylation form of tau proteins is generated. Accordingly, the tau would lose its ability to bind and stabilize microtubule. This leads to destabilizing microtubule, impairing of axonal transport and cell death. This is confirmed with the experimental results in which β-amyloid plaques increase the phosphorylation of tau protein in SN56 cholinergic cell lines (Kar et al., 2004).

3 -Formation of free radicals

When β-amyloid peptides bind to p75 receptors of neuron cells, free radicals are formed leading to apoptosis and loss of cholinergic neurons. This results in decreasing neurotransmitters

secretion from these cells. Since the level of p75 is highest in cholinergic neuron cells of the basal forebrain, the highest decrease would be in ACh level. This is consistent with experimental research where binding β-amyloid peptides to p75 receptors of rat brains showed colocalizations of p75 receptors (Ehrenstein et al., 1997; Peng et al., 1994).

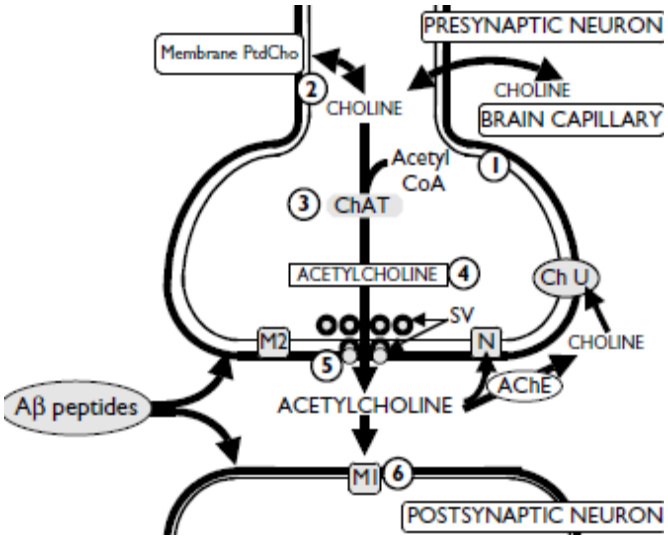

Figure 2.4: A graphical representation of β-amyloid peptides targets in cholinergic neuron cells (Kar et al., 2004)

4-Decreasing concentration of ACh through Positive feedback mechanism

The reduction in ACh concentration causes increase in β-amyloid aggregates concentration through two pathways: 1- Low ACh concentrations increase the synthesis of amyloid precursor protein (APP) in cerebral cortex by inducing high level of APP mRNA (Wallace et al, 1993). 2- Small level of ACh stimulates the cleavage of APP via β-amyloid pathway (Buxbaum et al., 1994; Hung et al., 1993). These two pathways lead to another increasing in β-amyloid peptides levels and hence a further decreasing in ACh levels. The positive feedback loop explains why some medications that increase ACh level such as AChE inhibitors have a limited success for AD treatment. This is because the decrease in ACh concentration is a continuous process due to

loss of choline by leakage action of β-amyloid peptide. Although the drug increases ACh level, β-amyloid peptides reduce it by depletion of its precursor like choline (Ehrenstein et al, 1997).

5-Leakage effect of β-amyloid peptides

The aggregates β-amyloid peptides in cholinergic cells cause formation pathways for leakage of choline and ions such as Calcium out of cholinergic neurons (Galdzicki et al., 1994). Because choline is the rate limiting substrate for ACh synthesis (Mustafa et al., 2009), leakage of choline out of cholinergic neurons induces a reduction in ACh concentrations, and hence AD.

This effect is as toxic as 2,4-dinitrophenol which causes a leakage pathway for protons to cross out cell membrane and leading to uncoupling of electron transport from ATP synthesis (Galdzicki et al., 1994). Choline leakage effect is consistent with experimental observations where the incubation of β-amyloid peptides with Pheochromocytoma PC12 cells increases choline conductance which is proportional to β-amyloid peptides concentrations (Galdzicki, 1994). In such case of low choline levels the cholinergic neurons try to provide choline from other sources like membrane phosphatidylcholine to compensate choline loss by leakage and to be able to synthesize ACh. This behavior of neuron cells is known as autocanabolism effect. The autocanabolism effect causes changes in phospholipids formation and thus in the lipid composition of cell membrane. This leads to neurodegeneration in which the membrane turnover and becomes unable to transmit chemicals impulses (Kar et al., 2004).

2.3) AD Pharmacotherapy

The numbers of patients with AD increase every day where there are 25 million people have dementia related disease, and this number is expected to reach to 81 million by 2040. The risk increases in the developed countries. For instance, in the US every 71 seconds there is one case of AD is estimated, and the cost of healthcare is around $180 billion annually (Walter Lukiw, 2008). Thus most of pharmaceutical research objectives are to develop medications for preventing and reducing AD. Until now there are no effective medication to arrest the developing progression of AD, but drugs provide only symptomatic relief and not useful as long term therapy (Walter J Lukiw, 2008). There are many drugs used for improving the quality of

life and behavior of AD Patients. These drugs are classified according to its molecular targets into different categories as follows:

1- Acetyl cholinesterase inhibitors (AChEIs)

AChEIs therapy is the drug of choice to treat AD. These medications are used to cure mild to moderate AD and considered the most widely prescribed drugs. Such kinds of medications were introduced more than 20 years ago. AChE is responsible for the degradation of ACh in synaptic cleft. As AD is characterized by low levels of ACh, some medications can be used to increase level of ACh by inhibition of AChE. Therefore, cholinergic neurotransmission in brain gets improving. Examples of these medications approved by FDA are donepezil (Aricept), galanthamine, revastigmine (Exelon), and tacrine. However, AChEIs have many side effects such as cardiovascular, cerebrovascular, urinary, and cognitive complications. Also, tacrine is withdrawal by FDA after severe adverse effects that are associated with its use where it is hepatotoxic leading to acute liver failure. Although a long of these (AChEIs) group Donepezil (Aricept) is the most common and favored drug, some researches in Canada and US have approved that the efficacy of this medication is not perfect and limited. Totally, using AChEIs have a definite effect as medicinal agents in AD treatment because the positive feedback effect which low level of ACh causes a further increase in β-amyloid peptides and as a result more decreasing in ACh level in the neurons (Ehrenstein et al., 1997).

2-N-methy-D-aspartate receptor (NMDAR) antagonists:

According to Walter Lukiw, (2008) β-amyloid peptides prevent glial cells from regulation of glutamate re-uptake and recycling resulting in glutamate over excitation and excitotoxicity. This leads to hyperstimulation and neural dysfunction which participates in etiopathogenesis of AD. Using NMDA receptor antagonist such as memantine (Namenda) plays a vital role in masking over stimulation effects of glutamate receptors. Memantine also has anticonvulsant and anti-parkinsonism properties. Recent studies show that NMDA antagonists have some neurotoxic effects and this depends on dose and patient age.

3-β-amyloid as a molecular target

There are different subcategory medications for β-amyloid peptides as follow:

A-γ-Secretase Inhibitors such as Semegacestat and Begacestat are used to inhibit amyloidogenic pathway for cleavage of amyloid precursor protein (APP). Ly450139, as another ɣ-Secretase inhibitor, is subjecting to clinical trials and it is expected to have a good ability in treatment of AD where single 140 mg dosage decreases $A\beta_{40}$ in plasma by 73%. Another compound is JLk6 which is also under research stage and it showed a good result in inhibition of $A\beta_{40}$ and $A\beta_{42}$ in HEk293 cells. However, ɣ-Secretase inhibitors have some concerns where they have some adverse reactions such as gastrointestinal bleeding, hyperplasia, immunological disturbance, and needed to large dosage to be able to cause a significant effect (Lukiw, 2008).

B- β-Secretase Inhibitors such as OM99-2 which is a high molecular weight peptide (peptidomimetic) with potent β-Secretase inhibition effects.

C- β-amyloid Aggregation Inhibitors

Native β-amyloid peptide is misfolded to form β-Sheet which aggregates into oligomer and protofibril. The latter is self-assembly to form insoluble fibril. Fibril deposits in the brain of AD patient to form β-amyloid plaques. Some medications are natural products obtained from plant source can inhibit aggregation of β-amyloid such as curcumine.

D- Immunization against β -amyloid peptides

Immunization against $A\beta_{1-42}$ peptides will be an effective solution for reducing $A\beta 1_{-42}$ peptide levels resulting in reducing pathology of AD. Amyloid over expressing transgemic PDAPP mice showed a good result in decreasing progression and level of neuropathology in AD. On the other hand, the human's clinical trials have not showed a significant success because of human patient body develops complex adverse reactions and meningo-encephalitic cellular inflammation effects. Immunotherapeutics possess significant properties to be used as a therapy for mild-to-moderate AD is under clinical phase III program (Lukiw, 2008).

3- Tau hyperphosphorylation inhibitors as a molecular target

Tau is a microtubule-associated protein in the CNS and promotes tubulin self-assembly into microtubules. Microtubules (MTs) are components of eukaryotic cellular cytoskeleton. Stabilization of microtubules depends on tau protein. Hyperphosphorylation of tau protein by β-amyloid peptides leads to microtubule disintegration and formation of neurofibrillary tangles (NFTs) which is a significant mark of AD. These aggregations of NFTs cause destabilization and disintegration of microtubule leading to collapsing the neurons and impairing axonal transport. Curcumin, Indirubin derivatives and Orange-G are considered good medications for tau hyperphosphorylation inhibition.

4-Oxidative stress as a molecular target

Oxidative stress is an imbalance between the formation of free radicals (reactive oxygen species (ROS)) such as nitric oxide ($NO^{\cdot}$), hydrogen peroxide (H_2O_2), peroxynitrite ($ONOO^{-}$), superoxide ($O_2^{\cdot-}$), and hydroxyl radical ($OH^{\cdot}$) inside the cells, and the ability of cells to protect themselves by scavenging through using detoxifying enzymes or antioxidants. Some metals (aluminum, zinc, copper, iron) can generate the production of free radicals. ROS can promote the generation of amyloid aggregations and neurofibrillary tangles in the brain which causes AD. Moreover, ROS can modify lipids, proteins, nucleotide by oxidation causing cell dysfunction and death. Some medications act as metal chelators or antioxidants used to protect cells against ROS such as desferrioxamine, curcumin, clioquinol, resveratrol, and vitamin-E (Branham, K.J. et al., 2004).

5 -Monoamine oxidase-B (MAO-B) as a molecular target for AD

Monoamine oxidase-B is an enzyme responsible for degradation of the neurotransmitter dopamine. As a result of degradation reaction of dopamine by MAO-B, toxic H_2O_2 and reactive quinone generate as metabolites of dopamine degradation. These toxic metabolites cause neurodegeneration in the CNS. So MAO-B Inhibitors act as neuroprotective agents in AD. Examples for drugs used for this purpose are Tacrine and Rasagiline.

6- G-protein Coupled Receptor 3 as a therapeutic target in AD

G-protein coupled receptor3 (GPR3) is an orphan receptor expressed in brain. GPR3 is a potential therapeutic target in AD because the over expression of GPR3 stimulates β-amyloid production, and hence causing AD. The genetic removal (deletion) of GPR3 in AD mouse model prevents β-amyloid aggregation in the brain (Bobba.et al., 2009).

7- **Gamma- Secretase Activating Protein as a molecular target for AD treatment**

Gamma-secretase activating protein (GSAP) is a protein that regulates gamma secretase processed cleavage of amyloid precursor protein (APP). Deletion of GSAP in mouse model of AD shows a reduction in β-amyloid formation. The anticancer imatinib (Gleevec) drug has a GSAP inhibition characters (Gen He et al., 2010).

8-Sirtuins are a therapeutic target for AD

Sirtuins (SIRT) are a group of enzymes involved in aging and longevity. Over expression of SIRT1 prevents oxidative stress and β-amyloid accumulation in AD. Activation of SIRT1by the antioxidant resveratrol is considered an effective goal for treatment ageing and Alzheimer disease (Bonda et al., 2011).

9- Other potential AD drug targeted against β-amyloid peptide generation

Some compounds are being under research and believed to have good roles in AD treatment. For instance, tramiprosate (Alzheimer NC-51; homotaurine) is a glycosaminoglycan-mimetic compound and it inhibits β-amyloid accumulation. Also, non-steroidal anti-inflammatory drugs (NSAIDs) have anti-inflammatory, antiamylodgenic characterizations like Flurbiprofen (Tarenflurbil; MPC-7869; flurizan) is attractive agent because it reduces $A\beta_{42}$ and it inhibits ɣ-secretase. Further, some herbs they would be expected to play a significant role in treatment of mild-to-moderate AD. For example, ginkgo biloba and uncararia rhynchophylla have antioxidant and antiangiogenic properties as well, also both of them could prevent β-amyloid aggregations. Other examples for herbal medications are tetrahydrcannabinol (THC) and marijuana both of

them are competitive AChE inhibitors. Also, satvia officinalis could improve cognitive impairment (Lukiw, 2008).

10 – Cholesterol lowering agent and their actions on β-amyloid peptide

Recent studies show that there is a relation between increasing weight and late-onset AD. In vitro and in vivo model lab researches have reached that contribution of high serum cholesterol concentration in pathology of AD where high cholesterol level increases processing APP into neurotoxic $A\beta_{40}$ and $A\beta_{42}$. Cholesterol lowering agents such as statins have ability to reduce cholesterol biosynthesis pathway by prevention HMG-CoA reductase enzyme, an enzyme that is responsible for production of cholesterol in liver, (Lukiw, 2008).

11-Omega-3 fatty acid (docosahexaenoic acid; DHA)

Omega-3 fatty acids have antioxidant, anti-inflammatory, and cholesterol lowering agent's properties. Docosahexaenoic acid (DHA) is a neuroprotective compound where it reduces APP processing into neurotoxic amyloidogenic pathway. In vitro studies using human brain cell tissue culture showed that depletion of DHA causes ROS production, and hence oxidative tissue damage. In animal studies using DHA supplementation results in lowering β-amyloid peptides aggregation, quenching ROS oxidative effect, and improving damaged synaptic contacts. This leads to improve cognitive impairment (Lukiw, 2008).

2.4) Pharmacokinetics (PK) and Pharmacodynamics (PD) of Drugs

2.4.1) Pharmacokinetics definition of drugs

It is very important to determine drug doses reaching its target site in the body and how long the drug takes. These questions give us fundamental definition of pharmacokinetic of drug (PK). The pharmacokinetics terms refers to the action of body on the drugs. In other words, a description for drug stages inside the body to reach its site of action as Figure 2.5 refers to.

Accordingly, for drugs to be accessible in the action site, they should pass through the following stages:

I) Adsorption: in which drug is transported from compartment of application to systemic circulation (blood plasma).

II) Distribution: equilibrium drug concentration between blood plasma and rest of organs.

III) Metabolism: this process happens usually in liver or kidney. Some drugs subject to metabolism by specific mechanisms according to drug nature structure. This process is important to make a drug in an easy form to be able to give its action or it is able to excrete easily out of the body.

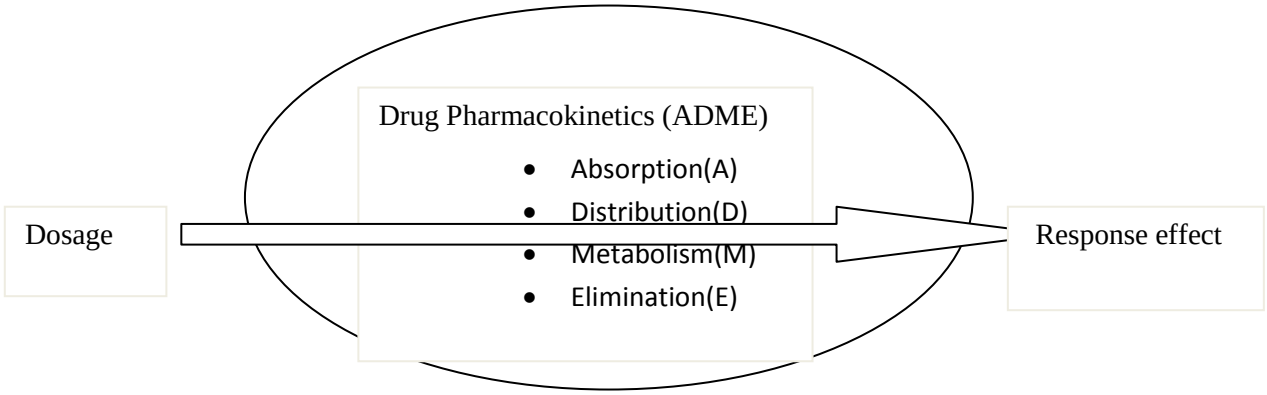

Figure 2.5: Pharmacokinetic principle of drug

IV) Elimination: excretion of drug outside the body via urine, sweat, breast milk or feces.

These four stages are for drugs that are not administered through intravenously (IV). In case of IV, the drug is injected directly into the blood stream; drugs do not need to be absorbed. In such case the bioavailability (percent of the drug that reaches to systemic circulation) of the drug is 100%. Whereas, for drug taken by other routes like oral their bioavailability is less than 100%. This is because the drug might be exposed to metabolism in liver before it becomes accessible in the systemic blood this is called first- pass effect.

2.4.2) Pharmacokinetic terms

There are many terms that should be determined in PK and PD study. These terms are:

1- Area under the curve (AUC): it measures plasma drug concentration time

2- Bioavailability (F): amount of given dose to reach systemic circulation.

3- Clearance (CL): rate of drug eliminated to its concentration in blood plasma.

4- Elimination half-life ($t_{1/2}$): the time needed for decreasing plasma drug concentration by half.

5- Maximum concentration (C_{max}): maximum drug concentration in plasma.

6- Time to maximum concentration (T_{max}): time needed for reaching maximum plasma concentration after taking the dose.

7- Volume of distribution: a relation between amount of drug in the body and concentration of drug in the plasma.

2.4.3) Pharmacodynamics (PD) definition

PD refers to the drug effects on the body. Most of the drugs set their action after binding to receptors of cell membrane surface, but others can affect the receptors inside the cell or the cell organelles.

2.4.4) Pharmacodynamics terms

There are many terms that should be determined in PD study. These terms are:

1- Agonist: drug that binds to its characterized receptor and generates its specific effects.

2- Antagonist: drug binds to receptor but does not produce effect by prohibiting a specific active agent from access to the receptors.

3- Potency: molar drug concentration required to give a specific high effect.

4- Efficacy (Intrinsic activity): maximum effect the drug can get.

5- Affinity: strength (intensity) of binding between drug and receptors.

6- Selectivity: separation between favorable and unfavorable drug action.

7- Therapeutic Window: the most safe and effective drug concentration that exists between effective dug concentration and toxic drug concentration.

8- Therapeutic Index: the ratio of toxic dose to effective dose (TD50/ ED_{50}).

9- Dose-response: simple relation between the mount of drug (dose) and the response (effect) that the drug does. All substances are toxic, the only thing that differentiates between effective and toxic effect is the right dose.

2.4.5) Pharmacokinetics/Pharmacodynamics (PK/PD) model

The application of mathematical modeling for pharmacokinetics/pharmacodynamics (PK/PD) analysis is very important for drug development and optimum therapy for patients. A PK model investigates the dynamics of drug levels in the body tissues such as blood, plasma livers, and heart while a PD model describes the dynamics of drug impacts (Tang et al., 2012). Furthermore, PD models could help for identification the most important factors for increasing the drug efficiency. PK/PD model can help in the design experiments on the large scale to understand the drug pharmacology acted inside biological systems (Gustafason and Bradashaw-pierce, 2011).

2.4.6) PK/PD modeling terms

There are many terms that should be determined in PK/PD modeling study. These terms are:

1- Pharmacokinetics (PK) models

PK models are mathematical models used for giving data about drug concentration in body vs. time. These mathematical equations are used to describe drug concentration in plasma and other tissues using different dosage regimes. Also by mathematical models all of absorption,

distribution, metabolism and elimination can be estimated. Differential equations are used to describe the dynamic behavior of drug from plasma compartments to tissue compartments and vice versa (Gustafason and Bradashaw-pierce, 2011).

2- Compartmental modeling is based on separating the body into different sections (compartments). Theses compartments have the same drug follow, blood flow, binding and similar elimination rate. These models are used for determining plasma concentration with time. There are two types of compartments models as follows:

A- One-compartment model

It is used to describe the distribution and the elimination of drug in the body using a single central compartment as shown in Figure 2.6. This compartment assumes that the change in blood concentration represents a suitable change in drug concentration in the tissue.

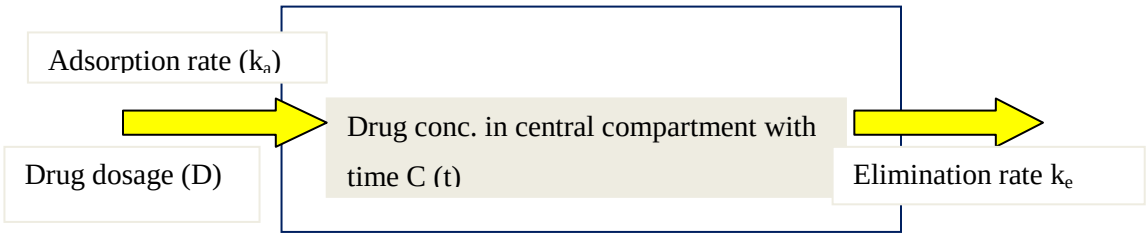

Figure 2.6: One-compartment model graph

B- Multi-compartments model

It is used to describe the drug eliminated by different mechanisms with different rate, and the drug that does not decay linearly with time. In this model the drug transports from a central compartment to peripheral compartments and vice versa with a first-order rate constant. For example, in two- compartment model there is no equilibrium in distribution of drug between blood and tissues. This means that the drug has bidirectional movement pathway between peripheral and central compartments as shown in Figure 2.7.

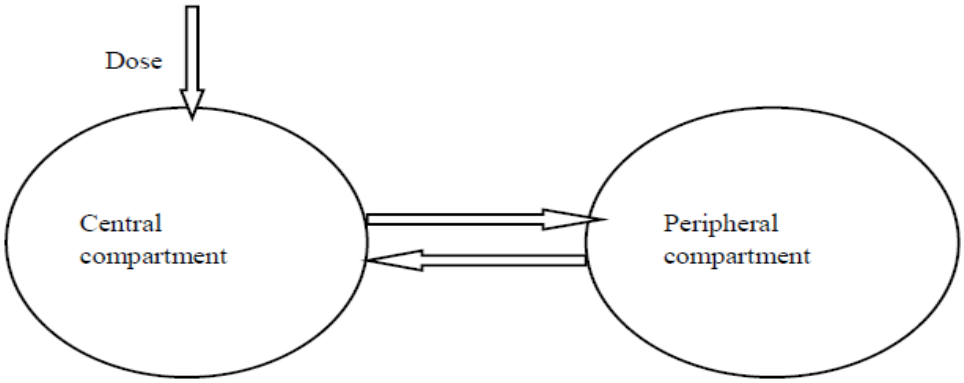

Figure 2.7 two-compartment models Scheme.

Chapter 3

Modeling the Effect of β-Amyloid as Direct Cholinergic Neuromodulator via Choline Leakage Hypothesis

3.1) Introduction

Alzheimer's disease (AD) is an advanced neurodegenerative disease that is considered one of the most dangerous diseases after cancer and heart attack in Canada and the USA. The aggregation of β-amyloid (Aβ) peptides and their plaques deposition in the central nervous system cause loss of neurons and lack of acetylcholine (ACh) which are considered the main symptoms of AD (Selkoe, 1999). Aβ is formed from its poly peptides called amyloid precursor protein (APP) by cleaving via β-secretase and γ –secretase enzymes (Craft 2002). Therefore, Aβ is considered one of the main reasons leading to AD where it rises the level of calcium ions inside the neurons by making a leakage pathways for Ca^{+2} to enter inside of the neurons (Hardy and Higgins, 1992). This leads to loss of neurons plasticity (Arispe et al., 1993). In addition, β-amyloid causes harmful effects on the function of cells. For example, it could prevent glutamate transport in cultured astrocytes and could alter salts and nutrients concentrations through cellular membrane as well (Allen et al., 1997). In this paper, we investigate the interaction between Aβ and ACh neurocycle through the choline-leakage mechanism leading to AD proposed by Ehrenstein et al., (1997). It is assumed that Aβ causes leakage in the plasma membrane leading to diffusion of choline outside the presynaptic membrane, and hence the rate of ACh production decreases. The effect of Aβ will be added to the two-enzyme/two-compartment model (2E2C) built by Mustafa et al., (2009) leading to a system of nine-first-order differential equations system. There are two sources for the choline substrate required for ACh synthesis in the brain: the first one is from compounds containing choline such as phosphatidylcholine and sphingomyelin and the other source is from the blood plasma which contains unbounded choline (Mustafa et al., 2009; Tucek 1985). Choline cannot be synthesized inside the neurons; however, it is produced from the hydrolysis of ACh and it is recycled to the presynaptic membranes via specific transporters

mechanisms existing in the membranes such as high affinity choline transporter mechanism (Bussiere et al., 2001) where the electrochemical gradient of salts like K and Na plays an important role for transporting choline from the synaptic cleft to the presynaptic membrane via high affinity choline transporter (Ehrenstein et al., 1997; Koliatsos and Price, 1991). Therefore, the brain gets choline in the form of either free or bound choline in phospholipids (Mustafa et al., 2009; Shawn et al., 2004). Tucek et al., (1985, 1987) showed that the brain can produce free choline where it was found that the blood stream entering the brain has choline levels lower than that in the leaving stream. Weckler (1988) showed that the experimental observations supported the importance of both forms of choline either free choline in the blood plasma or bound form such as lipoproteins and lysophospahtetidylcholine. Both forms provide the required amount of choline for ACh synthesis (Mustafa et al., 2009). In addition, the process of ACh degradation catalyzed by acetyl cholinesterase (AChE) in synaptic cleft is the most important source for providing the presynaptic neuron with choline (Tucek, (1985). Therefore, Choline recycled has a necessary function in ACh synthesis (Mustafa et al., 2009). Therefore, there are three main sources for choline supplied for ACh synthesis: free choline in the plasma of blood, bound choline in phospholipids, and choline coming from ACh hydrolysis process (Mustafa et al., 2009). Accordingly, if there is a shortage of choline resulting from ACh hydrolysis due to any reason such as AChE inhibition or Aβ aggregates, ACh concentrations in the presynaptic neuron will be affected significantly. This is because the choline is the rate limiting substrate for ACh synthesis in vivo (Mullen et al., 2007; Mustafa et al., (2009). Mustafa et al., (2012) showed that the choline recycled from the synaptic cleft to the presynaptic neuron is the rate limiting step in the whole neurocycle of ACh.

Mustafa et al., (2009) indicated that ACh concentrations in the presynaptic and postsynaptic neurons and synaptic cleft are affected directly by the level of feed choline substrate concentrations (Mustafa et al., (2009)). In addition, the feed choline is much more important than acetyl-coA where choline is the only substrate which is not synthesized in the brain as mentioned earlier (Mustafa et al., (2009)). Furthermore, the low levels of choline content lead to the less efficiency of the process of ACh synthesis and may lead to irregular cholinergic neurocycle behavior (Mustafa et al., 2009).

Ehrenstein et al., (1997) showed that the leakage of choline outside the presynaptic neuron is due to the high levels of Aβ leads to decreasing the internal concentrations of choline substrate. In addition, choline had been proved as the rate limiting substrate for synthesizing ACh (Mustafa et al., 2009; Tucek et al., 1985). Therefore, the final levels of the product ACh in the presynaptic neuron will be affected. Ehrenstein et al., (1997) presented experimental observations supporting the interaction between Aβ and leakage of intracellular choline where Aβ can cause ionic leakage in PC12 cells (Galdzicki et al., 1994). In addition, it is observed that the low levels of intracellular choline concentrations in the presynaptic neurons is one of the symptoms of AD even if the rate of choline transfer to the presynaptic neurons is high (Slotkin et al., 1990, 1994; Ehrenstein et al., 1997).

The main aim of this paper is to investigate the effect of β-amyloid via choline leakage hypothesis on the concentration of ACh, choline, and acetate in both compartments. In addition, we will study how the behaviors of the rate of ACh synthesis in compartment 1 catalyzed by the enzyme ChAT and the rate of ACh hydrolysis catalyzed by the enzyme AChE and pH levels in both compartments are affected by different Aβ levels. It is important to determine whether the choline leakage hypothesis on mechanism of cholinergic neurocycle inhibition AD is able to produce pronounced results compatible with physiological symptoms such as low level of ACh concentration.

3.2 Cholinergic cells and β-amyloid peptides

In cholinergic cells ACh neurotransmitter is responsible for transmission of chemical impulses from presynaptic neurons to postsynaptic neurons (Galdzicki et al., (1994)). ACh neurotransmitter is synthesized in the presynaptic neurons by interaction of choline (Ch) and acetyl-coenzyme A (AcCoA); the reaction is catalyzed by choline-acetyl transferase (ChAT) enzyme. AcCoA is the only substrate produced in axon terminal of presynaptic in the mitochondria, but the other substrates are supplied through different transport mechanisms (Mustafa et al., 2009). After ACh induces the effect on muscarinic receptors of post synaptic cell, it is hydrolyzed by acetylcholinesterase (AChE) into choline, acetate, and protons. The

choline is recovered back to the presynaptic neuron for further synthesis of a new ACh (Galdzicki et al., 1994).

Formation of Aβ plaques in the brain is considered a significant symptom of AD where the accumulation of Aβ in the brain can affect many stages of ACh synthesis and release. In vitro, observation of low concentration of Aβ (picomolar or nanomolar) lowers ACh production in rat hippocampal (Kar et al., 1998). Moreover, the continuous infusion of Aβ into rats was observed to reduce ChAT activity in frontal cortex (Nitta, 1994).

The high levels of β-amyloid plaques in the central nervous system are one of the well-known pathological characteristics for AD patients (Galdzicki et al., 1994). The interaction of β-amyloid with cholinergic neurocycle has attracted many researchers' interests such as Yankner et al., (1990), Galdzicki et al., (1994), Allen et al., (1997), Kar et al., (2004), and Mustafa et al., (2009, 2012). One of the mechanisms explaining the destructive effect of β-amyloid is that the leakage pathway built by the sticking of β-amyloid in the membrane of the presynaptic neurons leading to disruption of membrane transport and substrate diffusion such as choline out of the neurons and infusion of calcium ions into presynaptic neurons (Galdzicki et al., 1994; Aripse et al., 1993).

In this paper, we will focus on leakage pathways in the presynaptic neurons caused by β-amyloid aggregates and supported by many researchers such as Galdzicki et al., (1994) and Enshretein et al., (1997). The effect of β-amyloid aggregates on the dynamic behavior of ACh neurocycle is investigated where the dynamics of levels of ACh, choline, acetate, pH in both compartments are monitored at different concentrations of β-amyloid to determine which state variables are monitored with the various concentrations of β-amyloid. The kinetic parameters are evaluated in order to choose the most appropriate values that give results compatible with the experimental observations. In cell biology there are similar phenomena for the leakage pathways provided by inhibitors such as dinitrophenol to allow for ions to transport through the cell membranes and result in obstacles in ATP synthesis (Galdzicki et al., 1994). In the cholinergic neurocycle β-amyloid leakage pathways could explain the low levels of ACh concentrations in AD patients.

3.3) Modeling the effect of β-amyloid via the choline leakage hypothesis

The effect of β-amyloid on ACh neurocycle is investigated considering the choline leakage hypothesis from compartment 1. According to Ehrenstein et al., (1997) and Mustafa et al., (2009), the availability of choline is the rate-limiting step in the synthesis of ACh. Therefore, the loss of choline due to the leakage could produce significant effects on ACh levels in neurons resulting in low ACh concentration inside the cholinergic neurons. Depletion of choline makes neurons search for other sources of cholin such as phosphatidycholine of cell membrane. Furthermore, the membrane becomes turned over and unable to transport chemical impulses (Wurtman., 1992; Ehrenstein et al., 1997). Another negative effect is the increase β-amyloid aggregates levels by positive feedback. In such case the low ACh level leads to increase average of amyloid precursor protein (APP) mRNA and thereby β-amyloid (Ehrenstein et al., 1997; Wallace et al., 1993). Moreover, low ACh level stimulates cleavage of APP through amyloidogenic pathway (Ehrenstein et al., 1997; Buxbaum et al., 1994). These effects lead to an increase in Aβ levels and hence more choline leakage pathways and low ACh production. The latter case is known as a positive feedback mechanism. It had been observed that activating muscarinic receptors in rat hippocampus by ACh increases the regulation of nerve growth factor (NGF) mRNA and NGF protein (Knipper et al., 1994) while low ACh concentration could lead to neuron death by reduction of NGF. Ehrenstein et al., (1997) investigated the interaction between ACh and β-amyloid and found that the rate of reduction in ACh is proportional to the rate of production Aβ. Therefore, a reduction in ACh could cause low NGF (Ehrenstein et al., 1997; Knipper et al., 1994).

To incorporate β-amyloid into 2E2C model to induce the choline leakage effect the following modifications are performed: First the loss of intracellular choline is included by the addition of the term (- K_{bA3} bA) which is different from that considered by Ehrenstein et al., (1997) who did not consider mathematically the interaction between intracellular choline (Ch) concentration in compartment 1($S_{2(1)}$), and Aβ. This interaction can be formulated as below:

$$\frac{ds_{2(1)}}{dT} = s_{2f} + R * s_{2(2)} - \alpha_{S2_1}\left(s_{2(1)} - s_{2(2)}\right) - \frac{B_1}{S_{2refernce}} r(1) - K_{bA3}\, bA \tag{3.1}$$

Where bA is extracellular Aβ concentration and K_{bA3} is rate constant. This will yield significant effects because ACh is formed in compartment one and choline is the limiting substrate for formation of ACh. The second modification to 2E2C model is the introduction of extracellular Aβ (bA) as a new state variable by adding a new differential equation as shown below:

$$\frac{dbA}{dT} = K_{L2} - K_{L3}\, s_{1(1)} - K_{L4}\, bA \tag{3.2}$$

Equation (3.2) describes that the net increase in extracellular concentration of β-amyloid is proportional to each of K_{L2} which is the inlet concentration formed from APP, consumption by extracellular ACh (- $K_{L3}s_{1(1)}$), and decreasing in extracellular concentration of β-amyloid by acting through both absorption into neuronal membranes and enzymatic breaking down reaction (-K_{L4}bA).

The term K_{L2} refers to the rate of β-amyloid peptides generation. The numerical values of rate constants K_{L1}, K_{L2}, K_{L3} and K_{L4} are in the dimensionless form as shown in Table 1. To simplify the calculations, K_{L1}, K_{L3} and K_{L4} are expressed as a function of K_{L2}.

The third modification is based on the assumption that the rate of ACh reduction caused by decrease in choline levels in compartment 1 is proportional to the rate of β-amyloid production. Therefore, the effect of β-amyloid on ACh concentrations in compartment 1 can be formulated according to the following equation:

$$\frac{ds_{1(1)}}{dT} = s_{1f} - \alpha_{s1}\left(s_{1(1)} - s_{1(2)}\right) + \frac{B_1\, r(1)}{K_{s1}} - K_{bA2}\, s_{1(1)}\, bA \tag{3.3}$$

Equation (3.3) describes the rate loss of intracellular ACh ($s_{1(1)}$) which is assumed to be proportional to membrane concentration of β-amyloid (bA).

The 2E2C model considers that the presynaptic neuron is compartment one and both of the post synaptic neuron and the synaptic cleft as compartment two as shown in Figure 3.1. In 2E2C model every compartment is considered as a constant volume, isothermal continuous stirred tank reactor (CSTR) with constant flow rate, stable recycle ratio, and separated by a permeable membrane. S_1 refers to is ACh, S_2 is choline (Ch), h_1 hydrogen protons concentration, and S_3

refers to acetate (Ac). The feed streams of hydrogen, ACh, choline, and acetate (Q) are brought together in a stable stream to meet the choline recycle flow (RQ) before entering the presynaptic neuron. Also both the feed stream rate into compartment 1 and the outlet flow rate from compartment 2 are assumed to be constant values Q (1+R) as indicated in Figure 3.2.

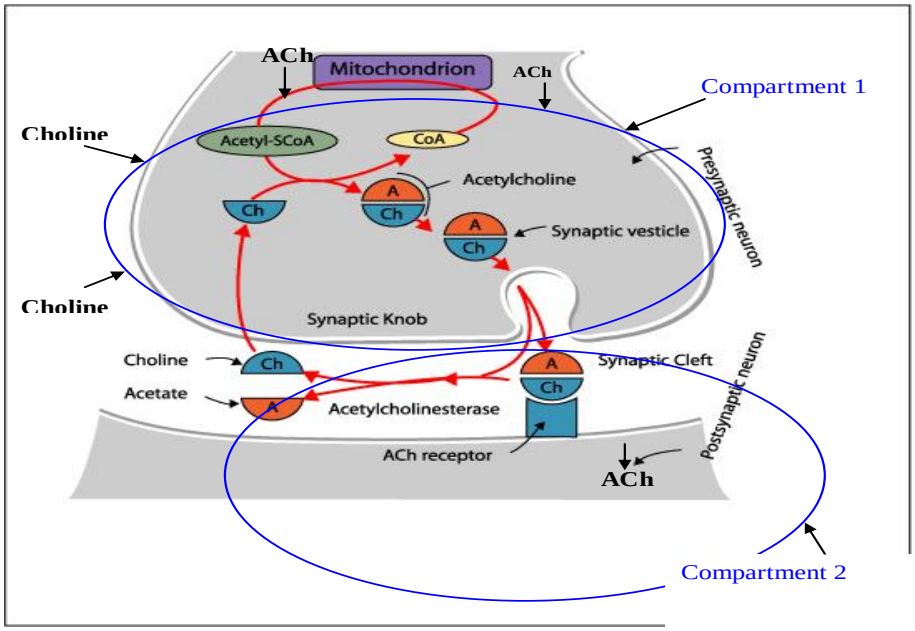

Figure 3.1: Two-enzyme/ two-compartment (2E2C) Model. Presynaptic neuron is compartment one, both synaptic cleft neuron and post synaptic is compartment two (Mustafa et al., 2009)

After incorporating the effect of β-amyloid through equations (3.1), (3.2), and (3.3), the two-enzyme two-compartment model consists of nine first-order differential equations as shown in Table 3.1 where the parameters and the ordinary differential equations of the nine state variables $h_{(1)}$, $h_{(2)}$, $s_{1(1)}$, $s_{1(2)}$, $s_{2(1)}$, $s_{2(2)}$, $s_{3(1)}$, $s_{3(2)}$, and bA are expressed in the dimensionless form.

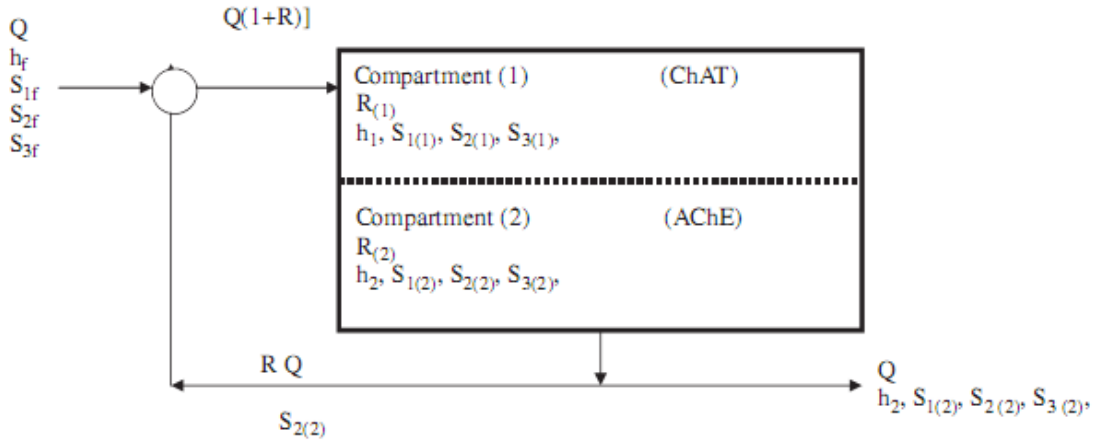

Figure 3.2: Schematic representation for two-enzyme/ two-compartment model

3.4) Model Assumptions

The following assumptions are considered in order to help simplify calculations. All assumptions made for investigating the effect of β-amyloid are compatible with the literature such as those studied by Mustafa et al., (2009). More justifications and assumptions are clarified as below:

1) The presynaptic of cholinergic nerve terminal is described by compartment 1 where ACh is synthesized by the reaction of choline and acetyl CoA in presence of the catalytic effect of ChAT enzyme.
2) Both postsynaptic neurons and synaptic cleft are considered as a compartment two. It is observed that both of them are unified to be in one compartment instead of two or three compartments because both of them are harmonized and interactive and also to simplify the model; particularly to reduce the dimensionality.
3) Both compartments are assumed to be separated by a permeable membrane.
4) The internal mass transfer in compartment one between synaptic vesicles and cytoplasm and in compartment two between ACh and postsynaptic receptors are neglected because every compartment is assumed to be homogenous.
5) All substrates in the presynaptic neuron are transported to the postsynaptic cleft via passive diffusion where all concentrations in compartment 1 should be higher than that in

compartment 2; however choline uptake from the postsynaptic cleft to the presynaptic neuron is performed by facilitated diffusion via high affinity choline uptake transporters (HACUTs).

6) The concentrations of all state variables in compartment two are the average of concentrations in the postsynaptic neuron and synaptic cleft.
7) Temperature is considered constant where the system is assumed to be isothermal and there is no effect for any temperate changes on the system.
8) In this paper we consider that the choline leaked out from the presynaptic neuron caused by β-amyloid aggregates is not transported to compartment 2 but it is leaked outside the two-enzyme/two-compartment system.
9) Transport of β-amyloid from compartment 1 to compartment 2 is neglected.
10) The initial concentration of β-amyloid is assumed to be zero.
11) Both feed flow rate to compartment one and outlet flow from compartment two are considered to be constant with a flow rate of q(m^3/sec).
12) The reactions that are carried out in connected compartments by ChAT and AChE are the following:

In compartment one; ACh is produced as indicated in the reaction below in presence of

$$R_{(1)}: \quad Choline + Acetyl - CoA \xrightarrow{ChAT} Acetylchol ine + CoA \tag{3.4}$$

In compartment two, ACh is hydrolyzed as the following reaction shows by AChE catalytic enzyme:

$$R_{(2)}: \quad Acetylchol ine + Water \xrightarrow{AChE} Choline + Acetate + H^+ \tag{3.5}$$

Both reaction rates $R_{(1)}$ and $R_{(2)}$ are assumed to be hydrogen ions dependent and substrate inhibited (Mustafa et al., 2009). The first order ordinary differential equations (ODEs) of the modified two-enzyme/two-compartment model are summarized in Table 3.1. The concentrations of choline and β-amyloid in cholinergic brain cells are not known either for healthy neurons or AD patients (Galadzicki et al., (1994). The values of kinetic parameters of the models and their sources are given in Table 3.2. Kinetic parameters related to β-amyloid effect such as k_{bA1}, k_{bA2}, k_{bA3}, K_{L1}, K_{L2}, K_{L3}, and K_{L4} are obtained by parameter estimation process and the remaining parameters are obtained from the literature as stated in Table 3.2.

Table 3.1: Dimensionless forms of the ordinary differential equations of choline leakage effects by β-Amyloid aggregates

Item	Compartment	Differential equation
Hydrogen protons	1	$\frac{dh_{(1)}}{dT} = h_f - \gamma_1 \left(\frac{1}{h_f}\right) - \alpha_H \left(h_{(1)} - h_{(2)}\right) + \alpha_{OH}\gamma_1 \left(\frac{1}{h_{(1)}} - \frac{1}{h_{(2)}}\right)$
	2	$\frac{dh_{(2)}}{dT} = V_R(\alpha_H \left(h_{(1)} - h_{(2)}\right) - \alpha_{OH}\gamma_1 \left(\frac{1}{h_{(1)}} - \frac{1}{h_{(2)}}\right) - \left(h_{(2)} - \frac{\gamma_1}{h(2)}\right) + \frac{B_2}{k_{h1}} r(2))$
Acetylcholine	1	$\frac{ds_{1(1)}}{dT} = s_{1f} - \alpha_{s1}\left(s_{1(1)} - s_{1(2)}\right) + \frac{B_1 r(1)}{K_{s1}} - K_{bA1}\, s_{1(1)}\, bA$
	2	$\frac{ds_{1(2)}}{dT} = V_R(\alpha_{S_1}\left(s_{1(1)} - s_{1(2)}\right) - s_{1(2)} - \frac{B_2\, r(2)}{K_{s1}})$
Choline	1	$\frac{ds_{2(1)}}{dT} = s_{2f} + R * s_{2(2)} - \alpha_{S2_1}\left(s_{2(1)} - s_{2(2)}\right) - \frac{B_1}{S_{2refernce}} r(1) - K_{bA2}\, bA$
	2	$\frac{ds_{2(2)}}{dT} = V_R(\alpha_{S2}\left(s_{2(1)} - s_{2(2)}\right) - (1+R) * s_{2(2)} + \frac{B_2}{S_{2reference}} r(2))$
Acetate	1	$\frac{ds_{3(1)}}{dT} = s_{3f} - \alpha_{S3}\left(s_{3(1)} - s_{3(2)}\right) - \frac{B_1}{S_{3refernce}} r(1)$
	2	$\frac{ds_{3(2)}}{dT} = V_R(\alpha_{S3}\left(s_{3(1)} - s_{3(2)}\right) - s_{3(2)} + \frac{B_2}{S_{3refernce}} r(2))$
β-amyloid aggregates	1	$\frac{dbA}{dT} = K_{L2} - K_{L3}\, s_{1(1)} - K_{L4}\, bA$
Rate of synthesis ($r_{(1)}$)	1	$r_{(1)} = \frac{\theta_1 s_{21} s_{31}}{\theta_2 / h_1 (h_1 + 1 + \delta h_1^2) + \theta_3 s_{31} + \theta_4 s_{21} + \theta_5 s_{21} s_{31}}$
Rate of hydrolysis ($r_{(2)}$)	2	$r_{(2)} = \frac{s_{12}}{s_{12} + 1/h_2 (h_2 + 1 + \delta h_2^2) + \alpha s_{12}^2}$

K_{bA2}	$0.075K_{L2}$
K_{bA1}	$0.06K_{L2}$

Table 3.2: Kinetic Parameter Values

Parameter	Value	Reference
θ_1	5.2(0.1)	Hersh & Peet (1977)
θ_2	12	Hersh & Peet (1977)
θ_3	1000	Hersh & Peet (1977)
θ_4	5	Hersh & Peet (1977)
θ_5	1	Hersh & Peet (1977)
α	0.5	Garhyan et al., (2006); Ibrahim et al., (1997); Elnashaie et al., (1984) and (1995))
δ	1	Garhyan et al., (2006); Ibrahim et al., (1997); Elnashaie et al., (1984) and (1995)
$K_a(k_h)$	$1.066*10^{-6}$ kMole/m^3(µMole/mm^3)	Garhyan et al., (2006); Ibrahim et al., (1997); Elnashaie et al., (1984) and (1995)
K_{s1}	50.33 µMole/l	Garhyan et al., (2006); Ibrahim et al., (1997); Elnashaie et al., (1984) and (1995)
S_{2ref}	100 µMole/l	Guyton and Hall, (2000)
S_{3ref}	1 µMole/l	Guyton Hall, (2000)
B_1	5.033×10^{-5} kMole/m^3(µMole/mm^3)	Garhyan et al., (2006)
B_2	5.033×10^{-5} kMole/m^3(µMole/mm^3)	Garhyan et al., (2006)
α_{H^+}	2.25	Elnashaie et al., (1984)

α_{OH^-}	0.5	Elnashaie et al., (1984)
α_{S_1}	1.5	Elnashaie et al., (1984)
α_{S_2}	1.5	Elnashaie et al., (1984)
α_{S_3}	1	Elnashaie et al., (1984)
V_R	1.2	Elnashaie et al., (1984)
pH_f	8.2	Guyton, 2000
s_{1f}	15	Garhyan et al., (2006)
s_{2f}	1.15	Garhyan et al., (2006)
s_{3f}	3.9	Garhyan et al., (2006)
γ_1	0.01	Garhyan et al., (2006); Ibrahim et al., (1997); Elnashaie et al., (1984) and (1995)
R	0.8	Tucek (1978)
K_{bAref}	20 nM/h	Ehrenstein et al., (1997)
K_{L2}	assumed	Dimensionless form
K_{L1}	$3K_{L2}$	Dimensionless form
K_{L3}	$0.035K_{L2}$	Dimensionless form
K_{L4}	$1.76K_{L3}$	Dimensionless form
T_{ref}	0.1 h	Assumed
BA_{ref}	20 nM/l	Kar et al., (2008)

3.5) Results and Discussion

The effect of Aβ on ACh neurocycle is investigated considering the choline leakage hypothesis from compartment 1. According to Mustafa et al., (2009) and (2012), the availability of choline is the rate limiting step in the synthesis of ACh. Therefore, the loss of choline due to the leakage pathways occurring in the membranes could produce significant effect on ACh concentration in neurons.

3.5.1) β- amyloid accumulation

The accumulation of β-amyloid in brains determines the onset of Alzheimer's symptoms (Lee et al., 2007). Figure 3.3 shows the dynamic behavior of the concentration of β-Amyloid. It is found that as the feed rate of β-amyloid (K_{L2}), which is the rate of β-amyloid formation representing the input of β-Amyloid to compartment 1, increases bA increases where it is produced from amyloid precursor protein (APP) in cerebral cortex. It is observed that no β-amyloid is generated at $K_{L2} = 0$ where bA is relatively zero which means healthy neurons. "$K_{L2} = 0$" means that there is no generation of Aβ in the neurons and ACh neurocycle behaves normally. The value of $K_{L2} = 0$ could be considered the control value of healthy neurons without Aβ aggregates. When K_{L2} increases to 0.5 in the dimensionless form (corresponding to 10 nM/h), bA increases rapidly in the time period (0-100) in the dimensionless form corresponding to (0-10 h), then bA reaches a plateau at bA = 9 in the dimensionless form (corresponding to 180 nM/h). When K_{l2} increases to 0.75 and 1 (corresponding to 15 and 20 nM/h respectively), bA increases fast to 9.5 and 9.8 in the dimensionless form (corresponding to 190 and 196 nM/h respectively) and then settles down in the end of the previous plateau period. These results are compatible with the theoretical results obtained by Ehrenstein (1997) who showed that the synthesis of APP promotes high concentrations of β-amyloid and creates pathways in the membranes of presynaptic neurons. The behavior of ACh neurocycle would be investigated at the previous different values of K_{L2} where all state variables in both compartments are studied in order to understand the physiological phenomena of the cholinergic neurocycle and their response to different values of β-amyloid inlet concentrations as will be shown later.

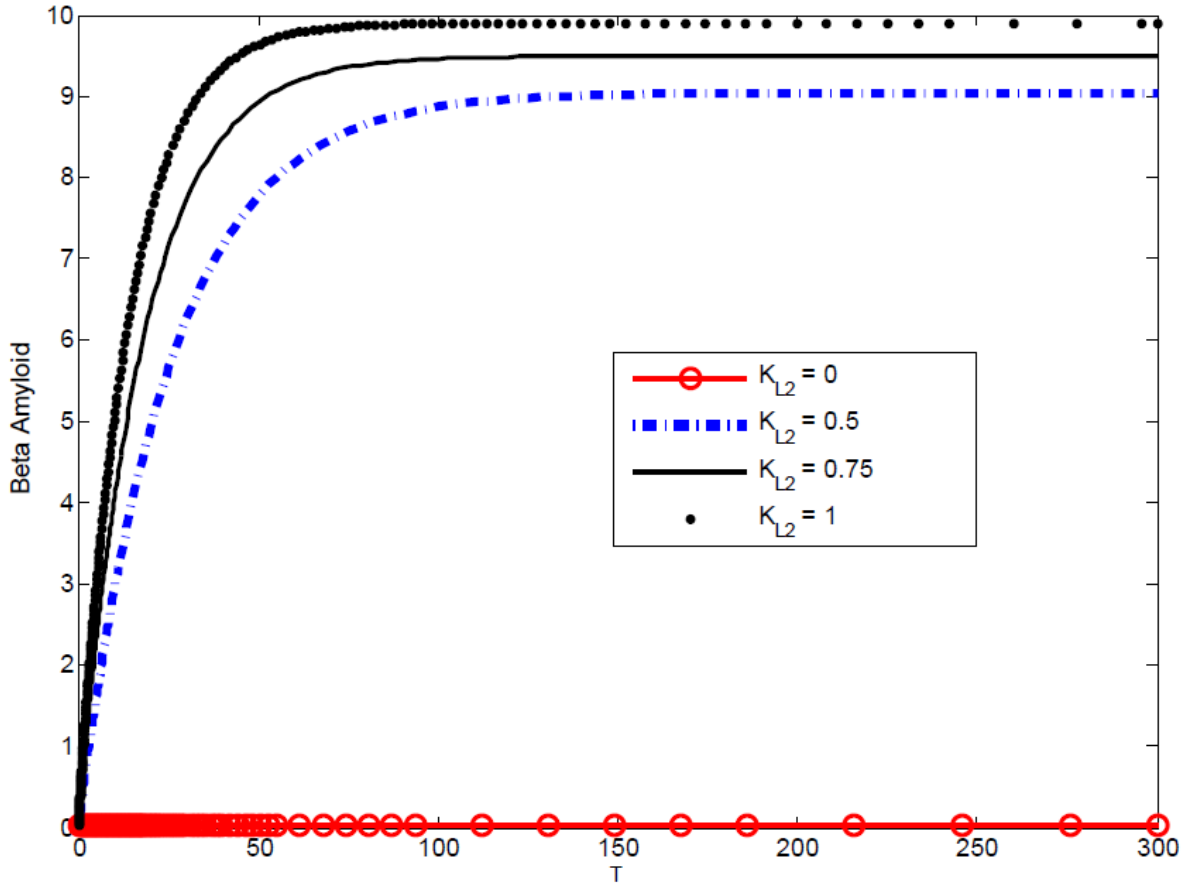

Figure 3.3 A graphical representation for Aβ concentration with time at different K_{L2} values

3.5.2) ACh concentrations in compartments 1 and 2

The dynamic behavior of ACh concentration in compartment 1 is investigated at different rates of Aβ production from APP (K_{L2}). The healthy normal cholinergic neurons is characterized by no existence of bA which corresponds to K_{L2} = 0. In this case no Aβ is produced inside the neuron as mentioned previously (Figure 3.3) and ACh level is normal where ACh_1 = 8.5 in the dimensionless form corresponding to 425 µM which represents a healthy concentration. On the other hand, as K_{L2} increases, there is a significant decrease in ACh_1 concentration in the period (0-100 h) until it reaches 5.8 in the dimensionless form corresponding to 290 µM at the end of the plateau period (100-300) in the dimensionless form corresponding to (10-30 h).

When K_{L2} increases to 0.75 and 1 (corresponding to 15 and 20 nM/h respectively), it is observed that there is a further significant decrease in ACh_1, where in the period of (0-100) in the dimensionless form, ACh_1 decreases fast to reach 5 and 4 in the dimensionless form (corresponding to (250 and 200μM). Then, ACh_1 decreases to reach the plateau at (4.7 and 3.8) in the dimensionless form corresponding to (235, and 190 μM) respectively. These values are lower than the healthy ACh levels in the end of plateau period as shown in Figure 3.4 (a). In the latter cases of K_{L2} = 0.75, and 1, it is observed that there is a much pronounced decrease in ACh_1. This can be explained by the mechanism of choline leakage pathways caused by high β-amyloid concentrations, as shown in Figure 3.3, which leads to decrease of choline concentrations in compartment 1 as will be studied later. The results are consistent qualitatively with the experimental results obtained by Kar et al., (1998) who showed that the small concentrations of β- amyloid lead to reduction of ACh concentrations in the presynaptic and postsynaptic neurons in rat hippocampal slices and guinea pig cortical synaptosomes. It is observed that reduction in ACh synthesis is accompanied by reduction in ACh hydrolysis.

As shown in Figure 3.4 (b) ACh_2 concentration in compartment two decreases as a consequence of decreasing ACh_1 in compartment one because the decrease in synthesis of ACh_1 leads to a reduction in ACh transport from the presynaptic neuron to the synaptic cleft. As shown in the figure ACh_2 has an exponential behavior and the more increase in the inlet rate of Aβ aggregates (K_{L2}), the more decrease in ACh_2 level in compartment 2. For example, at K_{L2} = 0 the level of ACh_2 is relatively high which is around 0.23 in the dimensionless form (corresponding to 11.5 μM) and this case represents the normal physiological condition where no bA is produced. However, at K_{L2} = 0.5 in the dimensionless form (corresponding to 10 nM/h), the level of ACh_2 decreases rapidly to 0.18 through the period of (0-100) in dimensionless form (corresponding to (0-100 h) until it reaches a plateau at 0.16 (corresponding to 8 μM). At K_{L2} = 0.75 (corresponding to 15 nM/h), ACh_2 has the same behavior as at K_{L2} = 0.5, but ACh_2 reaches a plateau at 0.15 (corresponding to 7.5 μM) at time t = 300 in the dimensionless form (corresponding to 30 h). At the maximum Aβ inlet rate K_{L2} = 1 (corresponding to 20 nM/h), ACh_2 concentration settles down at 0.12 (corresponding to 6 μM) at the end of the period which is much lower than the healthy ACh concentration.

The observed reduction in ACh_1 and ACh_2 concentrations at higher values of K_{L2} in comparison to the normal condition at $K_{L2} = 0$ is attributed to that the rate of production of Aβ is relatively high which leads to leaking choline (Ch1) from compartment 1. As the choline is the limiting substrate for ACh synthesis, with continuous leakage of choline, the net amount of choline available for synthesis of ACh decreases leading to lower generation of ACh_1. This low level of ACh release is compatible with experimental observations obtained by Kar et al., (2004) and Tohgi et al., (1994) who observed lower levels of ACh in guinea pig cortical synaposomes and rat neurons after incubation with Aβ and consistent with the observations of low levels in ACh concentration in cerebrospinal fluid (CSF) of AD patients (Ehrentein et al., 1997; Tohgi et al., 1994).

Ehrenstein et al., 1997 confirmed the reduction in intracellular ACh level observed in SN56 cells of cholinergic hybrid after two days incubations with small concentrations of $A\beta_{1-42}$. This reduction of intracellular ACh_1 level is due to shortage in availability of biosynthesis substrate material such as choline and acetyl-CoA, where Aβ peptide causes leakage of choline outside of the neuron (Ehrenstein et al., 1997) and Aβ reduces acetyl-coA synthesis in the neuron. Moreover, Kar et al., (2003) and Harkany et al., (1995) showed that a decrease in ACh release from hippocampus of rat occurs after its injection with $A\beta_{1-40}$. As shown in Figure 3.4, ACh_2 concentration in compartment two decreases as a consequence of decreasing its level in compartment one because reduction in ACh_1 synthesis leads to a decrease in ACh transport via presynaptic membrane to synaptic cleft, and hence lowering ACh_2 level.

3.5.3) Choline concentrations in compartments 1 and 2

As indicated in Figure 3.5 (a), there is a significant reduction in choline concentration in both compartments of 2E2C model (Ch_1) and (Ch_2) respectively due to choline leakage by the action of Aβ. Figure 3.5 (a), for instance, in compartment one at healthy neurons where $K_{L2} = 0$ (no inlet of Aβ peptides), choline concentration in compartment 1 (Ch_1) does not leak out of the presynaptic neuron. Accordingly, its level is normal and reaches 2.8 in the dimensionless form (Corresponding to 280 μM) at the end of the period of 300 corresponding to 30 hr.

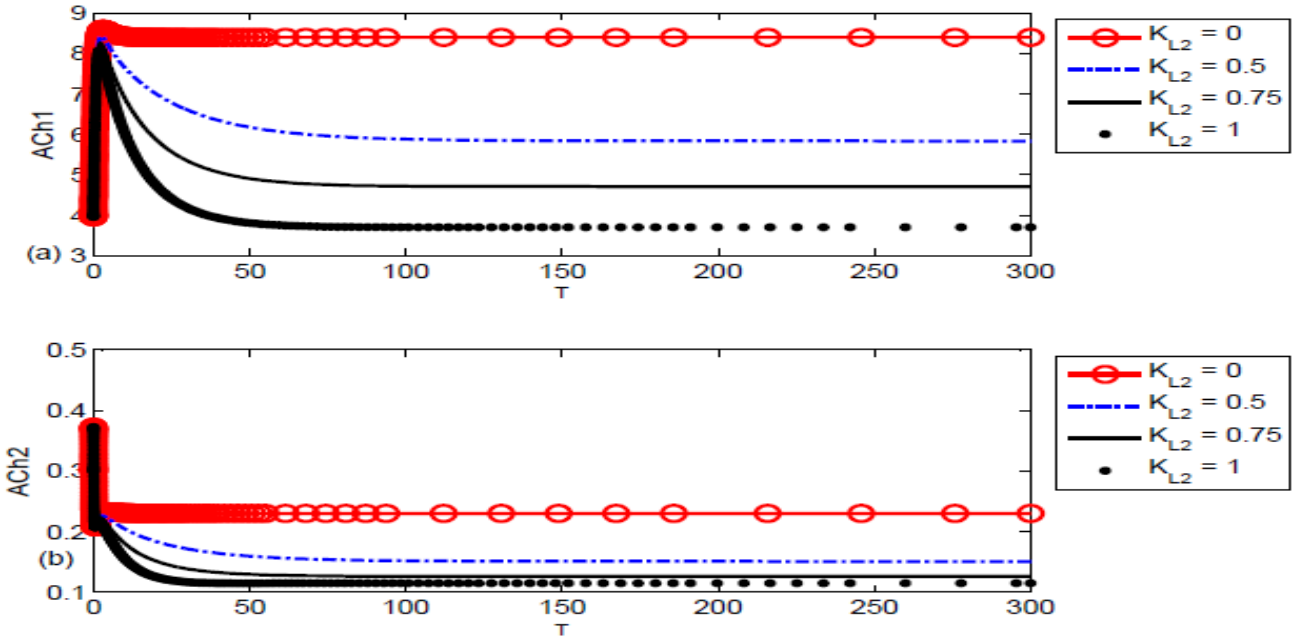

Figure 3.4: A schematic representation for ACh_1 and ACh_2 concentrations with time at different K_{L2} values.

At K_{L2} = 0.5 in the dimensionless form (corresponding to 10 nM/h), the level of ACh_2 decreases rapidly to 0.18 through the period of (0-100) in the dimensionless form (corresponding to ((0-10 h) until it reaches a plateau at 0.16 (corresponding to 8 µM). However, as shown in Figure 3.5 (a) when K_{L2} increases to 0.5 (corresponding to 10 nM/h), it is clearly observed that Ch_1 decreases to 2.3 (corresponding to 230 µM/h), at time (0-100) in dimensionless form (corresponding to 0-10 h). Then, Ch_1 is prolonged in reduction until it takes a plateau at 2 (corresponding to 200 µM) at the end of the period 30 h. While at K_{L2} = 0.75 (corresponding to 15 nM/h), Ch_1 reduces more significantly and settles down at 1.5 (corresponding to 150 µM/h) at the end of the period 30 h. When Aβ production rate propagates to K_{L2} = 1 (corresponding to 20 nM/h), Ch_1 decreases fast to reach 1 (corresponding to 100 µM/h) at the end of the period 300 (corresponding to 30 h). These results are in agreement with the theoretical and experimental results obtained by Ehrenstein et al., (1997) and Nitsch, (1992) who showed that the decrease in ACh levels in frontal cortex of AD patients was attributed to a decrease in choline concentration in the presynaptic neuron. Also our results are consistent with the experimental results obtained

by Kar et al (2004) who showed that an increase in choline conductance from PC12 cells after long exposure to molar concentrations of $A\beta_{1-40}$ was due to leakage of choline out of cells and low choline up-take. The leakage of choline from brain cell of AD patients is compatible with choline leakage from their red blood cells (Butterfield et al., 1985). Also, Aβ causes ionic leakage in PC12 cells (Galdzicki et al., 1994) and a further reduction in high-affinity choline uptake occurs after incubation of nanomolar concentration of $A\beta_{1-40}$ with hippocampus synaptosomal (Kar et al., 1998 and 2003).

Since the availability of choline in compartment two depends on the amount of ACh release existing in compartment 2 which depends on ACh transported from compartment 1 by membrane diffusion, choline level in compartment two (Ch_2) as shown in Figure 3.5 (b) decreases subsequently. This is because ACh in compartment two is susceptible to hydrolysis in synaptic cleft giving rise to choline, acetate and hydrogen ions. Accordingly, the reduction in ACh_2 leads to a corresponding reduction in Ch_2, as shown in Figure 3.5 (b). In the absence of β-amyloid production at $K_{L2} = 0$ as in healthy neurons, it is observed that the concentrations of Ch_2 is high. At $K_{L2} = 0.5$, Ch_2 decreases rapidly to 0.85 (corresponding to 42.5 µM/h) at the end of the period (0-100) in the dimensionless form (corresponding to 10 h). Then, Ch_2 reaches a plateau at 0.81 (corresponding to 40.5µM/h) at the end of 30 hr. It is observed that Ch_2, at $K_{L2} = 0.75$ (corresponding to 15 nM/h), behaves in the same way as at $K_{L2} = 0.5$ but it reaches a plateau at 0.62 (corresponding to 31 µM/h) after 300 hr. Figure 3.5 (b) at $K_{L2} = 1$ (corresponding to 20 nM/h) shows that the rate of Ch_2 reduction is fast and rapid and reaches nearly 0.4 (corresponding to 20 µM/h), after 30 hr which is less than healthy concentration which is 300 µM/h (Allen et al., (1997). However, the results in Figure 3.5 (b) are not compatible with observations obtained by Nitsch et al. (1992) and Slotkin et al., (1990), who observed that choline leakage could lead to increase in extracellular choline level noticed by high level of choline in cerebrospinal fluid (CSF). This discrepancy is because of our assumption that the choline leaked through β-amyloid pathways from compartment 1 does not enter to compartment 2. However, the result in Figure 3.5 (a) are in agreement with their observation which is low levels in Ch_1 is a result of choline leakage effect by β-amyloid (Ehrenstein et al., 1997; Elble et al., 1989; Nitsch et al. 992; Slotkin et al., 1990, 1994). Because ACh synthesis is based on

choline content in the presynaptic neuron, the reduction in Ch_1 via choline leakage pathways will affect significantly the rate of ACh synthesis and ACh_1 as well.

These results are compatible with those obtained by Galdzicki et al., (1994) who illustrated that the reduction of intracellular concentration of choline increases by the presence of β- amyloid aggregates and this could help explain the low concentrations of ACh in the tissue brains of AD patients (Galdzicki et al., (1994); Davis et al., 1982). Furthermore, These results are in agreement with the experimental results obtained, in-vitro, by Galdzicki et al., (1994) who showed that the interaction between PC12 cells and β-amyloid-(1–40) leads to reduction in free choline and increase in choline conductance which would result in increasing the concentration of β-amyloid. Furthermore, Galdzicki et al., (1994) illustrated that βA would decrease the choline levels in the presynaptic neurons; thereby ACh synthesized by the enzyme ChAT would decrease significantly where the decrease of concentrations of ACh is clearly one of the main symptoms existing in the central nervous system of AD patients (Galdzicki et al., 1994).

3.5.4) Acetate (Ac) concentrations in compartments 1 and 2

According to equation (3.4), the intracellular acetate substrate in the form of acetyl-CoA reacts with choline to produce ACh in the presence of catalytic effect of choline acetyl transferase (ChAT). Figure 3.6 (a) shows the dynamic behaviour of acetate level in compartment 1 (Acetate 1) at different values of K_{L2}. It is observed that at $K_{L2} = 0$ which represents healthy neurons without β-myloid effect, Acetate 1 decreases gradually from 8.5 in the dimensionless form (corresponding to 8.5 μM) and settles down to a plateau at 6.5 in the dimensionless form (corresponding to 6.5 μM) which represents the minimum concentration of Acetate 1 in comparison to its values at $K_{L2} = 0.5$, 0.75, and 1. It can be explained by that at $K_{L2} = 0$, no β-amyloid is produced as shown in Figure 3.3, no pathways are built in the membrane of the presynaptic membrane to allow for choline to be leaked outside the presynaptic neuron allowing for Acetate 1 to be consumed by the enzyme ChAT to synthesize ACh according to equation (3.3).

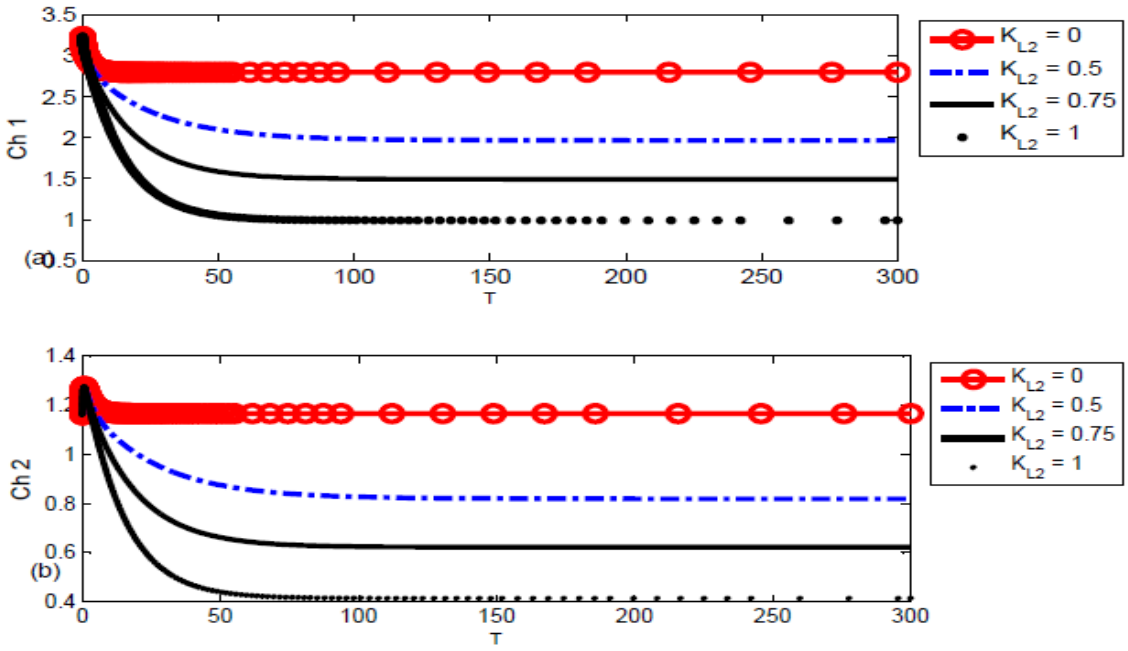

Figure 3.5: Ch_1 and Ch_2 concentrations with time at different K_{L2} values

However, at K_{L2} = 0.5 (corresponding to 10 nM/h) as shown in Figure 3.6 (a), Acetate 1 decreases gradually from 8.5 to reach 6.7 after passing time of 50 (corresponding to 5 hr) to be stable at 6.8 (corresponding to 6.8 µM) which is higher than Acetate 1 at K_{L2} = 0.0. It is observed that as K_{L2} increases β- amyloid aggregate is produced and builds leakage pathways allowing for choline to transport outside compartment 1 and reduction of intracellular choline concentration (Ch_1) and accumulation of intracellular acetate (Acetate 1). In addition, it is observed that Acetate 1 at K_{L2} = 0.75 (corresponding to 15 nM/h) decreases to reach 7 after a time of 50, then it increases to reach a plateau of around 7.4 (corresponding to 7.4 µM) at the end of the period 300 (corresponding to 30 hr), as illustrated in Figure 3.6 (a). However, at K_{L2} = 1 (corresponding to 20 nM/h), Acetate 1 decreases from 8.5 to around 7.8 (corresponding to 7.8 µM) at the end of the period 300 which is higher than that of K_{L2} = 0, 0.5, and 0.75 due to accumulation of Acetate 1 and low intracellular choline and choline leakage pathways of β-amyloid effect Figure 3.6 (a).

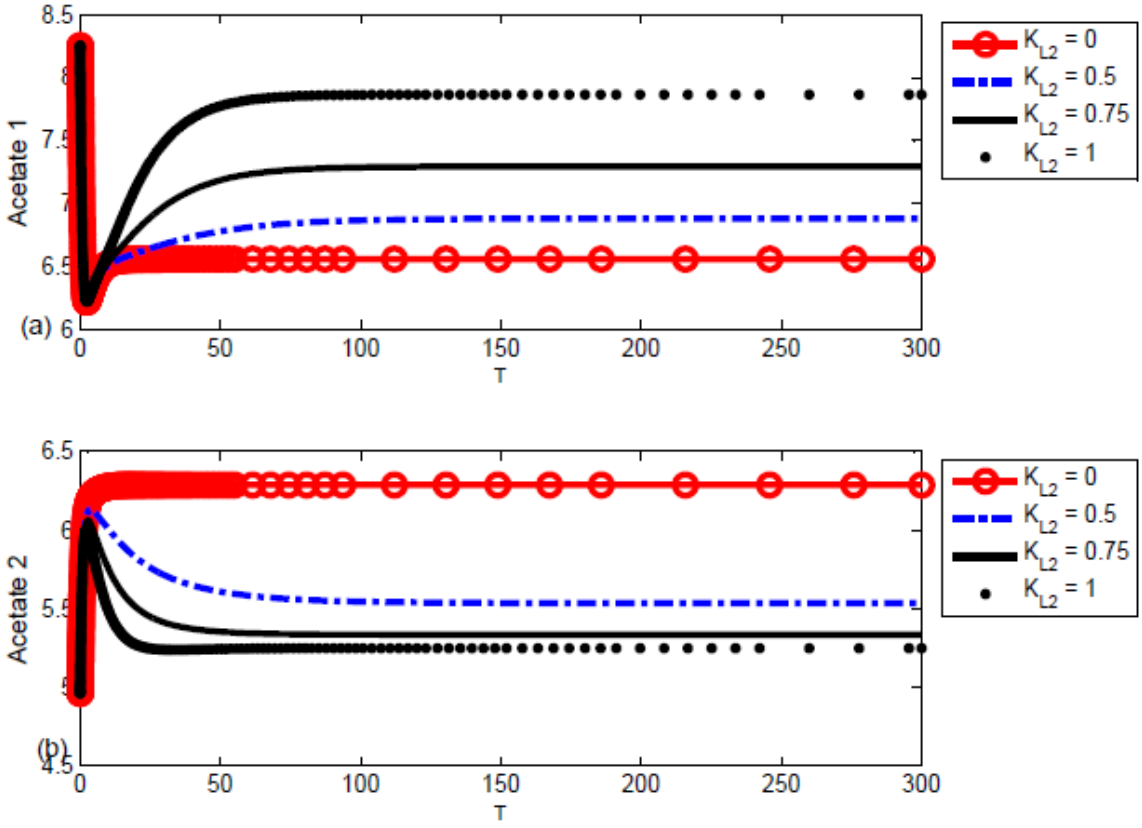

Figure 3.6 Dynamic behavior Ac_1 and Ac_2 concentrations at different K_{L2} values

Figure 3.6 (b) shows the dynamic behaviour of the acetate concentration in compartment 2 (Acetate 2) at different K_{L2} values. It is observed that the dynamic behaviour of Acetate 2 is different from that of Acetate 1 which increases with increasing of K_{L2}. This is due to the lower concentration of ACh_2 as shown in Figure 3.4 (b) where ACh_2 is the source for producing Acetate 2 according to the hydrolysis reaction (equation 3.5) catalyzed by AChE. As shown in Figure 3.6 (b) at $K_{L2} = 0$ (where no β-amyloid is produced) and ACh_2 has the maximum range, Acetate 2 settles down around 6.25 (corresponding to 6.25 µM) at the end of the period 300 (corresponding to 30 hr); however, as K_{L2} increases to 0.5, 0.75, and 1, Acetate 2 decreases to reach 5.52, 5.4, and 5.3 respectively (corresponding to 5.52 µM, 5.4 µM, and 5.3 µM respectively) at the end of the period 300 (corresponding to 30 hr). These concentrations are

lower than the healthy range and show the harmful effect of choline leakage pathways because of increase in β-amyloid aggregates concentrations.

3.5.5) Effect of β-amyloid on Synthesis and Hydrolysis Rates in compartments 1 and 2

The dynamic behaviors of ACh synthesis rate (Rate 1) catalyzed by ChAT in compartment 1 and ACh hydrolysis rate (Rate 2) catalyzed by AChE in compartment 2 are shown in Figure (3.7). Figure 3.7 (a) shows that Rate 1 does not change in the healthy range of $K_{L2} = 0$ where Rate 1 decreases from 0.0175 in the beginning of the reaction to settle down around 0.015 of the end of the period 300 (corresponding to 30 h). However, as K_{L2} increases to 0.5, 0.75 and 1 in the dimensionless form, Rate1 decreases continuously to reach a plateau at 0.01, 0.008 and 0.005 in the dimensionless form, respectively. As shown previously in Figure 3.5 (a), the intracellular choline concentrations (Ch 1) decreases with the increase of K_{L2}, and according to Table 3.1, Rate 1 depends on choline substrate concentration. In this case, ChAT activity decreases negatively with the increase in production of β-amyloid aggregates with an increase in K_{L2} as shown previously in Figure 3.3.

Figure 3.7 (b) shows that Rate 2 in compartment 2 which is catalyzed by AChE enzyme at different values of K_{L2}. It is observed that Rate 2 decreases slightly from 0.16 at the beginning of the reaction to reach 0.12 at the end of the plateau period of 30 hr. However, as K_{L2} increases to be 0.5, 0.75 and 1 in the dimensionless form, Rate 2 decreases significantly and reaches 0.78, 0.63, and 0.61, respectively. To explain the reduction of Rate 2, the hydrolysis rate in compartment 2 ($r_{(2)}$) in Table 3.1 depends on ACh_2 , which decreases with the increase in K_{L2} as shown in Figure 3.7 (b) leading to the reduction of Rate 2.

3.5.6) pH levels in compartments 1 and 2

Figure 3.8 shows the change of pH levels in both compartments at different K_{L2} values. As shown in Figure 3.8(a), at $K_{L2} = 0$ the level of pH_1 decreases very fast from 8.5 at the beginning of the period to reach the plateau where pH_1 is 5.5 at the end of the period 300 corresponding to

30h. At K_{L2} = 0.5, Figure 3.8(a) illustrates that pH_1 takes the same behaviour as at K_{L2} = 0 but settles down to a plateau at a high value of pH_1 = 5.75. In addition, at K_{L2} = 0.75, Figure 3.8 (a) shows that pH_1 settles at a high value of 6 at the end of the period 300 (corresponding to 30 hr). When K_{l2} increases to 1 (corresponding to 20 nM), it is observed that pH_1 stabilizes at a high value of 6.6 as shown in Figure 3.8(a). The phenomenon of increasing pH levels in compartment 1 with the increase of β-amyloid formation rate in terms of K_{l2}, can be attributed to the decrease in concentration of hydrogen protons in compartment 1(H^+) because of the increase in the difference between hydrogen ions levels in compartments 1 and 2 where hydrogen proton in compartment two (H^+) decreases as shown in Figure 3.8(b). The latter difference represents the driving force for transfer of hydrogen protons from compartment 1 to compartment 2.

Figure 3.8 (b) shows the dynamics of pH_2 in compartment 2 (pH_2). It is observed that at K_{L2} = 0 where no β-amyloid is produced, pH_2 decreases rapidly from 6.8 at the beginning of the period to settle down at 5.3 at the end of the period 300 (corresponding to 30 hr). When K_{L2} increases to 0.5, β-amyloid aggregate is generated leading to an increase of pH_2 which stabilizes around 5.6. As K_{L2} increases to 0.75 and 1 (corresponding to 15 and 20 nM respectively), it is observed that pH_2 settles down around 5.75 and 6.1 respectively as shown in Figure 3.8 (b). The reduction of pH_2 with the increase in β-amyloid aggregate production in terms of K_{L2} is attributed to the decrease in the rate of ACh hydrolysis as shown in Figure 3.7 (b) which is due to low available ACh_2 for hydrolysis.

From this study, it is clear that all system variables in addition to rate of ACh synthesis, rate of ACh hydrolysis - in all of presynaptic, postsynaptic cleft, and postsynaptic neurons have been affected significantly by lack of choline reflecting the sensitivity of cholinergic neurocycle in AD (Wurtman et al., 1990). As mentioned before, phospholipids in neuronal membranes are one of choline sources for ACh synthesis (Marie et al., 1985). A portion of membranes choline is proposed to transport into the presynaptic neuron to compensate the shortage of intercellular choline levels (Galdzicki et al., 1994; Wurtman et al., 1990). Therefore, the lipid composition of cell membranes could be affected leading to destruction of cholinergic neurons membranes [Ginsberg et al., 1993, Galdzicki et al., 1994; Wurtman et al., 1990). It has been found that low

levels of choline concentration and neuron cells membrane destruction are common features in the brain tissues of AD sick persons (Galdzicki et al., 1994).

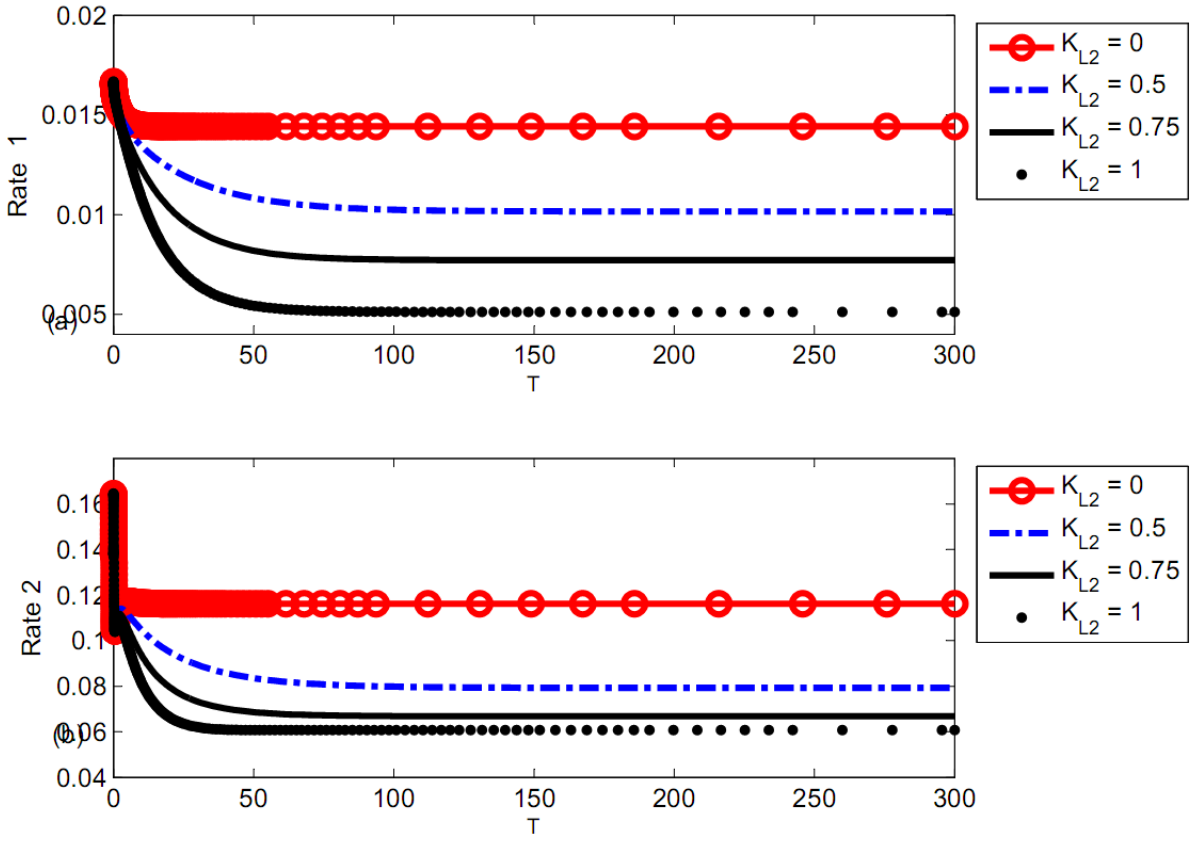

Figure 3.7 Dynamic behavior of ACh synthesis rate catalyzed by ChAT (Rate 1) and ACh hydrolysis rate catalyzed by AChE (Rate 2) at different K_{L2} values

Allen et al., (1997) investigated the neurotoxic effect on the membranes of PC 12 cells. They found that choline transport rate through PC 12 cells increases when exposed to a wide range of β-amyloid (1-40) concentrations. Allen et al., (1997) showed that the high levels of β-amyloid in cholinergic neurons could lead to loss of choline inside the neurons. Our results are in agreement with those obtained by Ehrenstein (1997), who showed that there is a mutual effect between the reduction of ACh concentration and the levels of β-amyloid. Where the synthesis of APP in the

neuron tissues of AD brain patients will be induced by the low levels of ACh and as a result more choline leakage pathways might be promoted (Buxbaum et al., 1994; Ehrenstein 1997). Therefore, the increase of β-amyloid will lead to a further decrease in ACh levels. This cycle of increasing β-amyloid and decreasing ACh continues resulting in a pronounced reduction in ACh in compartment 1. Furthermore, the results of the choline leakage model are compatible with those obtained by Tohgi et al., (1994) who observed low levels of ACh in the brains tissues of AD patients.

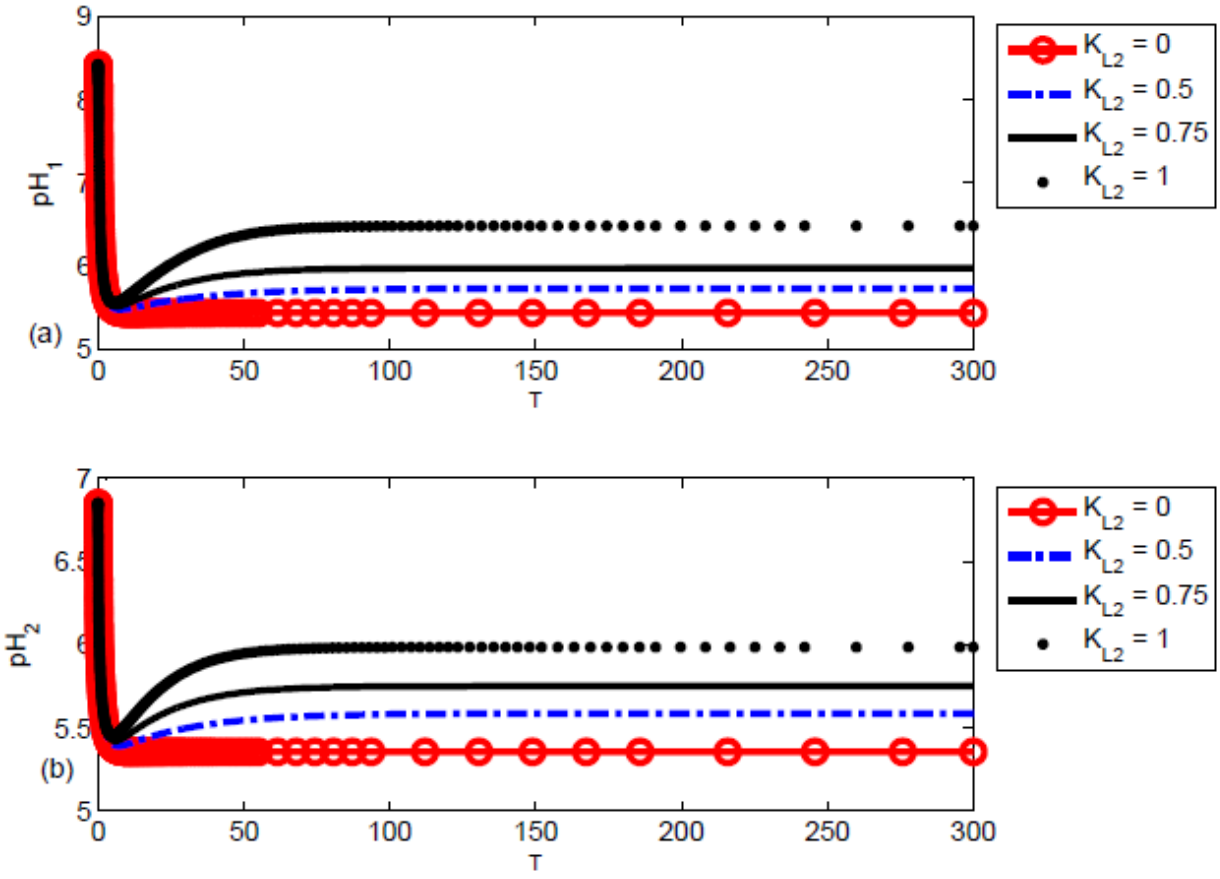

Figure 3.8 pH_1 and pH_2 levels with time at different K_{L2} values

3.6) Summary and Conclusions

Based on the results of the effect of β-amyloid on ACh neurocycle through the two-enzyme/two-compartment model, it is concluded that β-amyloid induces choline leakage from the brain presynaptic neurons (compartment 1) leading to a decrease of choline concentration in compartment 1 and compartment 2 as well. These reductions in choline concentrations in both compartments are promoted with the increase in the inlet β-amyloid (K_{L2}) where the portion of choline transported outside the presynaptic membrane increases. Additionally, the rates of ACh synthesis catalyzed by ChAT and rate of ACh hydrolysis in the post synaptic neurons (compartment 2) catalyzed by AChE decrease. Furthermore, the levels of ACh in both compartments are lowered as well as the levels of β-amyloid production (K_{L2}) increase in the range (0-1). However, the acetate concentration in compartment 1 increases in parallel with the increase of K_{L2} but the acetate level in compartment 2 decreases. As shown in Figure 3.3, β-amyloid production also increases with the increase of K_{L2} causing a more harmful effect. The results of the model show that choline leakage, induced by β-amyloid, could cause a reduction in choline and ACh concentrations in each of the presynaptic neuron and the synaptic cleft neuron, rate of ACh synthesis by ChAT, rate of ACh hydrolysis by AChE, and significant changes in pH levels and acetate concentrations in both compartments. The results are in agreement with that reported by Allen et al., (1994) and Kar et al., (2004) who showed that β-amyloid aggregates could lead to increase in choline loss from neurons and reduction in generated ACh levels.

Also, the results are in agreement with those obtained by Kar et al., (1998) who showed that when neuron tissues are exposed to low concentrations of β-amyloid for a while, choline uptake is reduced significantly. Therefore, ACh levels in the post synaptic cleft can be affected negatively. In addition, β-amyloid could influence ACh in compartment 1 by affecting transport rate of ACh in the presynaptic neuron and the fusion of synaptic vesicles with the membranes and thereby inhibiting ACh release. These results are compatible with the low levels of both ACh and choline in the neuron tissues of AD brains. Furthermore, our observations are consistent with the experimental findings such as those obtained by Kar et al., (1998, 2004), Galdzicki et al., (1994), and Allen et al., (1997) on PC 12 cells and with theoretical results obtained by Ehrenstein et al., (1997) and reflect the significance effect of β-amyloid in cholinergic disease

through choline leakage hypothesis. From this study it is proposed that medications should inhibit β-amyloid leakage effect as will be discussed in the next chapter to improve the choline recycle.

Chapter 4

Modeling the Interaction between β-Amyloid Peptides and Choline Acetyltransferase Activity and Its Relation with Cholinergic Dysfunction

4.1) Introduction

Cholineacetyltransferase (ChAT) is a single–strand globular protein, and it was discovered in rabbit brain by Nachmansohn and Machado in 1943 and catalyzes biosynthesis reaction of ACh neurotransmitter (Lips et al., 2007). ChAT is present in two forms in nerve terminal: (i) non-ionic membrane-bound and (ii) soluble form. ChAT synthesis occurs in the rough endoplasmic reticulum in cholinergic neuron cells. Then, it is transferred to axon terminal for ACh synthesis via rapid and slow axoplasmic flow (Oda, 1999). ChAT plays an essential role in cholinergic neuron cells and non-neuron cells. In neuron cells ChAT expression is a special marker for cholinergic system improvement during brain growth and development where ChAT is involved in activation of multiple neuropsychic functions such as memory, cognition, sleep, learning, and movement (Abreu-Villaca et al., 2011).Therefor, any disturbance in ChAT levels inside neuron cells could generate serious negative consequences. For example, (i) down-regulation of ChAT activity causes serious cholinergic disease such as dementia, schizophrenia, and Huntington's disease (Mustafa et al., 2009; Nuns Tavares et al., 2000), (ii) ChAT abnormalities in the brain could lead to sudden death in infants (Oda, 1999), (iii) ChAT inhibition leads to generation of Alzheimer's disease because ChAT is the enzyme that is responsible for ACh synthesis. Therefore, ChAT inactivation results in a decline of ACh levels in brain. Decreasing ACh concentration is the most common early stage features of AD. However, in non-neuron cells ACh generated by ChAT catalytic effect is secreted in extracellular space. ACh in extracellular space is necessary for maintaining homeostasis of cells, and for modulating many of the essential cell functions such as cell division, mitosis, cytoskeleton organization, interactions between cells, and maintaining the immune functions (Abreu-Villaca et al., 2011). As shown in Figure 4.1

ChAT is concentrated in the presynaptic neuron of the cholinergic neuron because of its necessity for ACh synthesis (Mustafa et al., 2009; Brandon et al., 2004) where ChAT catalyzes the reaction between choline (taken from extra cellular fluid by high-affinity transporter carrier) and acetyl-CoA (produced during glucose metabolism in mitochondria) to produce ACh; ChAT facilitates the transfer of acetyl moiety from acetyl-CoA to choline to give ACh and enzyme-CoA as indicated in equation 4.1.

$$\underset{\text{Choline}}{(CH_3)_3\overset{+}{N}CH_2CH_2OH} + \underset{\text{Acetyl coenzyme A}}{CH_3COSCoA} \xleftrightarrow{ChAT} \underset{\text{ACh}}{(CH_3)_3\overset{+}{N}CH_2CH_2OCOCH_3} + CoASH \qquad (4.1)$$

There are various factors that could affect negatively on ChAT activity such as excitatory amino acids (EAAs), reactive oxygen species (ROS), and β-amyloid peptides. The most serious defective factor is β-amyloid peptides (Zambrzycka et al., 2002). Incubation of nanomolar concentration of β-amyloid peptides with 50% cultured cholinergic neurons caused a complete ChAT inhibition (Nilson Nunes-Tavares et al., 2012). ChAT inhibition by β-amyloid peptides induces several cholinergic problems such as memory dysfunction, neuron impairment, and cognition declining. Since ChAT is an important indicator for healthy of cholinergic neurons and plays a necessary role for activating multiple neuropsychic functions, many researches focused on ChAT investigation such as Mustafa et al., (2009), Nunes-Tavares et al., (2000), and Waser et al., (1989).

The main goal of this chapter is to investigate the effect of wide range of concentrations of β-amyloid aggregates as inhibitor on ChAT activity in brain tissues and the consequences on the cholinergic neurocycle behavior such as concentrations of ACh, choline levels, acetate levels, and the rate of ACh synthesis and ACh hydrolysis in compartment 1 and compartment 2, respectively. In this study three different kinetic mechanisms describing the interaction between β-amyloid aggregates and ChAT activity are investigated and the results of each mechanism are compared to each other in order to understand how β-amyloid aggregates could affect ChAT activity. The rate of ACh synthesis catalyzed by ChAT and affected by β-amyloid inhibitor and derived from each kinetic mechanism is incorporated into the two-enzyme/two-compartment model explained in Chapter 3 to account for the effect of β-amyloid peptides.

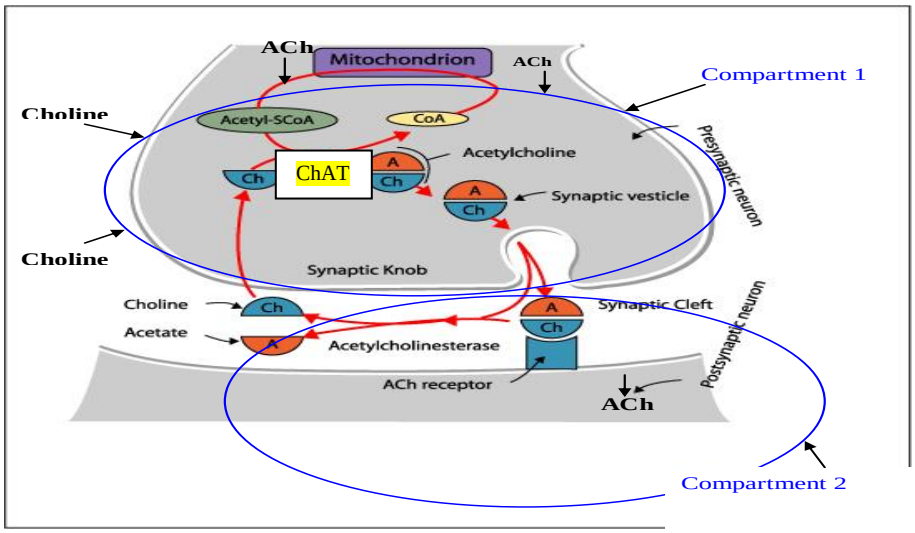

Figure 4.1: Schematic representation of ChAT catalytic role in ACh synthesis: two –enzyme/ two-compartment (2E2C) Model (Mustafa et al., 2009)

4.2 Formulation of the interaction between β-Amyloid peptides and ChAT kinetics through 2E2C Model

The ACh neurocycle is shown in Figure 4.1 where the presynaptic neuron represents the plant for ACh synthesis where it contains the enzyme ChAT, choline, and acetyl CoA. The presynaptic neuron is considered as compartment 1 while both synaptic cleft and postsynaptic neuron represent compartment 2. It is observed that choline is the only component produced from the hydrolysis which is recycled to compartment 1 and reused for ACh synthesis (Mustafa et al., 2009). Tucek (1985) showed that both ACh and acetyl-CoA are synthesized in compartment 1. Figure 4.2 shows a simple form of the feedback model of ACh cholinergic neurocycle shown in Figure 4.1. Every compartment is considered a constant volume and isothermal continuous stirred tank reactor (CSTR) with a constant flow rate and constant recycle ratio. Also, the two compartments are separated by a permeable membrane. β-amyloid peptides interact with ChAT inside compartment 1. Nunes-Tavares et al., (2012) reported that there is a strong relation

between β-amyloid peptides and cholinergic dysfunction which is one of the main symptoms of Alzheimer disease (AD). Furthermore, β-amyloid could inhibit the activity of the enzyme ChAT leading to reduction in the levels of ACh and memory impairment (Nunes-Tavares et al., 2012). ChAT activity could be completely reduced significantly with β-amyloid.

4.2.1 Model Assumptions

All assumptions made for investigating the effect of β-amyloid compatible with literature such as those cited by Mustafa et al., (2009) are shown in Chapter 3. More justifications and assumptions are clarified below:

1) The presynaptic of cholinergic nerve terminal is described by compartment 1. Inside this compartment ACh is synthesized by the reaction of choline and acetyl CoA in the presence of catalytic effect of ChAT enzyme.
2) Postsynaptic of neurons together with synaptic cleft are considered as compartment two. Both postsynaptic and synaptic cleft are unified to be in one compartment instead of two or three because both of them are harmonized and interactive and also to simplify the calculations in solving the model particularly when the dimensionality is too high.
3) Both compartments are assumed to be divided with a permeable membrane.
4) The internal masses transfer in compartment one between synaptic vesicles and cytoplasm and in compartment two between ACh and postsynaptic receptors are neglected because every compartment is assumed to be a homogenous
5) All matters in the presynaptic neuron are transported to the postsynaptic cleft via passive diffusion where all concentrations in compartment 1 should be higher than that in compartment 2; however, choline uptake from the postsynaptic cleft to the presynaptic neurons is performed by facilitated diffusion via high affinity choline uptake transporters, (HACUTs).
6) It is observed that concentrations of all state variables in compartment two are the average of concentrations in postsynaptic and synaptic cleft.
7) Temperature is considered constant where the system is assumed to be isothermal and there is no effect for any temperate changes on the system.

8) Transport of β-amyloid from compartment 1 to compartment 2 is neglected. To justify, it is noted that transport of β-amyloid from compartment 1 to compartment 2 is by passive diffusion and the transport rate is extremely lower than that from the cytoplasm to compartment 1. The latter transport (from cytoplasm to compartment1) addresses the blood brain barriers (BBB) according to saturable mechanism such as Monod and Michaelis-Menten kinetics (Craft et al., 2002; Zlokovic et al., 1993; Martel et al., 1996).
9) The initial concentration of β-amyloid is assumed to be zero.
10) Feed stream rate to compartment one and outlet flow from compartment two are considered to be constant with a value of q (m^3/sec).

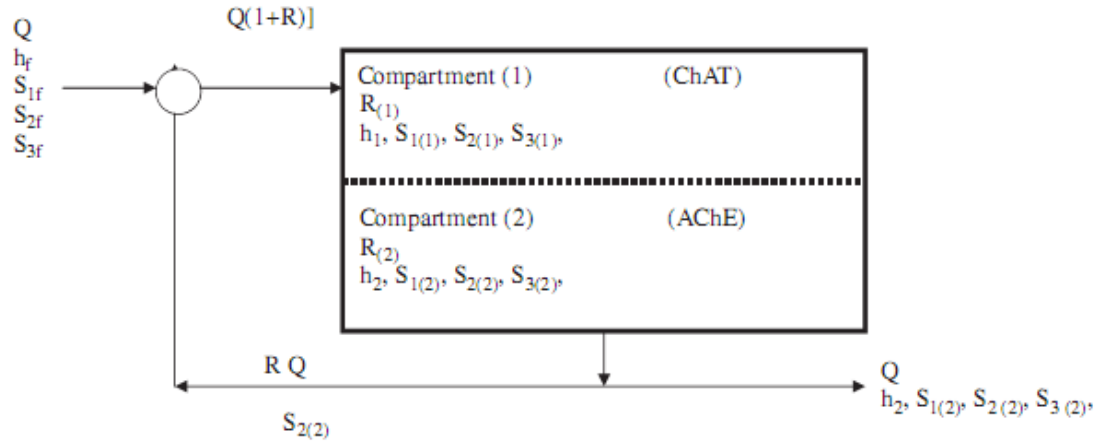

Figure 4.2: Schematic representation for two-enzyme/ two-compartment model

4.2.2 Competitive Inhibition of ChAT in Two Enzyme/Two Compartment Model

ChAT and AChE are the two cholinergic enzymes considered in the 2E2C model. ChAT is responsible for synthesis of ACh in compartment 1 of the 2E2C model, while AChE catalyzes the degradation of ACh in compartment 2. It is found that incorporation of β-amyloid into rat brains *in vivo* (Nitta, 1994) and at nano to pico molar concentrations into SN56 cell line *in vitro* (W.A. Pederson, 1996), shows significantly a decrease in ChAT activity and ACh production. However, detection of change in AChE activity was readily observed and reported (Auld, 1998).

This finding suggests that β-amyloid may act as a general modulator of ChAT enzyme activity leading to a reduction in ACh synthesis (Ehrenstein 2000).

The exact mechanisms of ChAT modulation by β-amyloid are still currently unknown. It is possible that β-amyloid aggregates may directly inhibit ChAT activity by competitively binding to active sites, or perhaps limit the activity of secondary proteins responsible for ChAT synthesis and regulation. Since level of intracellular ChAT is generally maintained at a concentration much higher than that of the reactants for ACh production (Blusztajn, 2000), modification of the 2E2C model to incorporate inhibition of ChAT activity is required to understand the mechanisms of the interaction between ChAT and β-amyloid aggregates.

To examine the phenomenon of ChAT activity inhibition by β-amyloid in a simpler model, β-amyloid is considered to act directly as a competitive inhibitor of ChAT enzyme.

Figure 4.3 illustrates a modified version of pH-dependent enzyme synthesis reaction model used in the two enzyme/two compartment model. The modification (represented in square brackets) takes into account two possible pathways in which β-amyloid may bind competitively to intermediate complexes, thereby inhibiting their ability to progress to the main reaction direction (in the vertical pathway) towards ACh synthesis. In such case β-amyloid may bind directly to the active form of the enzyme E_2H to generate the inactive E_2H [bA] complex (Figure 4.3 (a)), thus limiting the availability of active enzymes to carry out ACh synthesis and decrease net enzyme activity. Similarly, it is also possible that β-amyloid may bind to the enzyme intermediate complex X_2 thereby preventing ACh release from the complex (Figure 4.3 (b)).

The generation of β-amyloid is modeled by adding another differential equation identical to that of choline leakage hypothesis. However, note that the leakage term was not incorporated into the choline differential equation for compartment 1. The accumulation of Aβ is described by equation (4.2).

$$\frac{db}{dT} = K_{L2} - K_{L3} s_{1(1)} - K_{L4} b \qquad (4.2)$$

The value of K_{L2} is assumed to produce significant effects on other variables and the numerical relationships between K_{L3} and K_{L4} were kept the same as in the choline leakage hypothesis. The

numerical derivation of the rate equation for the modified pH-dependent ACh synthesis model with competitive inhibition of β- amyloid is shown below.

4.3. Kinetic Mechanism 1: Competitive inhibition of Aβ with all species activated enzyme complex E_2H

4.3.1 Formulation of Kinetic Mechanism1:

The synthesis rate for competitive inhibition of β- amyloid with activated enzyme complex E_2H can be derived as follow:

X_1 and X_2 are related to each other through the following equation:

$$X_1(Ch)k_1 = X_2k_{-1} \text{ or } X_1 = \frac{K_1}{Ch}X_2 \quad (4.3)$$

where $K_1 = k_{-1}/k_1$

By the assumption of rapid equilibrium, E_2H and X_1 can be related by:

$$k_2(AcCoA)E_2H = k_{-2}X_1 \text{ or } E_2H = \frac{K_1K_2}{(AcCoA)(Ch)}X_2 \quad (4.4)$$

Where $K_2 = k_{-2}/k_2$

By rapid equilibrium assumption, E_2H [bA] complex can be expressed as

$$k_iE_2H(bA) = k_{-i}E_2H[bA] \text{ or } E_2H[bA] = K_i(bA)(E_2H) \quad (4.5)$$

Where $K_i = k_i/k_{-i}$

From the ionization of E2H

$$E_2H(H^+)k_{-b} = E_2H^+ k_b \text{ or } E_2H^+ = \frac{(E_2H)(H^+)}{K_b} \quad (4.6)$$

From the deionization of E2H

$$E_2^- (H^+)k_a = E2H\,k_{-a} \text{ or } E_2^- = \frac{K_a(E_2H)}{(H^+)} \quad (4.7)$$

From equation (4.3), (4.4), (4.5), (4.6) and (4.7) we get,

$$E_{t2} = E_2H + E_2^- + E2H_1^+ + E_2H[bA] = \frac{K_2K_1}{(AcCoA)(Ch)}\left(1 + \frac{K_a}{H^+} + \frac{H^+}{K_b} + (bA)K_i\right)X_2 \quad (4.8)$$

X_2 and X_3 are related by:

$$X_3 = \frac{X_2}{K_3(AcCoA)} \quad (4.9)$$

where $K_3 = k_{-3}/k_3$

Since $E_t = E_{t2} + X_1 + X_2 + X_3$

$$E_t = X_2\left(\frac{K_2K_1}{AcCoA(Ch)}\left(1 + \frac{K_a}{H_1^+} + \frac{H_1^+}{K_b} + (bA)K_i\right) + \frac{K_1}{Ch} + 1 + \frac{1}{K_3(AcCoA)}\right) \text{ or}$$

$$X_2 = \frac{E_t(Ch)(AcCoA)}{\left(K_2K_1\left(1 + \frac{K_a}{H_1^+} + \frac{H_1^+}{K_b} + (bA)K_i\right) + K_1(AcCoA) + Ch(AcCoA) + \frac{Ch}{K_3}\right)} \quad (4.10)$$

Since $R_1 = K_2^{\backslash} X_2$, therefore

$$r_1 = \frac{\theta_1 s_{31} s_{21}}{\theta_2 / h_1(1 + h_1(1 + bAK_{I1}) + \delta h_1^2) + \theta_3 s_{31} + \theta_4 s_{21} + \theta_5 s_{31} s_{21}} \quad (4.11)$$

Where *bA* is the generated Aβ concentration in the dimensionless form and K_{I1} is the dimensionless equilibrium rate constant for the first proposed inhibition mechanism (Figure 4.3 (a)). Table 4.1 summarizes the nine ordinary-differential equations of 2E2C model considering ChAT-inhibition effect by β-amyloid based on the previous kinetic mechanism (1), and Table 4.2 gives the values of kinetic parameters.

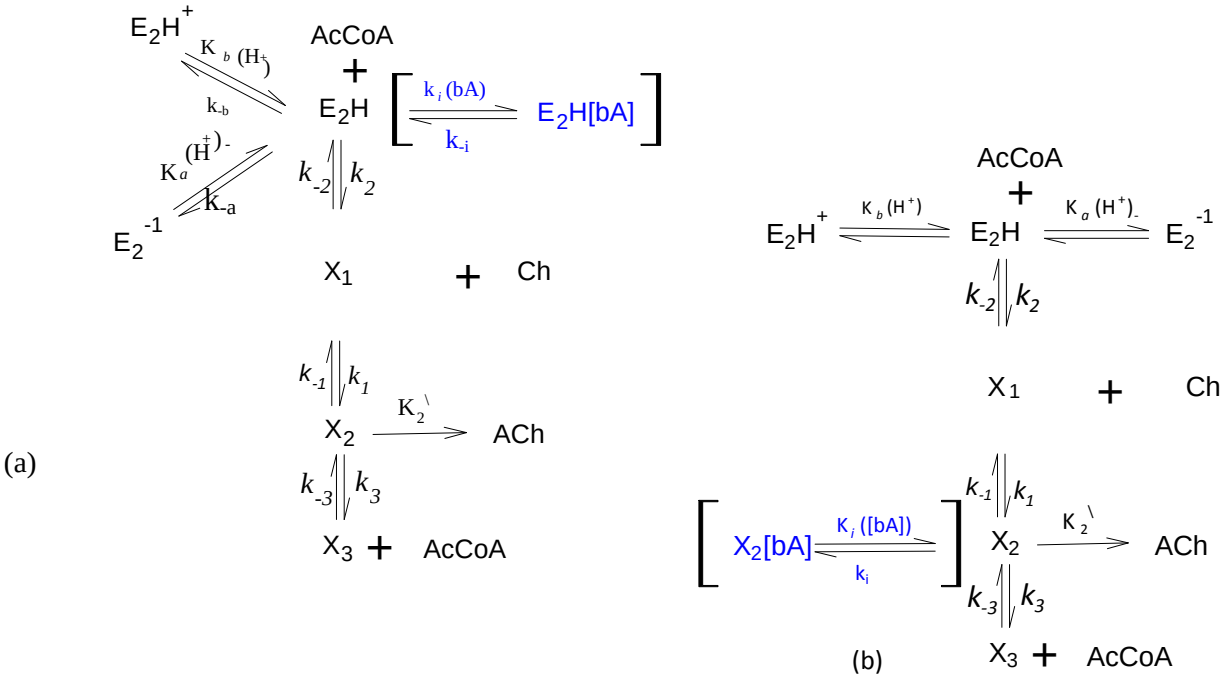

Figure 4.3: Possible competitive inhibition mechanisms for β-amyloid ([bA]) during pH-dependent ChAT synthesis of ACh (areas of inhibition are displayed in square brackets). The reaction route occurs in the vertical direction. E_2H is the active form of the enzyme; E_2H^+ and E_2^{-1} are the protonated and de-protonated inactive forms. X_1, X_2 and X_3 are enzyme intermediate complexes. a) β- -amyloid competitively binds to active enzyme complex E_2H; b) β- -amyloid competitively binds to enzyme intermediate X_2.

Table 4.1: Dimensionless forms of the ordinary differential equations of ChAT inhibition by β-amyloid aggregates

Item	Compartment	Differential equation
Hydrogen protons	1	$\frac{dh_{(1)}}{dT} = h_f - \gamma_1 \left(\frac{1}{h_f}\right) - \alpha_H \left(h_{(1)} - h_{(2)}\right) + \alpha_{OH}\gamma_1 \left(\frac{1}{h_{(1)}} - \frac{1}{h_{(2)}}\right)$
	2	$\frac{dh_{(2)}}{dT} = V_R(\alpha_H \left(h_{(1)} - h_{(2)}\right) - \alpha_{OH}\gamma_1 \left(\frac{1}{h_{(1)}} - \frac{1}{h_{(2)}}\right) - \left(h_{(2)} - \frac{\gamma_1}{h(2)}\right) + \frac{B_2}{k_{h1}} r(2))$
Acetylcholine	1	$\frac{ds_{1(1)}}{dT} = s_{1f} - \alpha_{s1}\left(s_{1(1)} - s_{1(2)}\right) + \frac{B_1 r(1)}{K_{s1}} - K_{bA1}\, s_{1(1)}\, bA$
	2	$\frac{ds_{1(2)}}{dT} = V_R(\alpha_{S_1}\left(s_{1(1)} - s_{1(2)}\right) - s_{1(2)} - \frac{B_2\, r(2)}{K_{s1}})$
Choline	1	$\frac{ds_{2(1)}}{dT} = s_{2f} + R * s_{2(2)} - \alpha_{S2_1}\left(s_{2(1)} - s_{2(2)}\right) - \frac{B_1}{S_{2refernce}} r(1)$
	2	$\frac{ds_{2(2)}}{dT} = V_R(\alpha_{S2}\left(s_{2(1)} - s_{2(2)}\right) - (1+R) * s_{2(2)} + \frac{B_2}{S_{2reference}} r(2))$
Acetate	1	$\frac{ds_{3(1)}}{dT} = s_{3f} - \alpha_{S3}\left(s_{3(1)} - s_{3(2)}\right) - \frac{B_1}{S_{3refernce}} r(1)$
	2	$\frac{ds_{3(2)}}{dT} = V_R(\alpha_{S3}\left(s_{3(1)} - s_{3(2)}\right) - s_{3(2)} + \frac{B_2}{S_{3refernce}} r(2))$
β- amyloid aggregates	1	$\frac{dbA}{dT} = K_{L_2} - K_{L_3}\, s_{1(1)} - K_{L_4}\, bA$
Rate of synthesis ($r_{(1)}$)	1	$r_1 = \frac{\theta_1 s_{21} s_{31}}{\left(\theta_2 / h_1 (h_1 + 1 + \delta h_1^2)(1 + K_{I1}\, bA) + \theta_3 s_{31} + \theta_4 s_{21} + \theta_5 s_{21} s_{31}\right)}$
Rate of hydrolysis ($r_{(2)}$)	2	$r(_2) = \frac{s_{12}}{s_{12} + 1/h_2 (h_2 + 1 + \delta h_2^2) + \alpha s_{12}^2}$

Table 4.2: Values of the kinetic parameters

Parameter	Value	Reference
θ_1	5.2(0.1)	Hersh & Peet (1977)
θ_2	12	Hersh & Peet (1977)
θ_3	1000	Hersh & Peet (1977)
θ_4	5	Hersh & Peet (1977)
θ_5	1	Hersh & Peet (1977)
α	0.5	Garhyan et al., (2006); Ibrahim et al., (1997); Elnashaie et al., (1983b), (1984), and (1995)
δ	1	Garhyan et al., (2006); Ibrahim et al., (1997); Elnashaie et al., (1983b), (1984), and (1995)
$K_a(k_h)$	$1.066*10^{-6}$ kMole/m^3(µMole/mm^3)	Garhyan et al., (2006); Ibrahim et al., (1997); Elnashaie et al., (1983b), (1984), and (1995)
K_{s1}	50.33 µMole/l	Garhyan et al., (2006); Ibrahim et al., (1997); Elnashaie et al., (1983b), (1984), and (1995)
S_{2ref}	100 µMole/l	Guyton and Hall, (2000)
S_{3ref}	1 µMole/l	Guyton Hall, (2000)
B_1	5.033×10^{-5} kMole/m^3(µMole/mm^3)	Garhyan et al., (2006)
B_2	5.033×10^{-5} kMole/m^3(µMole/mm^3)	Garhyan et al., (2006)
α_{H^+}	2.25	Elnashaie et al., (1984)
α_{OH^-}	0.5	Elnashaie et al., (1984)
α_{S_1}	1.5	Elnashaie et al., (1984)
α_{S_2}	1.5	Elnashaie et al., (1984)
α_{S_3}	1	Elnashaie et al., (1984)
V_R	1.2	Elnashaie et al., (1984)
pH_f	8.2	Guyton, 2000
s_{1f}	15	Garhyan et al., (2006)
s_{2f}	1.15	Garhyan et al., (2006)

s_{3f}	3.9	Garhyan et al., (2006)
γ_1	0.01	Garhyan et al., (2006), Elnashaie et al., 1983a; Elnashaie et al., 1983b; Elnashaie et al., 1984; Elnashaie et al., 1995; Ibrahim et al., 1997)
R	0.8	Tucek (1978)
K_{bAref}	20 nM/h	Ehrenstein et al., (1997)
K_{L2}	assumed	
K_{L1}	$3*K_{L2}$	Assumed
K_{L3}	$0.035K_{L2}$	Assumed
K_{L4}	$0.176K_{L3}$;	Assumed
K_{I1}	10.015	Assumed
K_{bA1}	0.05	Assumed
T_{ref}	0.1 h	Assumed
BA_{ref}	20 nM/l	Kar et al., (2008)

4.3.2 Results of Kinetic Mechanism 1

Based on the first kinetic mechanism of β-amyloid-ChAT competitive inhibition shown in Figure 4.3(a) and the derived ACh synthesis rate equation r_1 equation (4.11), the dynamic behavior of 2E2C model is investigated at different rates of β-amyloid production from APP (K_{L2}) as explained below.

4.3.2.1) β-Amyloid Generation

Figure 4.4 shows the dynamic behavior of β-amyloid concentrations. It is observed that at K_{L2} = 0, no β-amyloid is produced. However, when K_{L2} increases to 0.5 (corresponding to 10 nM), the concentration of generated β-amyloid increases in the period 0-150 (corresponding to (0-15hr) to reach the plateau at 9.75 (corresponding to 185 nM). However, when K_{L2} = 2.5 (corresponding to 50 nM), the produced β- amyloid increases rapidly to reach the plateau at the previous

concentrations which is 185 nM but through a shorter time which is 15 (corresponding to 1.5 hr) and remains constant until the end of the incubation period which is 30 (corresponding to 30 hr). When K_{L2} increases to reach the maximum value which is 25 (corresponding to 500 nM), the generated bA increases with a rate faster than the previous rates at K_{l2}=0.5 and 0.75 to reach the plateau in a period of 5 (corresponding to 0.5 hr only).

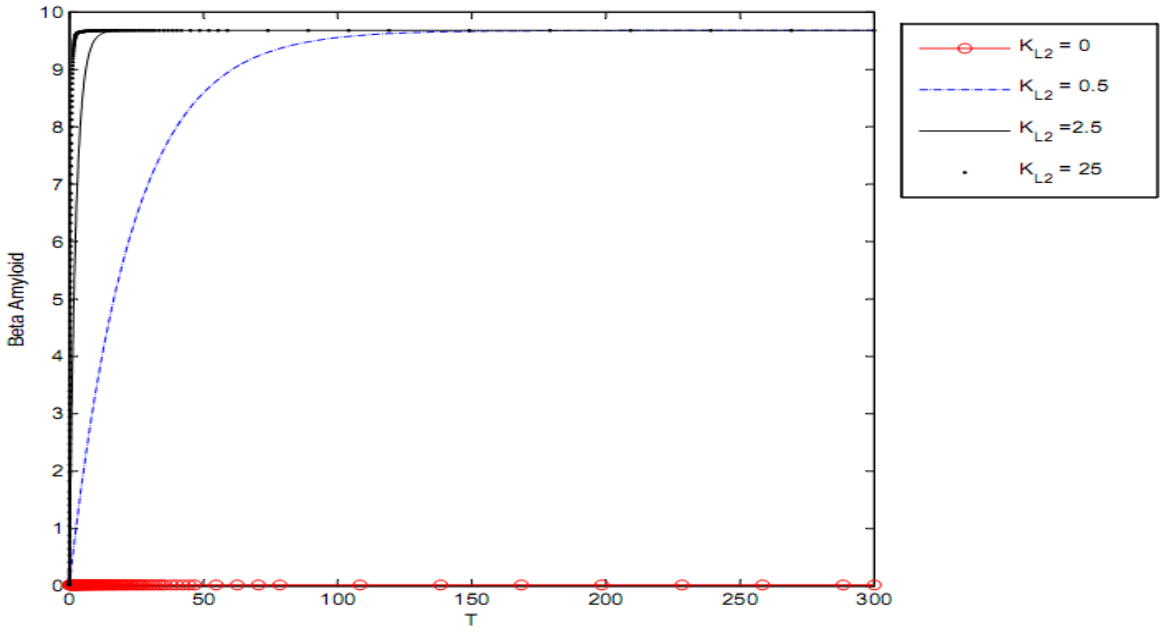

Figure 4.4: Time course of β-amyloid at different K_{L2} according to kinetic mechanism 1

4.3.2.2 Rate of ACh synthesis and hydrolysis

Figure 4.5 (a) shows the dynamics behavior of ACh synthesis (Rate 1) catalyzed by the enzyme ChAT. It is observed that rate 1 reaches steady state at a high value which is 0.01375 at K_{L2} = 0 where no β-amyloid is produced; however, when K_{L2} increases to 0.5, 2.5, and 25, rate 1 decreases significantly to reach a steady state around 0.0104. It is observed that the final value of Rate 1 at the end of the period (0-300) corresponding to (0-30) hr does not change with K_{L2} reflecting the neglected effect of the generated β-amyloid in this period. The rate of ACh synthesis is lowered by 25% through the effect of β-amyloid on ChAT. Figure 4.5 (b) shows that

there is no effect of K_{L2} on the rate of hydrolysis (rate 2) indicating that rate 2 is independent of the change of K_{L2} in the kinetic mechanism.

These results are compatible with the experimental results obtained by Nunes-Tavare et al., (2012) who showed that β-amyloid peptides could bind to a significant portion of cholinergic neurons and reduce ChAT activity. It is observed that the reduction in Rate 1 decreases from 0.0105 to 0.000125 which refers to a reduction in ChAT activity of 99.7% with an increase in K_{L2} from 0 to 25 (corresponding to 500 nM). In addition, Nunes-Tavares et al., (2012) showed that β-amyloid peptides have a very limited effect on the activity of AChE in comparison to ChAT activity which is in agreement with our results shown in Figures 4.5 (a) and (b).

4.3.2.3 ACh concentrations in compartments 1 and 2

One of the main physiological symptoms of AD is a reduction of ACh production in cholinergic neurons (Blusztajn, 2000). Therefore, the first step towards validating β-amyloid inhibition model is to see whether this physiological effect is reflected in the simulation results or not. As shown in Figure 4.6, it is an evidence of decreasing ACh concentration in compartment 1 (ACh 1) level in compartment1. Figure 4.6 (a) shows the dynamics of ACh1 which reaches steady state at a high value at K_{L2} = 0 where ACh1 settles down around 4.4 (corresponding to 221.5 μM) where no β-amyloid is produced, but when K_{L2} increases to 0.5, 2.5, and 25, it is observed that ACh1 decreases slightly to reach the steady state at 4.28 (corresponding to 215 μM). It is noted that the final value of rate at the end of the period (0-300) corresponding to (0-30 hr) does not change with K_{L2} reflecting the neglected effect of the generated β-amyloid in this period.

These results are compatible with experimental results obtained by Kar et al., (1998) who indicated that the decrease in ChAT activity leads to a reduction in ACh generated in the presynaptic neurons. Furthermore, Zheng et al., (2002) indicated that exposure of culture neurons to β-amyloid leads to decrease in ChAT activity. However, Pedersen and Blusztajn (1997) showed that only acetyl-coA not ChAT activity is affected negatively when exposed to β-amyloid leading to reduction of generated ACh similarly to the rate of ACh hydrolysis shown in Figure 4.5 (b) which exhibits no effect of K_{L2} where ACh2 does not change with any change in $K_{L2.}$ The absence of any observable effects in ACh_2 is mostly likely due to the relative magnitude

of the ACh synthesis rate (r_1) compared to the magnitude of other transport phenomena within the model. Focusing on the kinetics in compartment 2, ACh2 level is governed mainly by two processes; membrane diffusion of ACh from compartment 1 and the rate of ACh degradation (r_2)

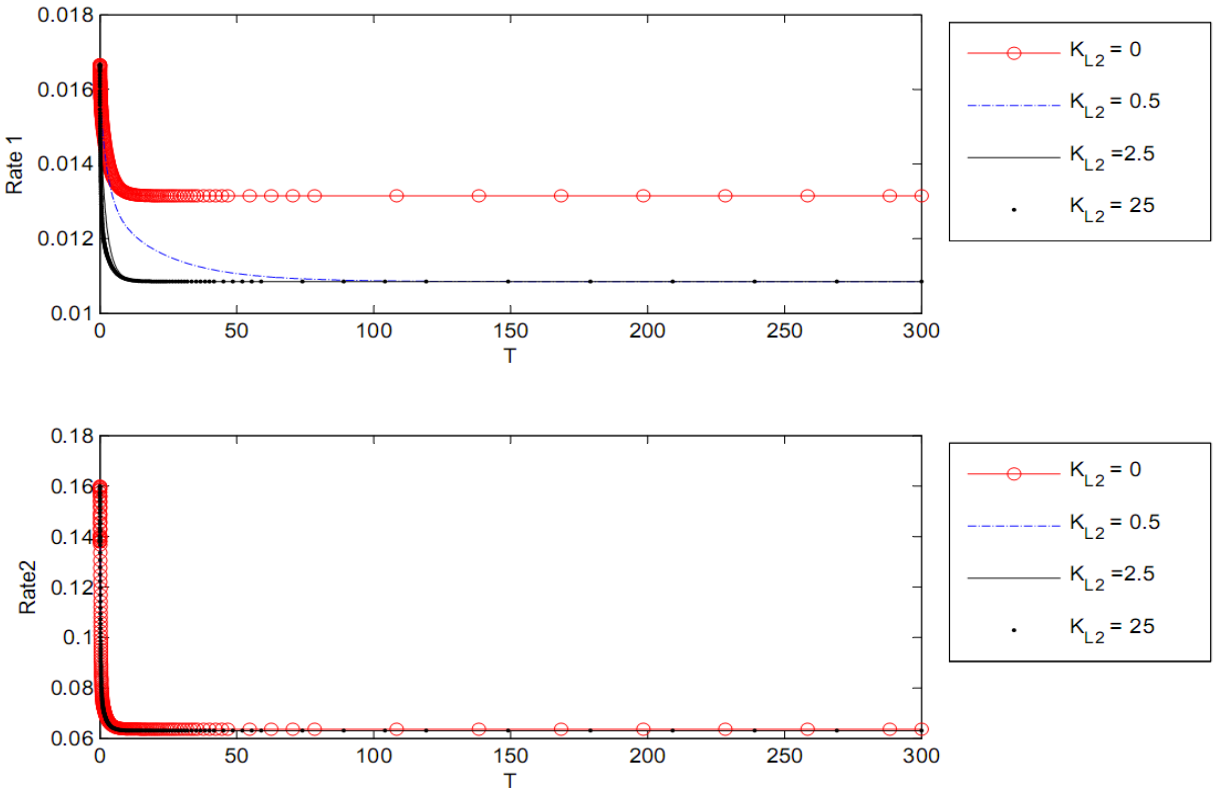

Figure 4.5: Time course according to kinetic mechanism 1 of: a) Rate of ACh Synthesis (Rate 1), b) Rate of ACh hydrolysis (Rate 2) at different K_{L2}

in compartment 2. The transport of ACh into compartment 2 through membrane diffusion is observed to slighly decrease due to reduced ACh1 levels from β-amyloid inhibtion. On the other hand, the rate of ACh break-down is maintained the same. It is expected that the influx of ACh into compartment 2 is approximately an order of magnitude higher than the consumption of ACh (r_2) in that compartment. This means that although the influx of ACh into compartment 2 is limited by β-amyloid inhibition, the fact that r_2 is so small in comparison infers that the overall level of ACh_2 will not be affected much.

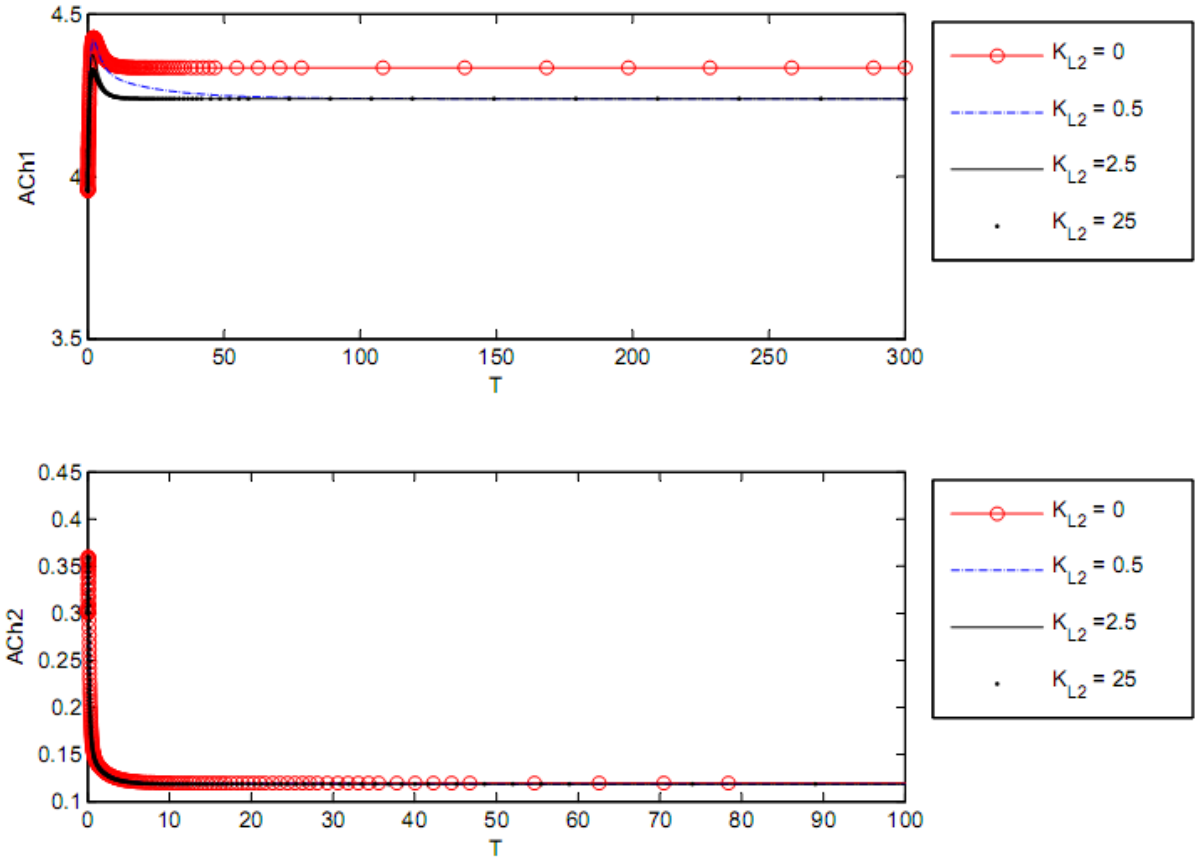

Figure 4.6: Time course according to kinetic mechanism 1 of: a) ACh concentration in compartment 1 (ACh 1), b) ACh concentration in compartment 2 (ACh 2) at different K_{L2} values

4. 3.2.4) Choline concentrations in compartments 1 and 2

Figure 4.7 (a) and Figure 4.7 (b) show the dynamic response for choline concentrations in compartment 1 (Ch1) and 2 (Ch2) respectively. It is observed that there is no effect of K_{L2} on the behavior of Ch1. This reflects that the uptake of choline to compartment 1 is not affected by any change in β-amyloid through the interaction between ChAT and β-amyloid via the relevant kinetic mechanism. This result is compatible with the experimental results obtained by Nunes et al., (2012) who showed that there is no effect of β-amyloid oligomers on choline uptake. Figure

4.7 (b) shows that K_{L2} does not affect Ch2. In other words ChAT inhibition β-amyloid in compartment 1 does not affect AChE activity in compartment 2.

4. 3.2.5) Acetate concentrations in compartments 1 and 2

Figure 4.8 shows the dynamic response for acetate concentrations in compartments 1 (Ac1) and 2 (Ac2). Figure 4.8 (a) shows that Ac1 increases from 8.25 at the beginning of the period then it reaches the steady state value which is 9.51 (corresponding to 9.51 μM) when K_{L2} increases to 0.5 , 0.75, and 1. Ac_1 increases slightly due to ChAT inhibition and accumulates due to low consumption of acetates by ChAT for synthesizing ACh. However, K_{L2} does not affect Ac_1 since the steady state behavior of Ac1 is obtained when K_{L2} is higher than zero. Figure 4.8 (b) shows that there is no influence of K_{L2} on Ac2 which is the same as Ch2 and Rate 2 reflecting the negligible effect of K_{L2} on compartment 2 through the proposed kinetic mechanism 1.

4. 3.2.6) pH in compartments 1 and 2

Figure 4.9 shows the dynamic response of pH in both compartments (pH_1) and 2 (pH_2). Figure 4.9 (a) shows that pH_1 is affected very slightly with changes in K_{L2} indicating that the inhibition of ChAT activity with the proposed kinetic mechanism 1 has a low effect on changing pH_1. Figure 4.8 (b) shows a negligible effect of K_{L2} on pH_2 which is the same as the behaviors of Ch2 and Rate 2 explained previously. According to kinetic mechanism 1, β-amyloid promotes a major reduction in ChAT activity while all other components in ACh cholinergic system remain unaffected.

The effect of β-amyloid inhibition on the remaining variables (pH and Ac) is observed to be negligible within the time frame studied. One likely explanation is that the feed concentrations of these chemical components into the 2E2C system are all much larger in magnitude compared to that of ACh. While they all have an indirect dependence on the activity of ChAT through changes in ACh1 concentration, the reduction in ACh is too small to produce a significant effect on the concentration of these components.

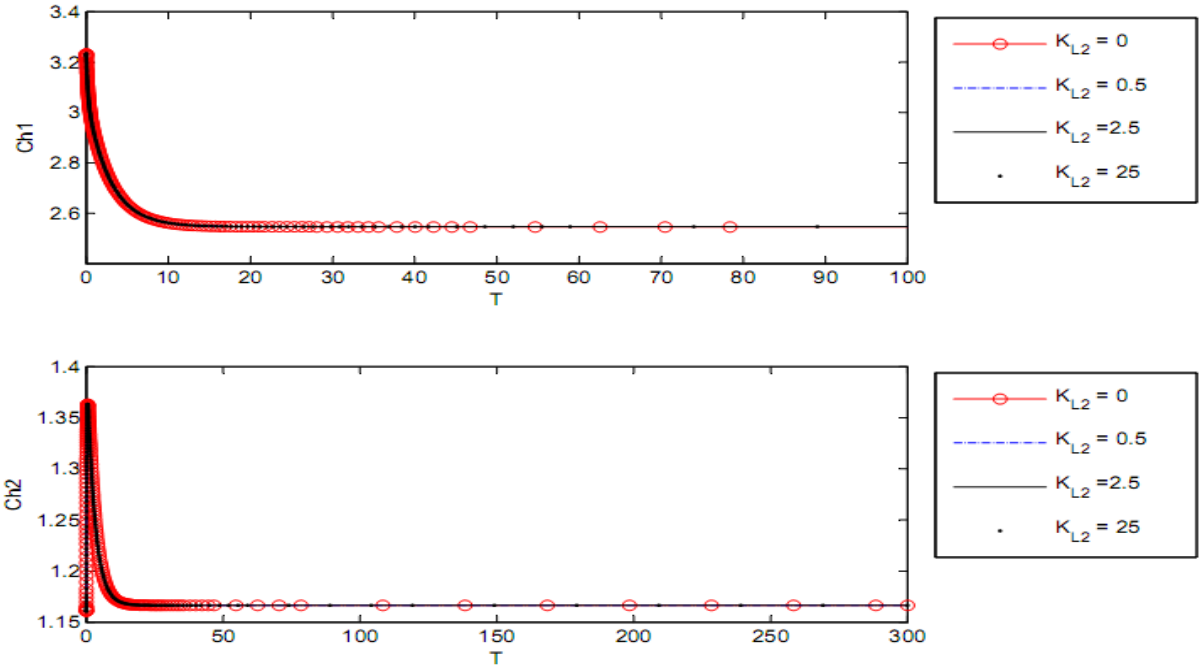

Figure 4.7: Time course according to kinetic mechanism 1 of: a) Choline concentration in compartment 1 (Ch 1), b) Choline concentration in compartment 2 (Ch 2) at different K_{L2} values

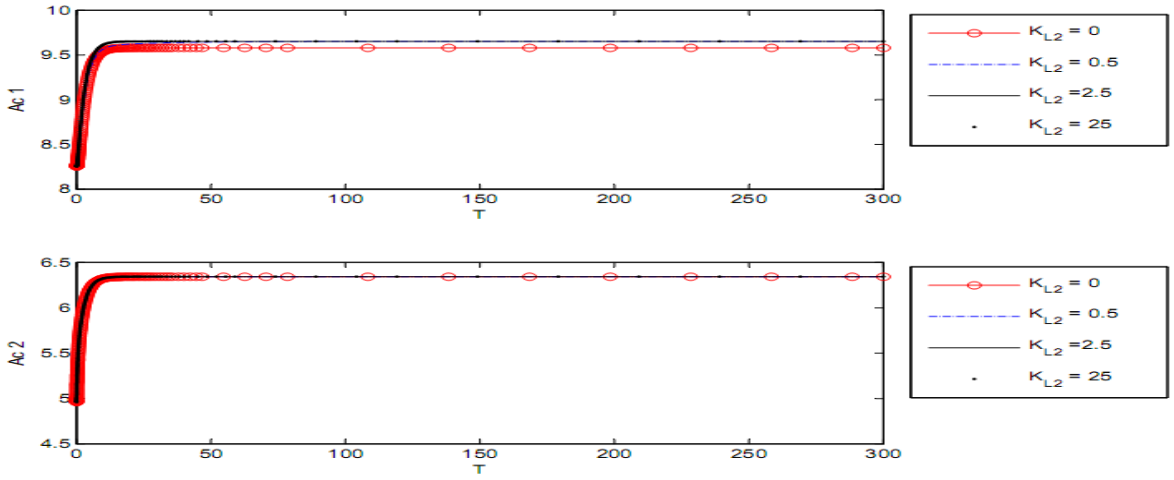

Figure 4.8: Time course according to kinetic mechanism 1 of: a) Acetate concentration in compartment 1 (Ac 1), b) Acetate concentration in compartment 2 (Ac 2) at different K_{L2} values

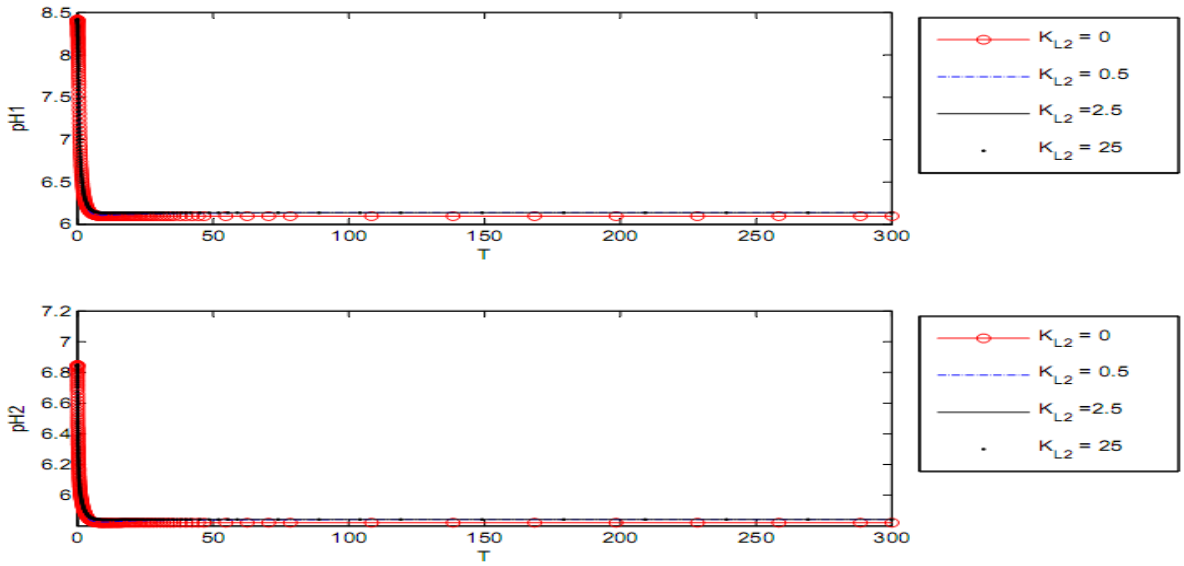

Figure 4.9: Time course according to kinetic mechanism 1 of: a) pH in compartment 1 (pH_1), b) pH in compartment 2 (pH_2) at different K_{L2} values

4.4 Kinetic Mechanism 2: Ccompetitive inhibition of β-amyloid with enzyme intermediate complex X2

4.4.1 Formulation of kinetic mechanism 2

In this kinetic mechanism, there is a competitive inhibition of β-amyloid with enzyme intermediate complex X_2. during ACh synthesis as shown in (Figure 4.3 (b)), the modified rate equation can be derived as shown below.

X_1 and X_2 are related through the following expressions:

$$X_1(Ch)k_1 = X_2k_{-1} \text{ or } X_1 = \frac{K_1}{Ch}X_2 \quad (4.12)$$

Where $K_1 = k_{-1}/k_1$

By the assumption of rapid equilibrium, E_2H and X_1 can be related by:

$$k_2(AcCoA)E_2H = k_{-2}X_1 \text{ or } E_2H = \frac{K_2X_1}{(AcCoA)} = \frac{K_2K_1}{(AcCoA)(Ch)}X_2 \quad (4.13)$$

Where $K_2 = k_{-2} / k_2$

From the ionization of E2H

$$E_2H(H^+)k_{-b} = E_2H^+ \; k_b \text{ or} \qquad E_2H^+ = \frac{(E_2H)\left(H^+\right)}{K_b} \tag{4.14}$$

From the deionization of E2H

$$E_2^- \; \left(H^+\right)k_a = E2H\, k_{-a} \text{ or} \qquad E_2^- = \frac{K_a(E_2H)}{\left(H^+\right)} \tag{4.15}$$

From equations (15), (16) and (17) we get:

$$E_{t2} = E_2H + E_2^- + E2H^+ = \frac{K_2K_1}{(AcCoA)(Ch)}\left(1 + \frac{K_a}{H^+} + \frac{H^+}{K_b}\right)X_2 \tag{4.16}$$

X_2 and X_3 are related by:

$$X_3 = \frac{X_2}{K_3(AcCoA)} \tag{4.17}$$

Where $K_3 = k_{-3} / k_3$

Also, $k_i X_2(bA) = k_{-i} X_2[bA]$ or $X_2[bA] = K_i X_2(bA)$ (4.18)

Where $K_i = k_i / k_{-i}$

Since $E_t = E_{t2} + X_1 + X_2 + X_3 + X_2[bA]$ we get:

$$E_t = X_2\left(\frac{K_2K_1}{AcCoA(Ch)}\left(1 + \frac{K_a}{H_1^+} + \frac{H_1^+}{K_b}\right) + \frac{K_1}{Ch} + 1 + \frac{1}{K_3(AcCoA)} + (bA)K_i\right) \text{ or}$$

$$X_2 = \frac{E_t(Ch)(AcCoA)}{\left(K_2K_1\left(1 + \frac{K_a}{H_1^+} + \frac{H_1^+}{K_b}\right) + K_1(AcCoA) + Ch(AcCoA) + \frac{Ch}{K_3} + (bA)K_iCh(AcCoA)\right)} \tag{4.19}$$

Since $R_1 = K_2^{\backslash} X_2$, therefore

$$r_1 = \frac{\theta_1 s_{21} s_{31}}{\left(\theta_2 / h_1(h_1 + 1 + \delta h_1^2) + \theta_3 s_{31} + \theta_4 s_{21} + \theta_5 s_{21} s_{31}(1 + K_{I1} bA)\right)} \tag{4.20}$$

Where bA is the concentration of generated β-amyloid in the dimensionless form and K_{I1} is the dimensionless equilibrium rate constant for the second proposed inhibition mechanism shown in

Figure 4.3 (b). In the next section, the results presented are based on the previous equation of r_1 replacing that r_1 in Table 4.1 while all other equations remain the same as the kinetic parameter values in Table 4.2.

4.4.2 Results of Kinetic Mechanism 2

Incorporating the rate of ChAT synthesis r_1 (equation 4.20) inhibited by β-amyloid peptides derived from the kinetic mechanism (2) into the 9th dimension 2E2C model shown in Table 4.1, the effect of β-amyloid peptides on ACh neurocycle is investigated to check the feasibility of kinetic mechanisms as a descriptor for the interaction between ChAT activity and β-amyloid peptides.

4.4.2.1) β. Amyloid Generation

Figure 4.10 shows the dynamic behavior of β-amyloid produced in compartment 1. It is clear that at $K_{L2} = 0$ where there is no inlet β-amyloid, there is no generation of β-amyloid. However, when K_{L2} increases to 0.5 (corresponding to 10 nM), β-amyloid is produced to reach 10 (corresponding to 200 nM) after a time of 150 (corresponding to 15 hr), then it becomes constant where there is no more generation until the end of the incubation period (300) corresponding to 30 hr. In addition, Figure 4.10 shows that when K_{L2} increases to 2.5 (corresponding to 50 nM), β-amyloid is generated faster than that at $K_{L2} = 0.5$ where β-amyloid reaches the stationery steady state after 15 (corresponding to 1.5 hr) then it does not change until the end of the incubation period. Furthermore, at K_{L2} =25 (corresponding to 500 nM), β-amyloid is produced much faster than before where it reaches the steady state value only after a dimensionless time of 7 (corresponding to 42 minutes). Comparing the dynamic behaviors of β-amyloid in kinetic mechanism 2 and kinetic mechanism 1, it is observed that the final steady state value of kinetic mechanism 2 is higher than that of kinetic mechanism 1. The increase of final β-amyloid might lead to changes in other state variables of the system.

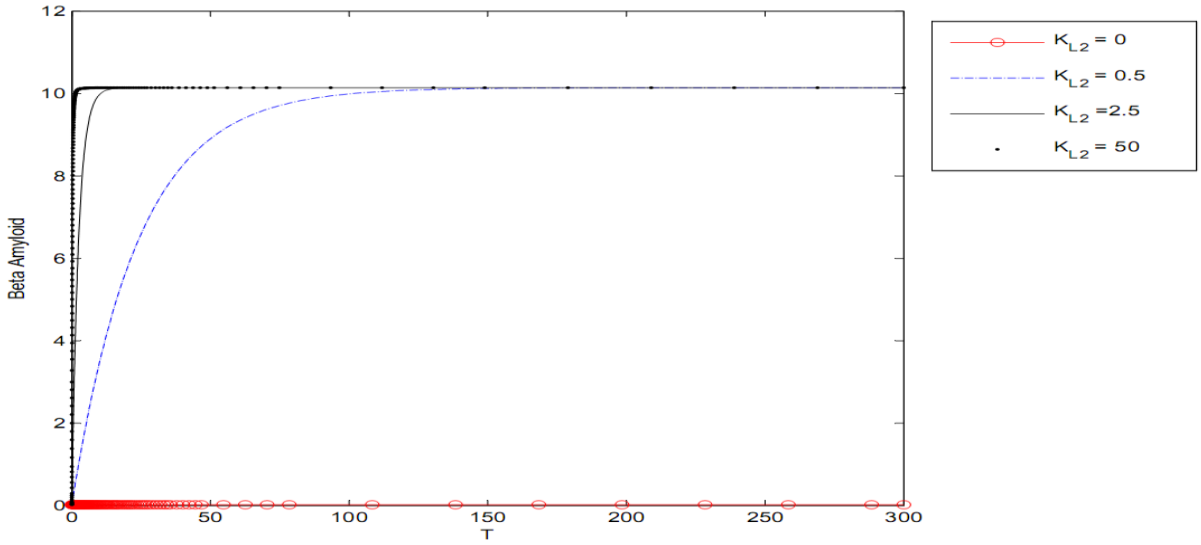

Figure 4.10: Time course of generated β-amyloid at different K_{L2} (according to kinetic mechanism 2)

4.4.2.2) Rates of ACh synthesis and hydrolysis

Figure 4.11 shows the dynamic behavior of rate of ACh synthesis catalyzed by ChAT (Rate1) and rate of ACh hydrolysis catalyzed by AChE (Rate 2). Figure 4.11 (a) shows that Rate1, at no β-amyloid production where $K_{L2} = 0$, decreases from 0.016 at the beginning of process to reach 0.0138 after passing 20 (corresponding to 2 hr), then it becomes constant until the end of the period. However, when ChAT activity is reduced according to kinetic mechanism 2 at $K_{L2} = 0.5$ (corresponding to 10 nM), Rate 1 decreases significantly as shown in Figure 4.11 (a) to reach 0.0103 at the end of the period but it reaches the steady state slower than that at $K_{L2} = 0$ where it takes time of 100 (corresponding to 10 hr) to reach the plateau. Furthermore, when K_{L2} increases to 2.5 and 50 (corresponding to 50 and 1000 nM, respectively) the generated β-amyloid takes the same behavior where both of them decrease with the same rate but faster than that at $K_{L2} = 0.5$. It is observed that the reduction in Rate 1 decreases from 0.01375 to 0.0105 which refers to a reduction in ChAT activity of 24.7% with an increase of K_{L2} from 0 to 25 (corresponding to 500

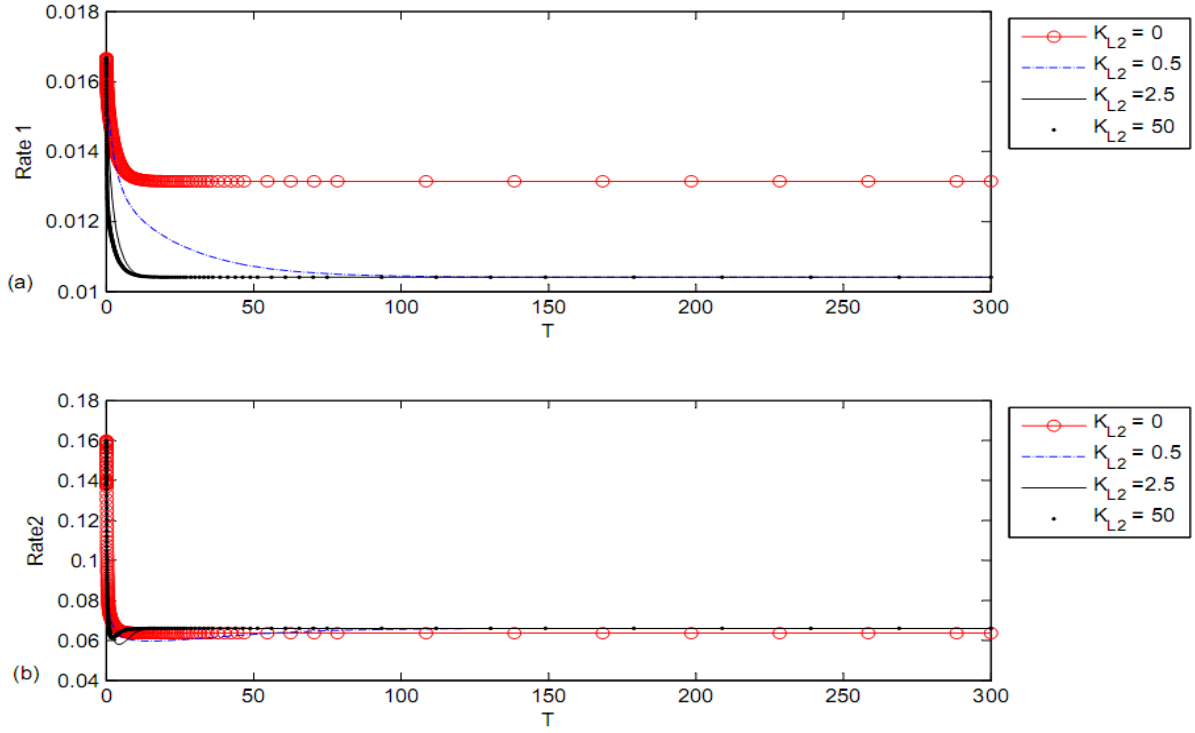

Figure 4.11: Time course of: a) Rate of ACh Synthesis (Rate 1), b) Rate of ACh hydrolysis (Rate 2) at different K_{L2} (according to kinetic mechanism 2)

nM). Figure 4.11 (b) shows that the effect of changing K_{L2} on Rate 2 is negligible according to the kinetic mechanism 2 indicating the same behavior as kinetic mechanism 1 as shown previously in Figure 4.7 (b).

4.4.2.3) ACh concentrations in compartments 1 and 2

Figure 4.12 (a) shows the dynamics of ACh1 with the rate of ChAT activity inhibition r_1 based on kinetic mechanism 2. It is observed that at K_{L2} = 0.5 ACh1 reduces from 4.3 (corresponding to 216.419 µM) at the beginning of β-amyloid incubation to reach to 3.15 (corresponding to 158.5µM) after passing 100 (10 hr) and it keeps at this value until the end of the period which is 300 (corresponding to 30 hr). Comparing ACh1 at K_{L2} = 0.5 to that in the first kinetic mechanism in Figure 4.6 (a), it is observed that the rate of ChAT activity affected by the interaction between competitive inhibitions of β-amyloid with enzyme intermediate complex X_2

in kinetic mechanism 2 leads to a more reduction in ACh_1. At K_{L2} = 2.5 and 50, the reduction of ACh1 is faster than that at K_{L2} = 0.5 where it occurs after passing 15 and 10 (corresponding to 1.5 and 1 hr respectively), then ACh1 remains at steady state around 3.15 (corresponding to 158.5μM) indicating that inhibition of ChAT activity by β-amyloid reached its maximum limit. Figure 4.12 (b) shows that ACh2 is not affected significantly with the change of K_{L2}; which is the same as in kinetic mechanism 1 as shown in Figure 4.6(b).

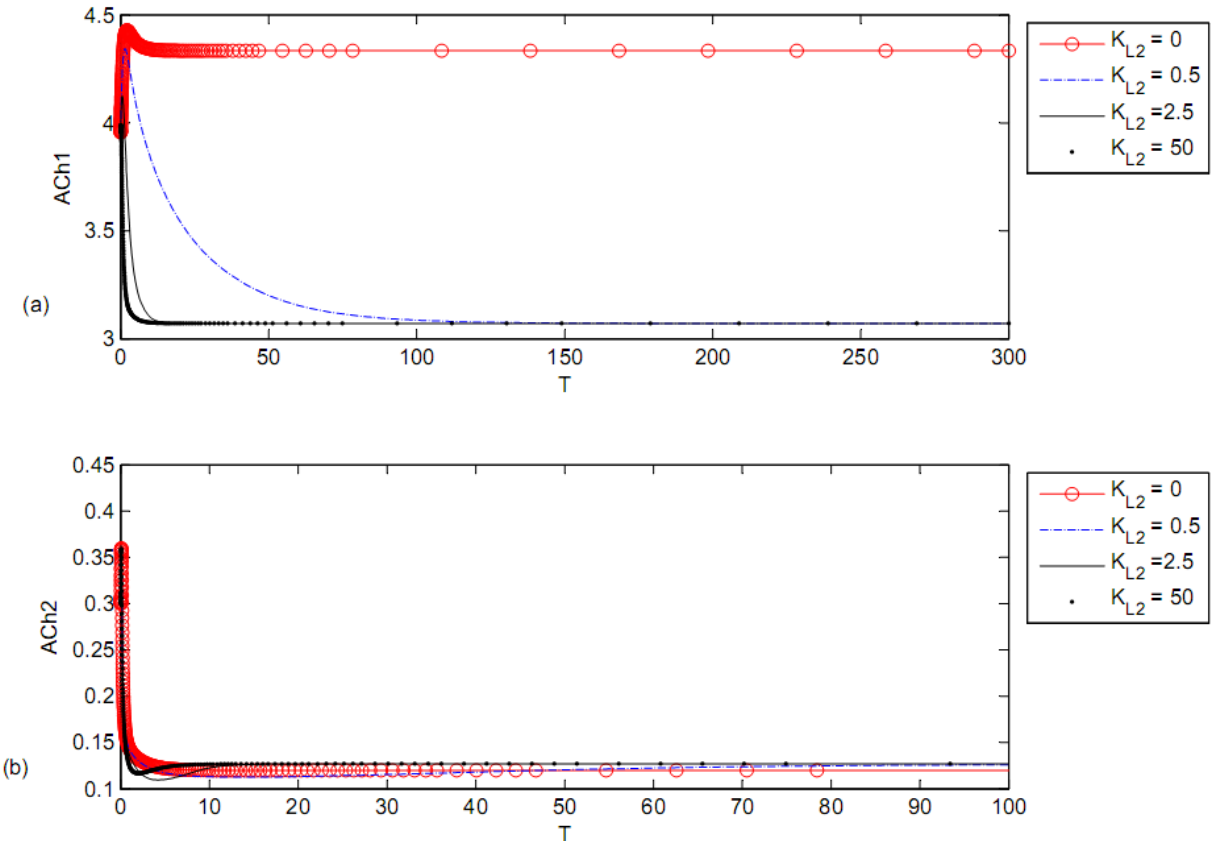

Figure 4.12: Time course of: a) ACh concentration in compartment 1 (ACh 1), b) ACh concentration in compartment 2 (ACh 2) at different K_{L2} values (according to kinetic mechanism 2)

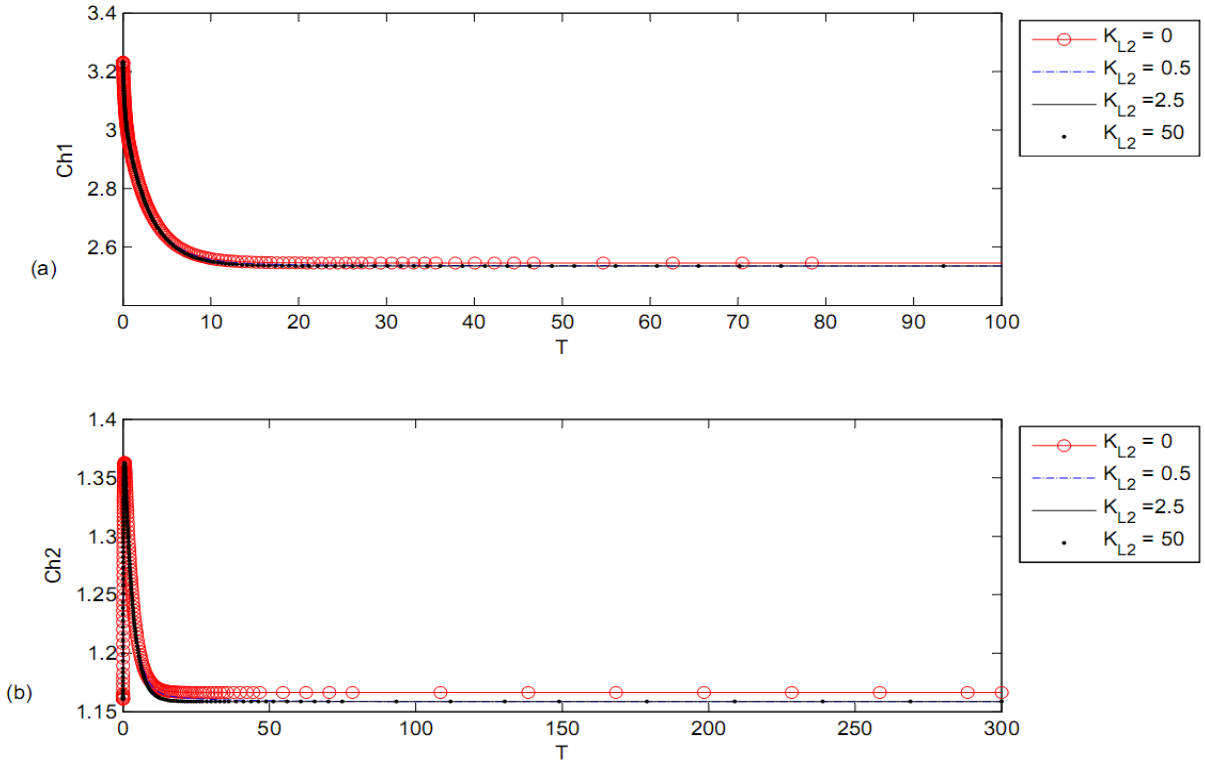

Figure 4.13: Time course of: a) Choline concentration in compartment 1 (Ch 1),
b) Choline concentration in compartment 2 (Ch 2) at different K_{L2} values (according to kinetic mechanism 2)

4.4.2.4) Choline concentrations in compartments 1 and 2

Figure 4.13 (a) and Figure 4.13 (b) illustrate the time course of choline concentrations in compartments 1 and 2 respectively. It is observed that K_{L2} has no effect on both Ch1 and Ch2 indicating that the inhibition of ChAT activity by β-amyloid does not affect choline uptake in compartment 1 and choline produced from hydrolysis in compartment 2 following the same behavior in kinetic mechanism 1 as shown previously in Figure 4.7 (a) and (b).

4.4.2.5) Acetate concentrations in compartments 1 and 2

Figure 4.14 (a) shows the effect of changing K_{L2} in terms of the inhibition of ChAT activity according to kinetic mechanisms 2 on intracellular concentration of acetate. At K_{L2} = 0, Ac1 increases through the first 30 (3 hr) and reaches steady state around 9.52 (corresponding to 9.52 μM) indicating that inhibition of ChAT activity by β-amyloid reached its maximum limit.

However, after incorporating β-amyloid generation in terms of K_{L2} = 0.5, 2.5, and 50 (corresponding to 10, 25, 1000 nM), there is a significant decrease in Ac1, where the final steady state concentration of Ac1 is around 8.95 (corresponding to 8.95 µM). It is clear that competitive inhibition of β-amyloid with enzyme intermediate complex X_2 in kinetic mechanism 2 has moreeffect on Ac1 than that in kinetic mechanism 1. Figure 4.14 (b) shows that Ac2 is affected clearly with any increase in inlet β- amyloid concentrations (K_{L2}) where at K_{L2} = 0, the steady state of Ac2 = 6.4 (corresponding to 6.4 µM) while with the increase of K_{L2} to 0.5, 2.5 and 50, the steady state value of Ac2 will be around 5.6 and not varying with changing K_{L2} as illustrated in Figure 4.14 (b). This indicates again that inhibition of ChAT activity by β-amyloid reaches the maximum effect.

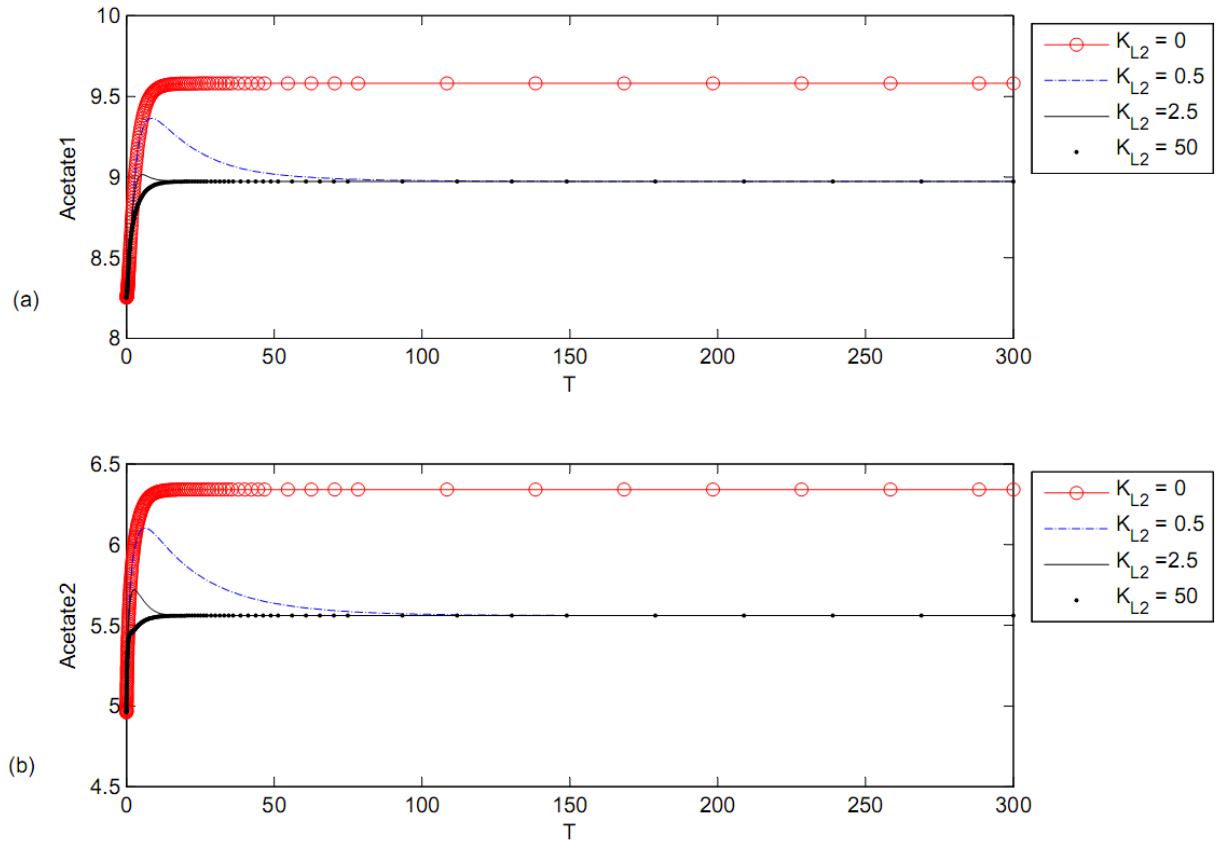

Figure 4.14: Time course according to kinetic mechanism 2 of: a) Acetate concentration in compartment 1 (Ac1), b) Acetate concentration in compartment 2 (Ac 2) at different K_{L2} values

4.4.2.6) pH in compartments 1 and 2

Figure 4.15 (a) shows the dynamics of pH_1 with changing K_{L2}. It is observed that at $K_{L2} = 0$, pH_1 decreases from 8.5 at the beginning to settle down around 6.2 at the end of the period. However, as K_{L2} increases to 0.5, 2.5, and 50, pH_1 decreases clearly to settle down around 7.75 indicating that the inhibition of ChAT activity by β-amyloid reaches the maximum limit. It is concluded that the rate of transport of hydrogen protons from compartment 1 to compartment 2 is still higher than the rate of accumulation of hydrogen protons due to the inhibition of ChAT catalytic effect according to kinetic mechanism 2. Figure 4.15 (b) shows the dynamic behavior of pH_2 where pH_2 increases from 5.85 at $KL_2 = 0$ to the steady state value of 6.23 with increasing K_{L2} from 0.5 to 50.

It clear that kinetic mechanism 2 in terms of competitive inhibition of β-amyloid with enzyme intermediate complex X_2 has more effect on pH_1 and pH_2 than that in kinetic mechanism 1. It is observed that after time 100 (corresponding to 10 hr), there is no effect for any further change of β-amyloid production rate (K_{L2} from 0.5 to 25), where all state variables reach the same steady state values indicating that the activity of ChAT is fully inhibited. These results are compatible with that obtained by Nunes-Tavares et al., 2012) who showed that there is no significant effect for any further β-amyloid concentration more than 100 nM. According to kinetic mechanism 2, β-amyloid peptides promote a major reduction in ChAT function, ACh1, acetate 1 and acetate 2, pH_1, and pH_2 while all other components in ACh cholinergic system remain unaffected.

4.5 Kinetic Mechanism 3: Non-competitive inhibition of β-amyloid with all species ChAT

4.5.1 Formulation of kinetic mechanism 3

β-amyloid inhibitor behaves as a non-competitive inhibitor and could attack all ChAT species in the synthesis reaction in compartment 1 with the same affinity if the reaction follows either a rapid equilibrium random mechanism or an ordered sequential (Cheng and Prusoff, 1973). Figure 4.16 shows the kinetic mechanism 3 for the synthesis reaction catalyzed by ChAT

where all species in ChAT can be exposed to β-amyloid peptide, where E = ChAT, I = β-amyloid, A = Choline, B = Acetyl-coA. In the same way as the previous kinetic mechanisms 1 and 2 were derived, the final form of the rate of ACh synthesis derived is shown as below:

$$r_1 = \frac{\theta_1 s_{21} s_{31}}{\left(\theta_2 / h_1 (h_1 + 1 + \delta h_1^2) + \theta_3 s_{31} + \theta_4 s_{21} + \theta_5 s_{21} s_{31}\right)\left(1 + K_{I1} bA\right)} \qquad (4.21)$$

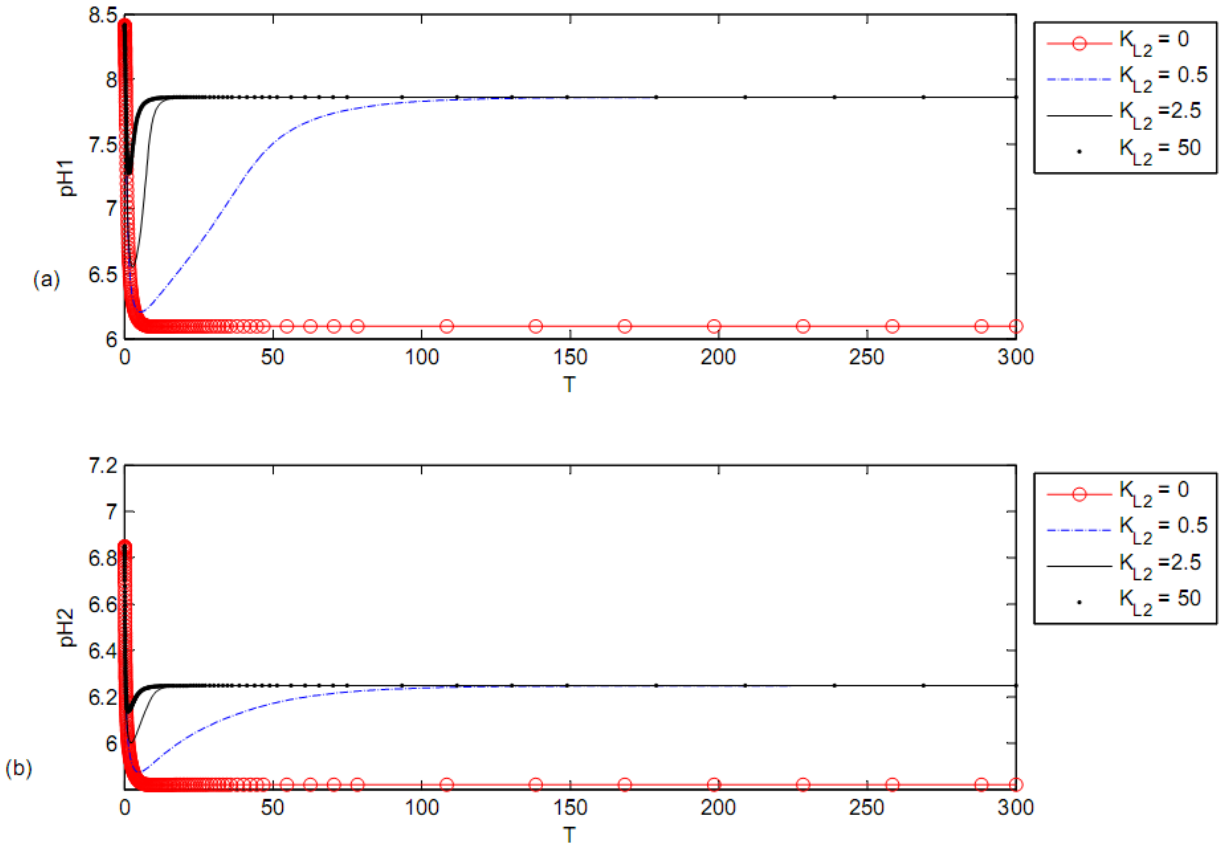

Figure 4.15: Time course according to kinetic mechanism 2 of: a) pH in compartment 1 (pH $_1$), b) pH in compartment 2 (pH $_2$) at different K_{L2} values

By using equation (4.21) for the rate equation r_1 in 2E2C of Table 4.1 and keeping all other equations the same and incorporating K_{I1} into Table 4.2, the effect of β-amyloid peptide as an inhibitor for ChAT activity on 2E2C model can be simulated as discussed in the next section:

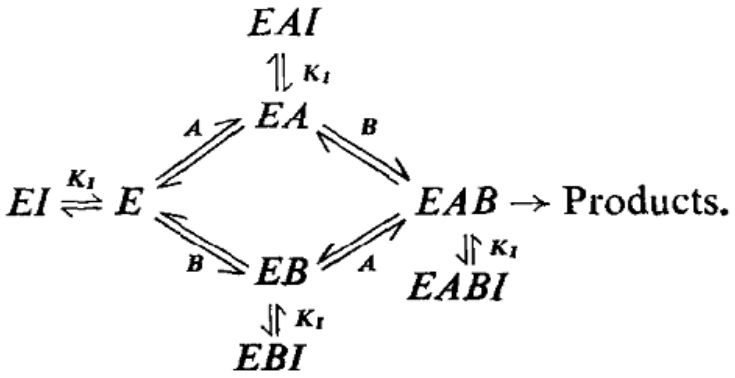

Figure 4.16: Possible non-competitive inhibition mechanisms for β-amyloid during pH-dependent ChAT synthesis of ACh: E = ChAT, I = β-amyloid, A = Choline, B = Acetyl-coA, Products = ACh

4.5.2 Results of Kinetic Mechanism 3

4.5.2.1) β-Amyloid Generation

Figure 4.17 shows the dynamic response at different K_{L2} values. At K_{L2} = 0 where there is a normal ChAT activity without inhibition, it is observed that there is no β-amyloid generated where β-amyloid concentration = 0. At K_{L2} = 0.5, β-amyloid is produced significantly and increases to 10.2 (corresponding to 204 nM) after passing time of 100 (corresponding to 10 hr), where it reaches steady state at this value. At K_{L2} = 25 (corresponding to 500 nM), it is observed that β-amyloid oscillates in a narrow range (10-10.2) corresponding to (200-204 nM). The oscillatory behavior is an interesting phenomenon because it may affect other state variables of the system as will be investigated below.

4.5.2.2) Rate of ACh synthesis and hydrolysis

Figure 4.18 (a) shows the effect of varying inlet β-amyloid K_{L2} on ACh synthesis rate 1 under the condition of ChAT fully inhibited according to equation (21). At normal ChAT synthesis where there is no β-amyloid generation, rate 1 decreases from 0.014 at the beginning to 0.0105 which is the steady state value after passing time 200 (corresponding to 20 hr). However, when K_{L2} increases to 0.5 and 25 (corresponding to 10 and 500 nM), rate 1 decreases from 0.014 at the beginning of β-amyloid incubation to reach a very small value close to zero indicating that ChAT activity is completely inhibited by β-amyloid peptides which attack every species in ChAT enzyme. It is observed that the reduction in Rate 1 decreases from 0.0105 to 0.000125 which refers to a reduction in ChAT activity of 99.7% with increasing K_{L2} from 0 to 25 (corresponding to 500 nM). This result is consistent with the experimental results obtained by Nunes-Tavares et al., 2012) who showed that β-amyloid could inhibit ChAT completely.

Figure 4.18 (b) shows that a very interesting phenomenon which is the oscillatory behavior at a high inlet β-amyloid K_{L2} = 25 where rate 2 oscillates in the range (0.05-0.32). This oscillatory behavior reflects the disturbances occurring in the cholinergic system at which β-amyloid is generated at a high rate as shown in Figure 4.17 and acts severely as an inhibitor ChAT.

4.5.2.3) ACh concentrations in compartments 1 and 2

Figure 4.19 (a) shows that ACh_1 is synthesized with a high rate at K_{L2} = 0 where ACh1 settles down to around 4.35 (corresponding to 219 µM) at the end of the time T = 200 (corresponding to 30 hr). When K_{L2} = 0.5 (corresponding to 10 nM), the levels of ACh_1 decrease to 2.7 (corresponding to 136 µM) after passing T = 100 (corresponding to 10 hr) then ACh1 remains constant at the latter concentration until the end of the incubation period which 30 hr. As K_{L2} increases to 25 (corresponding to 500 nM), the interesting oscillatory phenomenon appears where ACh_1 oscillates in a wide range from 2.6-3.4 corresponding to 131-322 µM. This range shows that the ACh_1 moves in a disturbance and could be related to irregular behavior leading to impaired memory. Figure 4.19 (b) shows that at the highest value of K_{L2} =25, ACh_2 fluctuates in a wide range (0.1-1.38) corresponding to (5-69.5) µM. The latter fluctuation shows the irregular behavior of ACh_2 released in compartment 2 and could lead to unreasonable electrical and

chemical messages to the postsynaptic receptors and finally dysfunctions of the memory. The latter disturbances show the harmful effect of high concentration β-amyloid and the consequences of inhibition action with all species in ChAT.

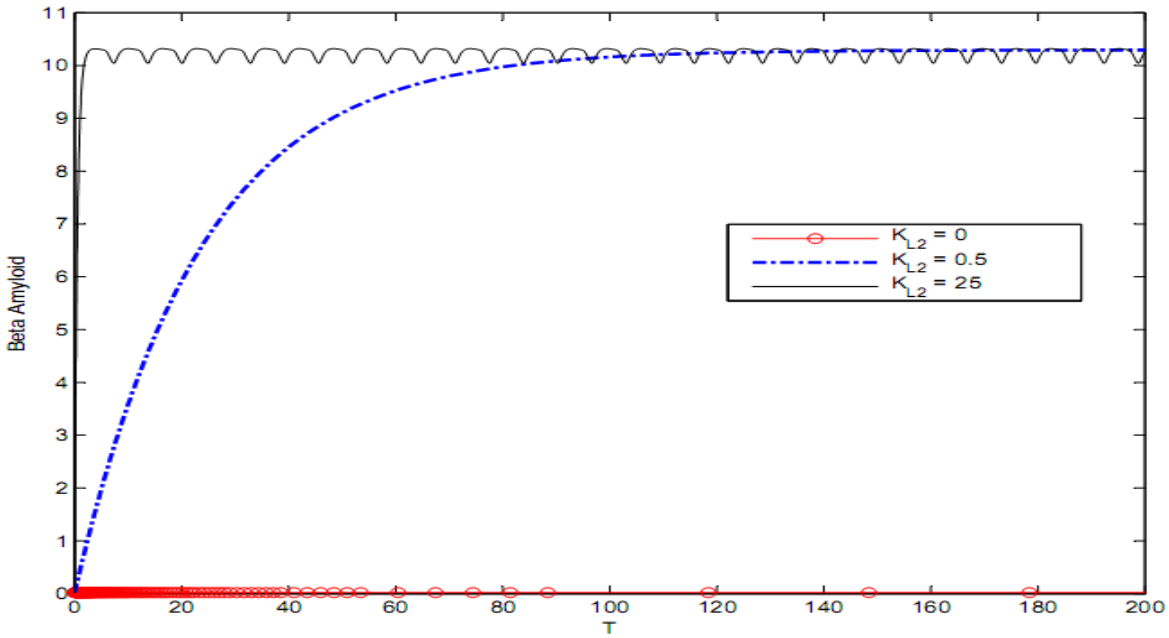

Figure 4.17: Time course of β-amyloid at different K_{L2} (according to kinetic mechanism 3)

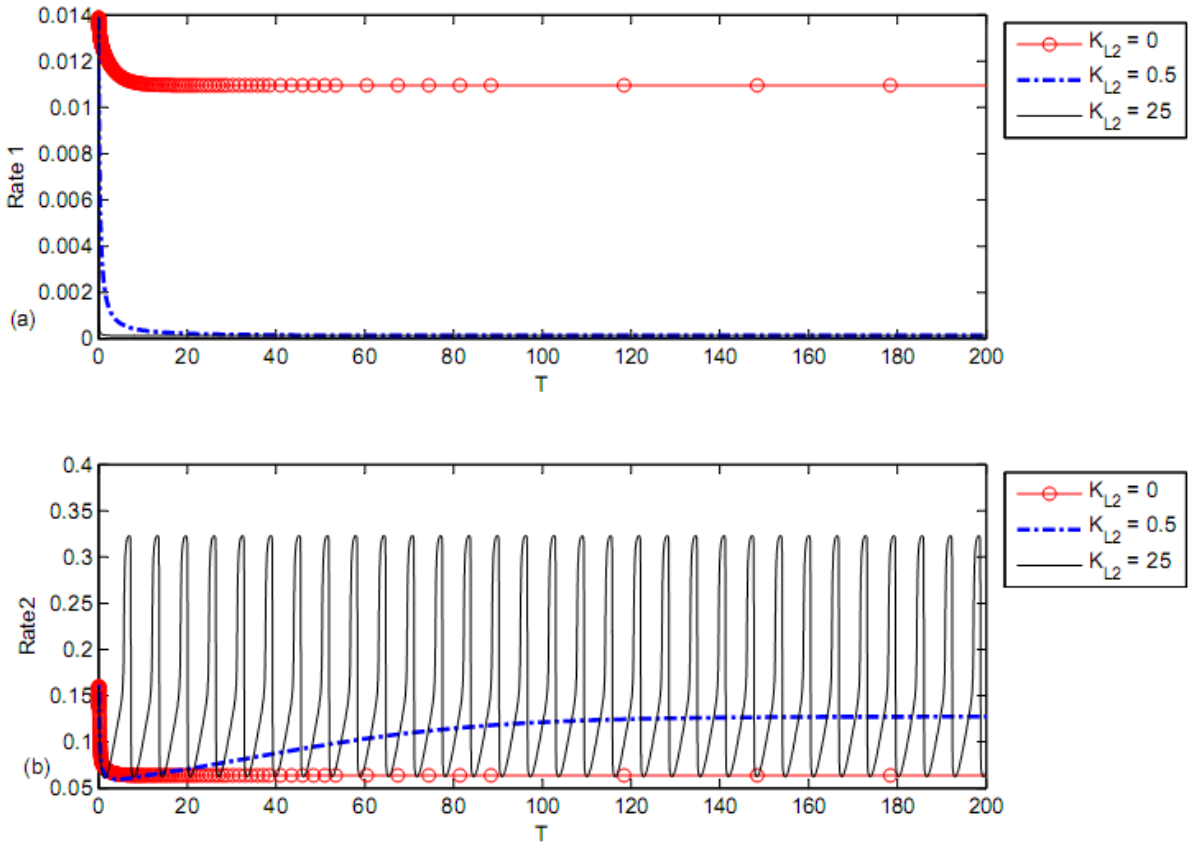

Figure 4.18: Time course of: a) Rate of ACh Synthesis (Rate 1), b) Rate of ACh hydrolysis (Rate 2) at different K_{L2} (according to kinetic mechanism 3)

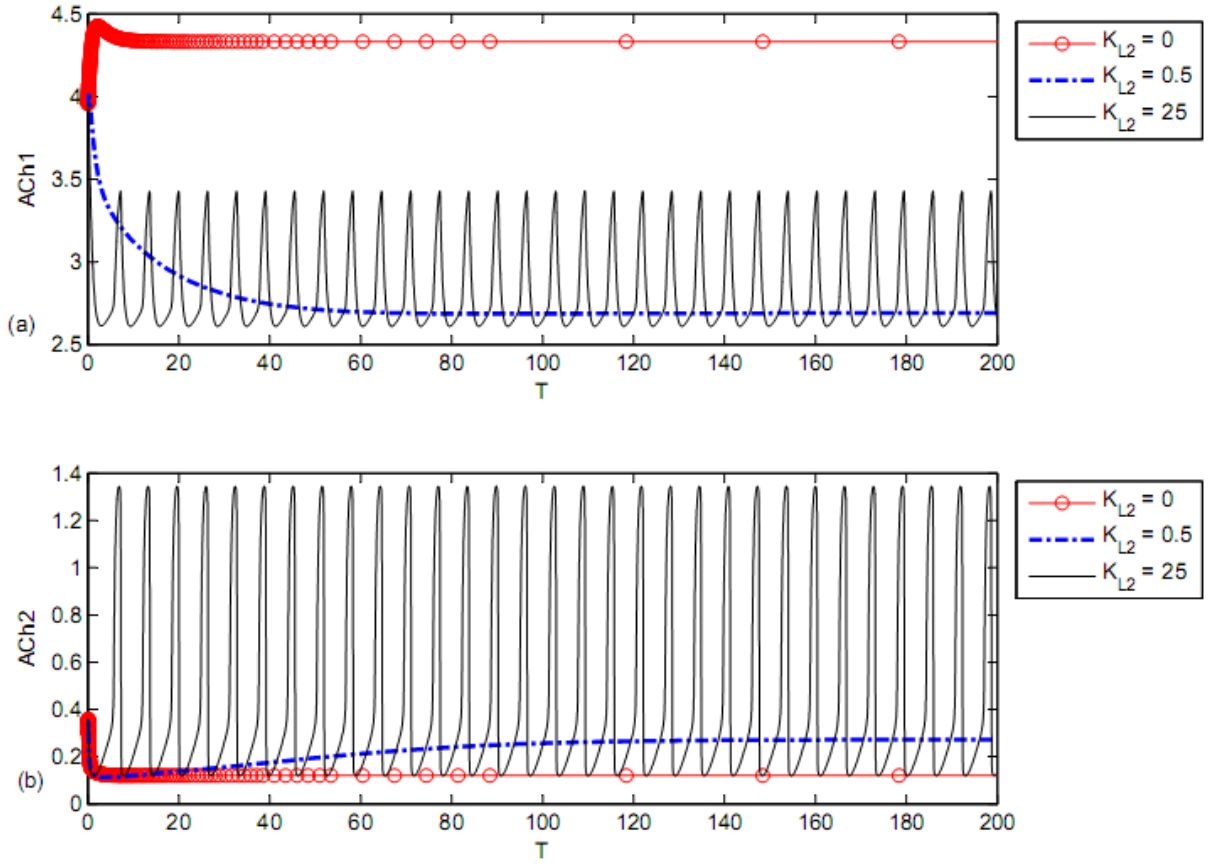

Figure 4.19: Time course of: a) ACh concentration in compartment 1 (ACh_1), b) ACh concentration in compartment 2 (ACh) at different K_{L2} values (according to kinetic mechanism 3)

4.5.2.4) Choline concentrations in compartments 1 and 2

Figure 4.20 (a) shows that there are no observable effects in the bahavior of Ch_1. This refelcts that there is no effect of ChAT-inhibition by β-amyloid on intracellular choline concentration indicating that both choline uptake and choline transport between compartments 1 and 2 are able to keep balanced intracellular choline concentration. It is observed that Ch_1 decreases from 3.22 (corresponding to 322 µM) at the beginning of incubation to 2.55 (corresponding to 255 µM). Figure 4.20(b) shows a limted efect of varying K_{L2} on Ch_2. Ch_2 increases very fast at the beginning of the reaction from 1.15 (corresponding to 115 µM) to 1.36 (corresponding to 136 µM) in just a short time T = (0-2) corresponing to (0-0.2 hr) then decreases to settle down at

1.16. Figure 4.21 (a) shows that Ch_1 decraeses from 3.2 (corresponding to 320 µM) to 2.52 (corresponding to 252µM) after passing T = 20 (corresponing to 2 hr). Figures 4.22 (a) and (b) are enlargement of Figures 4.20 (a) and (b) where it is observed that Ch1 oscilates in a narrow range (2.532-2.538) (corresponding to 253.2-2538 µM) at K_{L2} = 25 (corresponding to 500 nM) as shown in Figure 4.22 (a). Figure 4.22 (b) shows that Ch2 oscialtes through a limted range of 1.1548-1.1558 (corresponding to 115.48-155.8 µM).

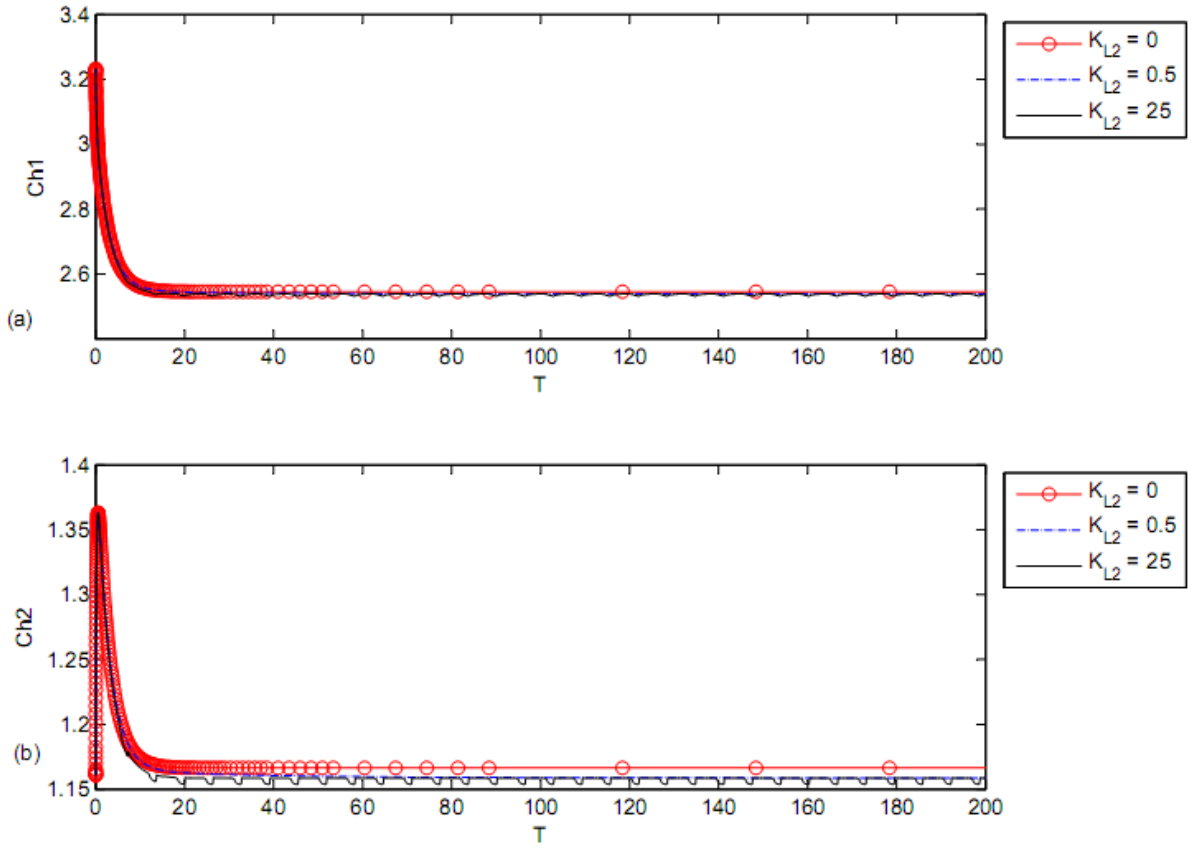

Figure 4.20: Time course of: a) Choline concentration in compartment 1 (Ch_1), b) Choline concentration in compartment 2 (Ch_2) at different K_{L2} values (according to kinetic mechanism 3)

The limited effect of Aβ inhibition on Ch_1 and Ch_2 is found to be negligible within the time frame studied. One likely explanation is that the choline uptake and the rate of ACh hydrolysis are all much larger in magnitude compared to that of ACh. While they all have an indirect

dependence on the activity of ChAT through changes in ACh_1 concentration, the reduction in ACh is too small to produce a significant effect on the concentrations of these components.

4.5.2.5) Acetate concentrations in compartments 1 and 2

Figure 4.23 (a) shows the dynamic behaviors of Acetate 1 at different K_{L2} values. It is observed that at K_{L2} = 0 where no β-amyloid is produced, Acetate 1 increases to settle down at the stationery state value of 9.6 (corresponding to 6.6 µM). As K_{L2} increases to 0.5 (corresponding to 10 nM), Acetate 1 settles down at a lower value of 9.45 (corresponding to 9.45 µM). When K_{L2} increases to the highest value of 25 (corresponding to 500 nM), Acetate 1 fluctuates in the range of 9-9.5 (corresponding to 9-9.5 µM).

Figure 4.23 (b) shows that Acetate 2, at K_{L2}= 0, takes steady state behavior which is around 6.4 (corresponding to 6.4 µM). While K_{L2} increases to 0.5 (corresponding to 10 nM), Acetate 2 deceases to settle down around 5.6 (corresponding to 5.6 µM) which is lower than that at no inhibition K_{L2} = 0). When K_{L2} increases to 25 (corresponding to 500 nM), the oscillatory behavior dominates the system where Acetate 2 fluctuates in the range 5- 5.63 corresponding to 5-5.63 µM.

4.5.2.6) pH in compartments 1 and 2

Figure 4.24 (a) shows the dynamic response of pH_1 at different K_{L2} values. It is observed that at K_{L2} = 0 where no β-amyloid is produced, pH_1 decreases rapidly from 8.5 to settle down at 6.2. At K_{L2} = 0.5, pH_1 decreases from 8.5 to 6.75 in the period 0-5 corresponding to (0 - 0.5 hr) then it increases to settle down around 8.4 which is the steady state value. When K_{L2} increases to the high value of 25 (corresponding to 500 nM), pH_1 oscillates in the range of 7.8-8.6.

Figure 4.24 (b) shows that at K_{L2}= 0, pH_2 settles down of around 5.8; when K_{L2} increases to 0.5 (corresponding to 10 nM), pH_2 decreases from 6.65 to 6.1 in the period 0-5 corresponding to (0 - 0.5 hr) then it increases to settle down around the steady state value of 6.8. It is observed that at K_{L2} = 25, pH_2 fluctuates in a wide range of 6.35-8.2 causing disturbances to the cholinergic system.

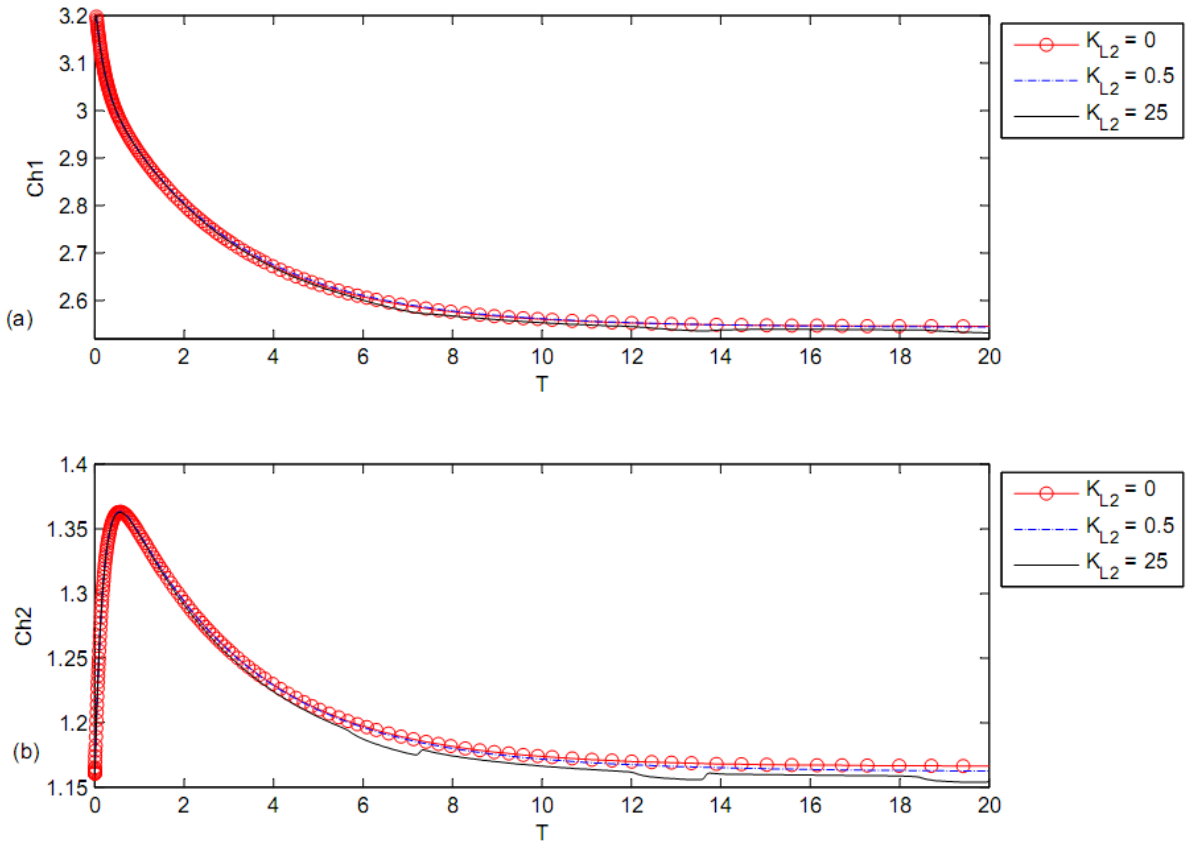

Figure 4.21: Magnification to Figure 4.20: a) Choline concentration in compartment 1 (Ch 1),

b) Choline concentration in compartment 2 (Ch 2) at different K_{L2} values (according to kinetic mechanism 3)

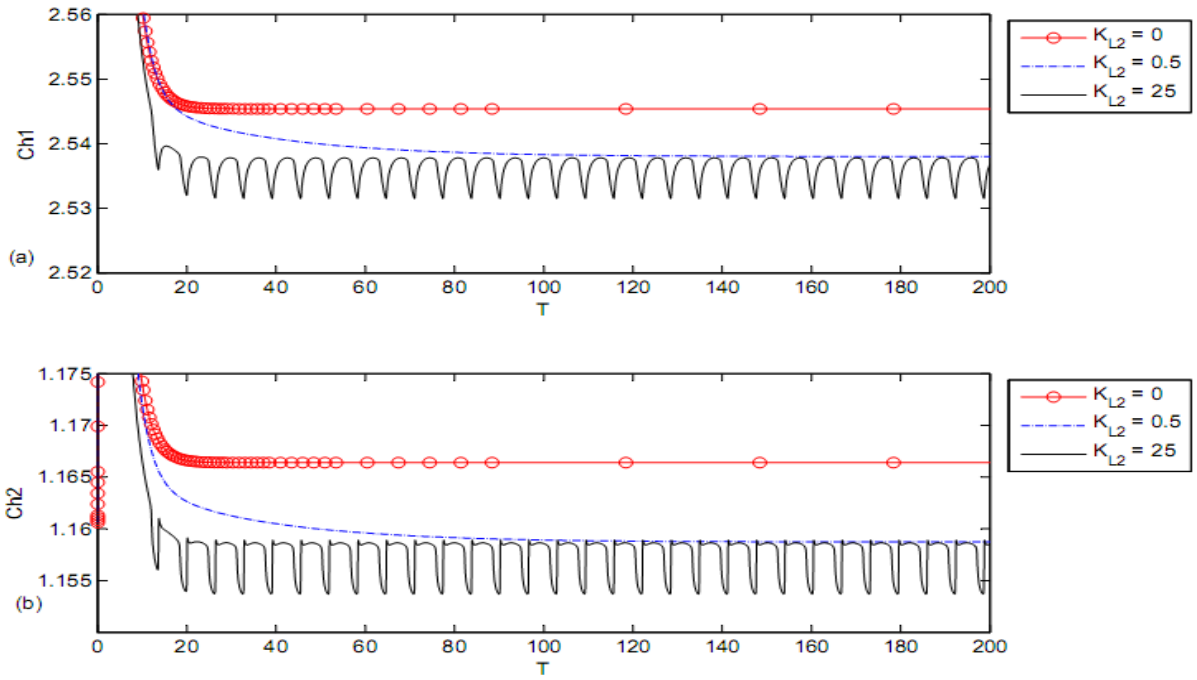

Figure 4.22: Magnification to Figure 4.20: a) Choline concentration in compartment 1 (Ch 1), b) Choline concentration in compartment 2 (Ch 2) at different K_{L2} values (according to kinetic mechanism 3)

4.6 Discussion

The effect of β-amyloid inhibition on ChAT activity is investigated through proposing three different kinetic mechanisms. The first kinetic mechanism is that β-amyloid binds to active enzyme complex E_2H in ChAT for producing ACh while in the second kinetic mechanism β-amyloid competitively binds to enzyme intermediate X_2. In the third kinetic mechanism, β-amyloid binds all species in ChAT enzyme. In each kinetic mechanism, a rate equation of ACh synthesis (r1) is derived and incorporated into the two-enzyme/ two –compartment model to get a cholinergic system with nine first-order ordinary differential equations. The concentrations of all state variables in compartments 1 and 2 in addition to the rates of ACh synthesis and ACh hydrolysis are investigated at different rates of β-amyloid generation (K_{L2}) and compared with normal cholinergic neurons where there is no inhibition with β-amyloid.

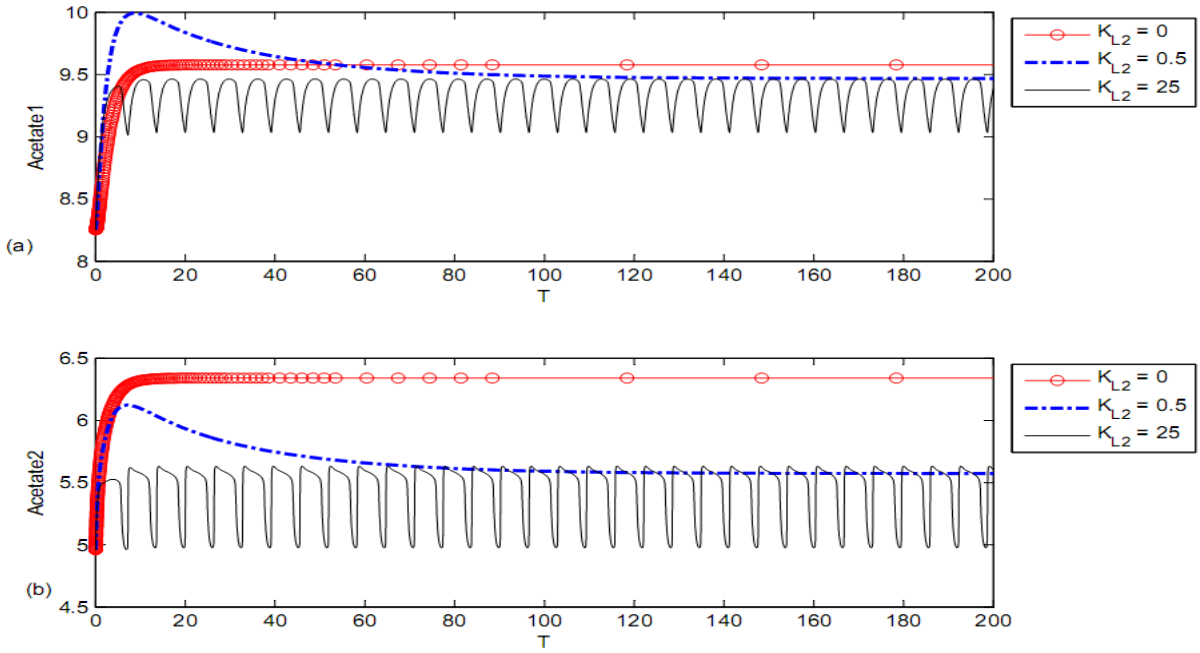

Figure 4.23: Time course of: a) Acetate concentration in compartment 1 (Ac 1),
b) Acetate concentration in compartment 2 (Ac 2) at different K_{L2} values (according to kinetic mechanism 3)

It is found that for all kinetic mechanisms the concentration of generated β-amyloid increases with increasing β-amyloid peptides production until it reaches saturation levels where there is no further increase with any additional increase of K_{L2}. In the first kinetic mechanism where β-amyloid attacks only the active enzyme complex E_2H in ChAT, it is found that each of the rate of ACh synthesis and the concentration of intracellular ACh (ACh1) decrease significantly with an increase in K_{L2} referring to the inhibition effect of ChAT activity while all of the other rates of ACh hydrolysis are not affected. In addition, ACh concentration in compartment 2 (ACh2), choline concentrations in compartments, pH in both compartments, acetate concentrations in both compartments are not affected by any change in K_{L2}. Therefore, the interaction between β-amyloid peptides and enzyme complex E2H in ChAT has a limited effect on most of elements of ACh neurocycle. One of the main explanations is that the limited effect of β-amyloid peptide on substrates such as choline and acetyl CoA in kinetic mechanism 1 is because that supply of these substrates such as choline from compartment 2 to compartment 1 and choline transport from compartment 1 to compartment 2 and acetate transport from compartment 1 to compartment 2

can compensate any reduction due to the inhibiting effect of β-amyloid on the active site E_2H. However, the significant reduction in ACh concentrations due to ChAT activity inhibition is one of the hallmarks in cholinergic dysfunctions.

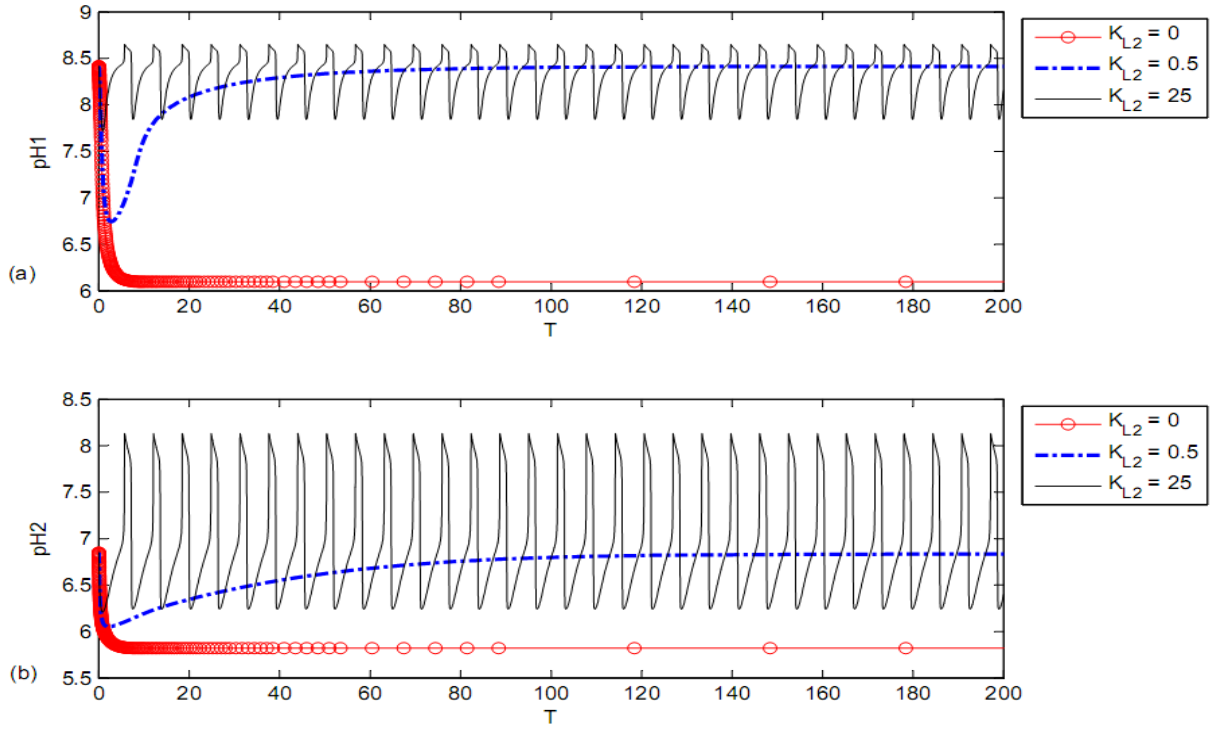

Figure 4.24: Time course of: a) pH in compartment 1 (pH 1),
b) pH in compartment 2 (pH 2) at different K_{L2} values (according to kinetic mechanism 3)

The results of the second kinetic mechanism where β-amyloid competitively attacks the enzyme intermediate X_2 are similar to that of the first kinetic mechanism except that acetate concentration in compartments 1 and 2 decrease significantly while pH_1 and pH_2 in both compartments increase with the increase in K_{L2} where the attack of β-amyloid on intermediate X_2 of ChAT leads to a decrease in the consumption of acetyl-CoA in compartment 1 and the lower production of acetate in compartment 2. The reduction in Rate 1 or ChAT activity in kinetic mechanisms 1 and 2 decrease with around 25 % with increase K_{L2} from 0 to 25 (corresponding to 500 nM).

In the third kinetic mechanism where β-amyloid binds to all species in ChAT, it is found that at low values of K_{L2}, the behavior of cholinergic ACh looks like that of the second kinetic mechanism. However, at high values of K_{L2} (e.g. 25), an interesting phenomenon arises for all state variables of the system where all variables fluctuate in a wide range (as shown from Figures 4.17 to 4.22) leading to irregular behavior of the cholinergic system. These disturbances occurring in the cholinergic system is one of the main features of AD (Nunes-Tavare et al., 2012). According to kinetic mechanism 3, β-amyloid peptides promote a major reduction in ChAT activity. Kar et al., (2004) indicated that decline of intracellular ACh concentration is due to reduction in ChAT catalytic action. Moreover, it was observed that long incubation of rat primary septal culture neurons with micro molar concentration of β-amyloid peptides caused a reduction in ChAT function and cell death (Kar et al., 2004; Olesen of et al., 1998).

The results of kinetic mechanism 3 are compatible with the experimental results obtained by Nunes-Tavare et al., (2012) who showed that β-amyloid peptides could bind to a significant portion of cholinergic neurons and reduce ChAT activity completely. It is observed that the reduction in Rate 1 in kinetic mechanism 3 decreases from 0.0105 to 0.000125 which refers to a reduction in ChAT activity of 99.7% with increasing K_{L2} from 0 to 25 (corresponding to 500 nM). The results are in agreement with the experimental results obtained by Nunes-Tavares et al., 2012) who showed that β-amyloid could inhibit ChAT completely.

It is observed that after time 100 (corresponding to 10 hr), there is no effect for any further change of β-amyloid production rate (K_{L2} from 0.5 to 25), where all state variables reach the same steady state values. These results are compatible with those obtained by Nunes-Tavares et al., 2012) who showed that there is no significant effect for any further β-amyloid concentration higher than 100 nM. It is also observed that ChAT inhibition by β-amyloid could cause severe consequences for the rate of ACh synthesis and ACh concentrations in compartments 1 and 2 as well where ChAT inhibition could reach 100 % as shown in Figure 4.18 (a).

4.7 Summary and Conclusions

In this chapter, the effect of β-amyloid peptide as an inhibitor on ChAT activity for ACh synthesis through the two enzyme/two compartment (2E2C) model in a variety of situations is analyzed through suggesting three different kinetic mechanisms for the inhibition effect. Overall, numerical solutions to the modified 2E2C with β-amyloid were in accordance with three significant, widely reported symptoms of AD; loss of ChAT activity (Pederson 1996), reduced choline uptake (Kar 1998) and reduced ACh production (Pederson 1996). This in turn means that the direct inactivation of ChAT by β-amyloid may be a probable mechanism contributing to the development of AD. The incorporation of ChAT inhibition by β-amyloid into the 2E2C model is able to yield dynamic solutions for concentrations of generated β-amyloid, ACh, choline, acetate, and pH in addition to the rates of ACh synthesis and ACh hydrolysis in compartment 1 and 2. This correlates well to the physiological understanding since the production of β-amyloid is not generally known to be highly reversible. One of the most significant physiological symptoms of AD is the reduction of ACh neurotransmitter concentration within cholinergic neurons. In this investigation, the effect of ChAT activity inhibition via β-amyloid is considered an individual basis in order to evaluate the validity of each kinetic mechanism. Since it is highly likely that physiologically more than one single mechanism can contribute to the generation of AD symptoms. In comparison to the effect of β- amyloid via choline leakage hypothesis, it is observed that ChAT activity needs a high concentration of β-amyloid production rate (K_{L2}). This is in agreement with the experimental results obtained by Kar et al., (1998) who showed that the exposure to small concentrations of β-amyloid has no impact on ChAT activity in cortex tissues. However, the results are in agreement with those obtained by Zambrzycka et al., (2002) who showed that when neurons tissues exposed to high concentrations of β- amyloid for a while, ChAT activity is reduced significantly. The results of kinetic mechanism 3 are in agreement with that obtained by Mustafa et al., (2012) who indicated the oscillatory behavior of ACh neurocycle at low ChAT activity.

Chapter 5

Pharmacodynamics/Pharmacokinetics, Modeling, and Simulation for the Effect of Drugs on β-amyloid Aggregates and Cholinergic Neurocycle

5-1 Introduction

Alzheimer's disease (AD) is a progressive neurodysfunction illness and responsible for high mortality rate worldwide and is considered the main cause of dementia. Loss of memory, cognition impairment, and behavioral deficits are common characterizations of AD. AD is considered the fourth reason of death in the United States. In addition, the number of AD patients increases every day; now 25 million worldwide have AD, 4 million of them are in the USA. AD etiology is still unknown accurately; however, many researchers such as Hardy and Higgins, (1992) supported the hypothesis of β-amyloid cascade as the main reason of AD where β-amyloid aggregates are deposited in the brain slices (Lu, 2012). β-amyloid is produced through sequential enzymatic cleavages of APP. Lowering of β-amyloid aggregates in the brain is considered a strategy for AD therapeutics (Pettersson et al., 2011; Lu, 2012). These aggregates of β- amyloid are formed by proteolytic cleavage of a transmembrane protein known as amyloid precursor protein (APP). There are two possible ways for cutting APP: (1) via α- secretase to produce sAPPα which is non amyloidogenic and neuroprotective agent. This is because sAPPα induces expression of transthyretin (TTR), a transport protein in cerebrospinal fluid (CSF) and blood, which prevents β-amyloid aggregation; (2) via β- and ɣ- secretase. The latter pathway is amyloidogenic because it releases β- amyloid that deposits as fibrillar aggregates in the brain and known as senile plaques (Liu and Murphy, 2006). Senile plaques are dense plaque cores of β-

amyloid deposits plus activated microglia and active astrocytes, where they together form damaged neutrophil (Teplow, 1998). Aggregates of amyloid plaques in the brain of AD patients cause negative consequences in cholinergic neurons. Examples for sever neurodegenerative disorders are: (1) disturbance in choline level a rate limiting substrate for ACh synthesis, in cholinergic neurons by inducing a leakage in the presynaptic membrane as indicated in Chapter 3, (2) Inhibition of ChAT activity, an enzyme responsible for ACh synthesis, as presented in Chapter 4, (3) Other effects such as formation of neurofibrillary tangles (NFT) which are aggregation of hyper phosphorylated tau protein: an enzyme that is responsible for stability of microtubules and enhances assembly of tubulin into microtubules, the cytoskeleton of cells, and hence hyper phosphorylation of tau protein causes instability and disintegration of microtubules that results in neuron cells degeneration and death (Mandelkow E.M., and Mandelkow, E. (2012)).

From Chapter 3, it was found that the lower concentration of β- amyloid aggregates could cause significant reductions in the levels of choline and ACh. Therefore, therapeutic agents have become extremely important to abrogate the toxicity effect of β- amyloid aggregates and inhibit aggregation. Since β-amyloid plaques are the key to neurons damage which initiates AD, the challenge for research is to find a promising and safe therapy for preventing β-amyloid formation and accumulation. Examples for promising drugs candidate that are currently under studies for developing an effective therapy for AD:

(1) Transthyretin (TTR), a transport protein in plasma and cerebrospinal fluid (CSF) with molecular weight 55 kDa, is able to reduce dementia in AD patient by binding to β- amyloid and preventing its toxicity and aggregation. The hopeful research is to find a compound that mimics TTR or increases level of TTR in CSF. Stein et al., (2002) and (2004); Lui and Murphy,(2006) showed that incubation of 50 μM of β- amyloid with hippocampal slices caused cell death, but this effect is completely abolished after the addition 3 μM of TTR. Also, processing APP by α-secretase to produce sAPPα increases TTR expression, and hence increase TTR.

(2) β- amyloid vaccination helps stop β- amyloid aggregation and moves it from brain to blood. In 2000 the immunization therapy showed good results in enhancement memory function of

participants but did not achieve the required objectives due to problems related to brain inflammation and bleeding in brain besides cerebral blood vessel disease (Teplow, 1998; Liu and Murphy, 2006). Currently, there is a product produced by researchers at Cardiff University namely 2B12 which is antibody that binds to amyloid precursor protein (APP) and prevents its cutting by amyloidgenic β-secretase. 2B12 inhibits β- amyloid aggregation in culture cells. This product is still under lab trials for human use (Teplow, 1998; Liu and Murphy, 2006).

(3) Nicotine for AD treatment: Researchers at Lancaster University found that nicotine is able to arrest β-amyloid aggregation. An optimist result had been obtained in lab trial on nicotine using animal model (Pollack et al., 2005).

Overall, the key element for AD treatment is to understand its etiology and pathobiology. Since the main pathological feature of AD is the presence of β-amyloid aggregation in the brain, a drug that could prevent β-amyloid formation and accumulation could achieve the greatest success in AD cure (Teplow, 1998). Using traditional trials for improving and testing new drugs is based on carrying a series of experiments on number of healthy volunteers in order to determine the correlation between potential doses and medical effects for testing drug. Moreover, the traditional resources of research are money, time, and effort consuming besides risk effects due to adverse drug interactions. Therefore, the need for developing new methods for drug testing and development become necessary. An example for these new techniques is the application of computational modeling for the analysis of pharmacokinetics (PK) and pharmacodynamics (PD) of drugs.

PK/PD modeling helps to understand the mechanisms leading to intimation and development of diseases and develop therapeutics of different diseases and integrate with experimental knowledge and improve in vivo /vitro clinical potentials (Lu, 2012). However, not all factors of all aspects of AD can be considered in mathematical models. These factors such as temperature, environment, diet, and presence of any other disease could have a significant effect on PK and PD of drugs. PK models can predict and define time course of drug concentration in different body compartments such as blood, brain, and plasma, but PD models describe time course of drug effect at the site of action. Both PK and PD models play an important role in

current drug research. However, the accuracy of these models is limited because they did not consider the biophysical properties of different body tissues and the interstitial space.

In AD, PK/PD models are helpful in predicting the time course of β- amyloid concentrations after treatment. PK/PD models have many advantages: they can predict the reduction of β- amyloid aggregates, ACh and choline levels as will be shown from PD time course. The prediction of time course of β- amyloid aggregates facilitates selection of appropriate doses and sampling time points to ensure that the outcomes are informative. Moreover, PK/PD models help design preclinical studies and clinical experiments. In addition, modeling and simulation are good tools for hypothesis testing. The simulations of β- amyloid aggregates profiles after treatment are then compared with observations from a subsequent preclinical study. Therefore, modeling and simulations could provide a good feedback that could speed-up drug development.

Because the importance and necessity of AD therapy and the big need for improving and developing drug techniques, we propose an integrated mechanistic model for AD drug that integrates PK and PD of drug and elucidate the relationship between dose and drug action at cholinergic neuron cells in brain. This is an effective way in determining the best strategies for AD treatment. Our model describes the dynamic concentration of AD drugs, β- amyloid aggregates, and ACh neurocycle components with time.

This Chapter is based on Chapter 3 at which the interaction between β- amyloid and ACh neurocycle was investigated through incorporation of the effect of β- amyloid aggregates into two-enzyme/two-compartment model via choline leakage hypothesis. The presynaptic neuron was considered as compartment 1 while both synaptic cleft where ACh hydrolysis process occurs by the enzyme AChE and postsynaptic neuron are considered as compartment 2. Furthermore, it was found that β-amyloid aggregates formed from APP interact with ACh synthesized in compartment 1 and the membrane of the presynaptic neurons lead to formation of pathways in the membranes and allowed the opportunity for choline content in compartment 1 to leak out of the cholinergic system. Therefore, choline substrate reduction in compartment 1 affects the levels of produced ACh. Furthermore, it was found in Chapter 3 that as the rate of β- amyloid

production (K_{L2}) increases, the number of channels formed in the membranes increase and levels of ACh and choline in both compartments decrease significantly.

In this chapter, a PK and PD one-compartment model is proposed to study the drug behavior in the presynaptic neurons. It is proposed that the drug interacts only with one compartment which is compartment 1 where ACh is synthesized by the catalytic effect of the ChAT enzyme. It is suggested that the drug interacts with β- amyloid peptides to prevent formation of β- amyloid aggregates (polymers) more than monomers. Therefore, β- amyloid aggregates will not be able to form pathways in the membranes of the presynaptic neurons allowing saving choline levels inside the presynaptic neurons.

The main objective of this chapter is to evaluate the impact of AD drugs on β- amyloid levels, ACh, choline, acetate, pH, and rates of ACh synthesis and hydrolysis in ACH cholinergic system. This is performed by incorporating the proposed one-compartment PD/PK model into the two-enzyme/two-compartment model built in Chapter 3. The effect of drugs on the percent of β- amyloid aggregates removal is investigated at different feed drug rates. The maximum concentration of drug content in the presynaptic tissues giving the maximum effect is investigated with the area under the curve (AUC) for drug concentration with time.

5.2) Formulation of PD/PK model of the ACh system

It is very important to understand the effect of drug feed rates on its pharmacokinetic and pharmacodynamics behavior because it helps to maximize the drug effect (Wakelkamp et al., 1998). Controlling the drug input rate can help to develop advanced drug delivery systems to accomplish the best efficiency Wakelkamp (1997). In this chapter PD and PK model is used to evaluate the impact of AD drugs on β- amyloid aggregates levels, ACh, choline, acetate, pH, and rates of ACh synthesis and hydrolysis in two-enzyme/two compartments of cholinergic neurons. The drug concentrations inside neuronal tissues are calculated through one-compartment model which is the presynaptic neuron where both β- amyloid inhibitor and the produced ACh exist. The feed production of the drug (K_{U2}) is assumed to be zero-order. However, the clearance rate is assumed to be first order that is proportional to the accumulation concentration of drugs (Wakelkamp et al., 1998). The drug consumption rate is assumed to be second order where it is

proportional to the concentrations of accumulated drugs and β- amyloid (Wakelkamp et al., 1998). The first order differential equation for the drug concentration can be formulated as follows:

$$\frac{dU}{dT} = \frac{K_{U2}}{1+\psi e^{\omega t}} - K_e(bA)(U) - K_{Cl}(U) \quad (5.1)$$

It is observed that K_{U2} is multiplied by the sigmoid function which is a special case of logistic functions. The sigmoid function helps to simulate the cholinergic cycle system. This saturates after a long period of time. Gibbs (2000) used sigmoidal functions in different natural processes characterized by continuous development from low levels to the saturation through time. Lu (2012) and Group et al., (2013) used the sigmoidal function to modify the input rate of the inhibitory effect.

It is expected that the drug could prevent the aggregation of β-amyloid and inhibit pathways formation in the presynaptic membrane according to choline leakage hypothesis investigated in Chapter 3. Therefore, the intracellular choline concentration could be kept inside the presynaptic neuron to react with acetyl-coA to form ACh. The final concentration of β- amyloid aggregates existed in the presynaptic neurons after incorporation of drugs through oral input is obtained as follows:

$$\frac{dbA}{dT} = K_{L2} - K_{L3}\, s_{1(1)} - K_{L4}\, bA - KU_{11}(bA)(U) \quad (5.2)$$

The potency and efficacy of lowering β-amyloid aggregates can be defined by the function $\% X_s$ which measures the average β-amyloid aggregates reduction after treatment. It defines the intrinsic PK/PD relationship for the drug which is equivalent to the relationship between an exposure and time-weighted-average β-amyloid aggregates lowering after treatment:

$$\% X_S = \frac{bA(0) - bA(f)}{bA(0)} \; x \; 100 \quad (5.3)$$

Where *bA*(0) refers to the initial concentration of β-amyloid aggregates at time (zero) where there is no drug added, and *bA (f)* refers to the final concentration of β- amyloid aggregates after

incorporating the drug. The last term refers to the reduction of β-amyloid aggregates concentrations due to interaction with the drug (U). It is noticed that the latter reduction is proportional to the concentrations of drugs and β- amyloid aggregates as well. Furthermore, the reduction of intracellular choline concentration will be lowered due to interaction of β- amyloid aggregates with the drug. The final concentration of choline in compartment 1 can be formulated as follows:

$$\frac{ds_{2(1)}}{dT} = s_{2f} + R^{*} s_{2(2)} - \alpha_{S2_1}\left(s_{2(1)} - s_{2(2)}\right) - \frac{B_1}{S_{2refernce}} r(1) - K_{bA3}\, bAK_{UU} \tag{5.4}$$

Where:

$$K_{UU} = 1 - \frac{V_m(U)}{K_{sm} + K_{sU}(U^{\lambda})} \tag{5.5}$$

The term K_{UU} refers to the effect of the drug on the intracellular choline concentrations. It takes the form of Monod kinetics to show the dynamic effect of the drug. It is observed that the drug should be kept in a certain range where it should be neither too low in order to give the required effect nor too high to avoid the toxicity (Moore et al., 2004). The form of K_{UU} is obtained through assuming values for V_m (the maximum effect of the drug), and the constants K_{sm} and K_{sU} in order to give reasonable effect for the drug.

Equations from equation 5.1 to 5.5 of PK/PD model are incorporated into two-enzyme/two-compartment model to evaluate the impact of Alzheimer's drug on β- amyloid levels, ACh, choline, acetate, pH, and rates of ACh synthesis and hydrolysis in two-enzyme two-compartment model of cholinergic neurons via β- amyloid-choline leakage mechanism studied in Chapter 3. The response of the cholinergic system through the time course of β- amyloid aggregates levels in compartment 1 in addition to concentrations of ACh, choline, acetyl CoA concentrations and pH levels in both the presynaptic neurons (compartment 1) and the postsynaptic cleft (compartment 2) are investigated. Furthermore, the impact of the drug on the rate of ACh synthesis catalyzed by the enzyme ChAT in compartment 1 and the rate of ACh hydrolysis catalyzed by the enzyme AChE in compartment 2 are investigated.

Table 5.1 provides a summary of ordinary differential PK/PD equations where there are ten-first order differential equations through the 2E/2C cholinergic ACh system and one compartment for the drug effect. The effect of AD drugs is assumed to be only one compartment which is compartment 1 because β- amyloid aggregates which cause choline leakage exist only in compartment 1. In addition, it will help to focus on choline leakage hypothesis and how AD drugs affect β- amyloid aggregates in the presynaptic neurons in addition to simplify the calculations of the system. Table 2 shows the values of PK/PD parameters and other kinetic and operating parameters used previously in Chapter 3.

Model Assumptions:

Each compartment is assumed to be isothermal continuous-stirred tank reactor (CSTR); the components in each compartment are assumed to be well-mixed and homogenous. In addition, it is assumed that choline which is leaked due to the pathways caused by the β- amyloid aggregates in the membrane of compartment 1, is settled out of the two-enzyme/two-compartment systems where it is not settled down in compartment 2 or compartment 1 as shown in Figure 5.1.

A one-compartmental model is enough to describe the pharmacokinetics of orally administered drugs where K_{U2} represents zero-order rate constant for drug feed rate, K_{cl} is the first order rate constant for drug clearance. In addition, it is assumed that drug exerts action by inhibiting β-amyloid aggregation. Transport of both β-amyloid aggregates and drug from compartment 1 to compartment 2 are neglected. To justify these considerations, we note that the transport of β-amyloid and drugs from compartment 1 to compartment 2 is by passive diffusion and the transport rates are extremely lower than those from the cytoplasm to compartment 1 (Wakelkamp (1997)). The latter transport (from the cytoplasm to compartment 1) addresses brain boundary barriers (BBB) according to saturable mechanism such as Monod and Michaelis-Menten kinetics (Craft et al., 2002; Zlokovic et al., 1993; Martel et al., 1996).

One of the main assumptions is this Chapter is that the drugs are administered orally to let the drug absorption be as fast as possible and could give a direct effect on the neuron tissues in the

brain. In addition, the drug is assumed to be on a single-dosing regimen whereby after a duration drug concentration reaches a steady state level. The measure of the capability of the body to eliminate a drug is defined in terms of clearance (Bent and Zia-Amirhosseini, 1995). The extraction ratio (ER) of the drug which is the ratio of the rate of elimination to the rate of presentation is assumed to be 0.55. The latter value is considered a medium ER for AD drugs (Bent and Zia-Amirhosseini, 1995). This means that around 45% of the drug is absorbed in the blood. ER is calculated according to the following equation:

$$ER = \frac{Q(C_A - C_V)}{QC_A} = \frac{C_A - C_V}{C_A} \tag{5.6}$$

C_A refers to concentration in the feed stream to the liver, while C_V refers to the exit concentration from the liver. Q (C_A – C_V) refers to rate of elimination.

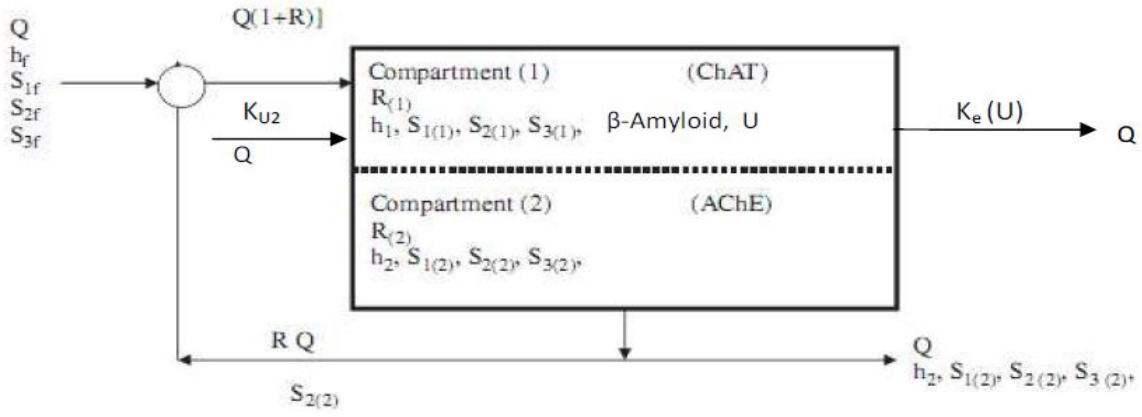

Figure 5.1: Schematic representation for Pharmacodynamics one-compartment drug and two-enzyme/ two-compartment model

Table 5.1: Dimensionless forms of the ordinary differential equations of drug effect on β- amyloid aggregates via choline leakage hypothesis

Item	Compartment	Differential equation
Hydrogen protons	1	$\frac{dh_{(1)}}{dT} = h_f - \gamma_1 \left(\frac{1}{h_f}\right) - \alpha_H \left(h_{(1)} - h_{(2)}\right) + \alpha_{OH}\gamma_1 \left(\frac{1}{h_{(1)}} - \frac{1}{h_{(2)}}\right)$
	2	$\frac{dh_{(2)}}{dT} = V_R(\alpha_H \left(h_{(1)} - h_{(2)}\right) - \alpha_{OH}\gamma_1 \left(\frac{1}{h_{(1)}} - \frac{1}{h_{(2)}}\right) - \left(h_{(2)} - \frac{\gamma_1}{h(2)}\right) + \frac{B_2}{k_{h1}} r(2))$
Acetylcholine	1	$\frac{ds_{1(1)}}{dT} = s_{1f} - \alpha_{s1}\left(s_{1(1)} - s_{1(2)}\right) + \frac{B_1 r(1)}{K_{s1}} - K_{bA2}\, s_{1(1)}\, bA$
	2	$\frac{ds_{1(2)}}{dT} = V_R(\alpha_{S_1}\left(s_{1(1)} - s_{1(2)}\right) - s_{1(2)} - \frac{B_2 r(2)}{K_{s1}})$
Choline	1	$\frac{ds_{2(1)}}{dT} = s_{2f} + R^* s_{2(2)} - \alpha_{S2_1}\left(s_{2(1)} - s_{2(2)}\right) - \frac{B_1}{S_{2refernce}} r(1) - K_{bA3}\, bA K_{UU}$
	2	$\frac{ds_{2(2)}}{dT} = V_R(\alpha_{S2}\left(s_{2(1)} - s_{2(2)}\right) - (1+R)^* s_{2(2)} + \frac{B_2}{S_{2reference}} r(2))$
Acetate	1	$\frac{ds_{3(1)}}{dT} = s_{3f} - \alpha_{S3}\left(s_{3(1)} - s_{3(2)}\right) - \frac{B_1}{S_{3refernce}} r(1)$
	2	$\frac{ds_{3(2)}}{dT} = V_R(\alpha_{S3}\left(s_{3(1)} - s_{3(2)}\right) - s_{3(2)} + \frac{B_2}{S_{3refernce}} r(2))$
β- amyloid aggregates	1	$\frac{dbA}{dT} = KL_2 - KL_3\, s_{1(1)} - KL_4\, bA - K_{U11}(bA)(U)$
Drug	1	$\frac{dU}{dT} = \frac{K_{U2}}{1+\psi e^{\upsilon t}} - K_e(bA)(U) - K_{Cl}(U)$
Rate of synthesis ($r_{(1)}$)	1	$r_{(1)} = \frac{\theta_1 s_{21} s_{31}}{\theta_2 / h_1 (h_1 + 1 + \delta h_1^2) + \theta_3 s_{31} + \theta_4 s_{21} + \theta_5 s_{21} s_{31}}$
Rate of hydrolysis ($r_{(2)}$)	2	$r_{(2)} = \frac{s_{12}}{s_{12} + 1/h_2 (h_2 + 1 + \delta h_2^2) + \alpha s_{12}^2}$
K_{UU}		$1 - \frac{V_m(U)}{K_{sm} + K_{sU}(U^{\lambda})}$

V_m	0.068 K_{U2}
K_{sm}	9.5
K_{sU}	0.034 K_{U2}
λ	1.25
K_{bA3}	0.075 K_{L2}
K_{bA2}	0.06 K_{L2}
K_{abs}	0.375
K_e	0.7205
K_{Cl}	0.125
υ	0.05
ψ	0.001

Table 5.2: Values of the Kinetic Parameters

Parameter	**Value**	**Reference**
θ_1	5.2(0.1)	Peet & Hersh (1977)
θ_2	12	Peet & Hersh (1977)
θ_3	1000	Peet & Hersh (1977)
θ_4	5	Peet & Hersh (1977)
θ_5	1	Peet & Hersh (1977)
α	0.5	Garhyan et al., (2006); Ibrahim et al., (1997); Elnashaie et al., (1983a), (1983b), (1984), and (1995)
δ	1	Garhyan et al., (2006); Ibrahim et al., (1997); Elnashaie et al., (1983a), (1983b), (1984), and (1995)
$K_a(k_h)$	$1.066*10^{-6}$ kMole/m^3(µMole/mm^3)	Garhyan et al., (2006); Ibrahim et al., (1997); Elnashaie et al., (1983a), (1983b), (1984), and (1995)
K_{s1}	50.33 µMole/l	Garhyan et al., (2006); Ibrahim et al.,

		(1997); Elnashaie et al., (1983a), (1983b), (1984), and (1995)
S_{2ref}	100 µMole/l	Guyton and Hall, (2000)
S_{3ref}	1 µMole/l	Guyton Hall, (2000)
B_1	5.033×10^{-5} kMole/m^3(µMole/mm^3)	Garhyan et al., (2006)
B_2	5.033×10^{-5} kMole/m^3(µMole/mm^3)	Garhyan et al., (2006)
α_{H^+}	2.25	Elnashaie et al., (1984)
α_{OH^-}	0.5	Elnashaie et al., (1984)
α_{S_1}	1.5	Elnashaie et al., (1984)
α_{S_2}	1.5	Elnashaie et al., (1984)
α_{S_3}	1	Elnashaie et al., (1984)
V_R	1.2	Elnashaie et al., (1984)
pH_f	8.2	Guyton, 2000
s_{1f}	15	Garhyan et al., (2006)
s_{2f}	1.15	Garhyan et al., (2006)
s_{3f}	3.9	Garhyan et al., (2006)
γ_1	0.01	Garhyan et al., (2006); Ibrahim et al., (1997); Elnashaie et al., (1983a), (1983b), (1984), and (1995)
R	0.8	Tucek (1978)
K_{L2}	1	
K_{U2}	assumed	
K_{L1}	$3K_{L2}$	
K_{L3}	$0.035K_{L2}$	
K_{L4}	$1.76K_{L3}$	
K_{U11}	0.0425	
BA_{ref}	20 nM/l	Kar et al., (2008)

5.3) Results and Discussion

On the basis of Figure 5.1 and the model equations described in Table 5.1 and the kinetic parameters values in Table 5.2, the results illustrated from Figure 5.3 to Figure 5.8 show the predicted time course of all state variables in two-enzyme/two-compartment (2E2C) model where the impact of AD drug on 2E2C model is incorporated by solving numerically the system ODEs of Table 5.1. It is assumed that the patient is in pre-treatment with maximum β- amyloid concentration according to choline leakage hypothesis obtained at K_{L2} =1 as investigated in Chapter 3. Then, a drug is administered in order to lower the production of β- amyloid aggregates through the period (0-300) corresponding to (0-30 hr).

Figure (5.2) depicts the dynamic behavior of the drug concentration at different feed drug administrations (K_{U2}). It is observed that the drug administered orally takes the bell shape where the left branch represents the absorbance after administration while the right branch is the clearance part through urine or the liver. It is observed that at K_{u2} = 0 which is considered as the control value where no drug is administered, the drug concentration (U) in the presynaptic neurons is zero. As K_{u2} = 2.25 (corresponding to 225 mg), it is observed that the drug is absorbed to allow for its concentration in the presynaptic neurons to increase to reach 0.37 (after passing 37 (corresponding to 3.7 hr) then the drug is cleared slowly to reach 0.36 (corresponding to 0.36 μM) after passing 70 (corresponding to 7 hr). Afterwards, the drug starts to be eliminated completely to reach the pretreatment case where the drug content is zero after passing 250 (corresponding to 25 hr).

When K_{u2} increases to reach 4.5 (corresponding to 450 mg), drug is absorbed to allow for its intracellular concentration to increase and reach 0.95 (corresponding to 0.95 μM) as a high level then it decreases slowly due to complete removal after passing 250 (corresponding to 25 hr). Furthermore, at K_{U2} = 9 (corresponding to 900 mg), the absorbance increases very fast to reach to 1.3 and the drug content (U) increases reach 1.3 (corresponding to 1.3 μM). Then the drug absorbance increases to reach 3.8 after passing 63 (corresponding to 6.3 hr). Then, it decreases fast to reach 0.5 after passing 175 (corresponding to 17.5 hr); then it is cleared slowly to be removed completely after passing 250 (corresponding to 25 hr).

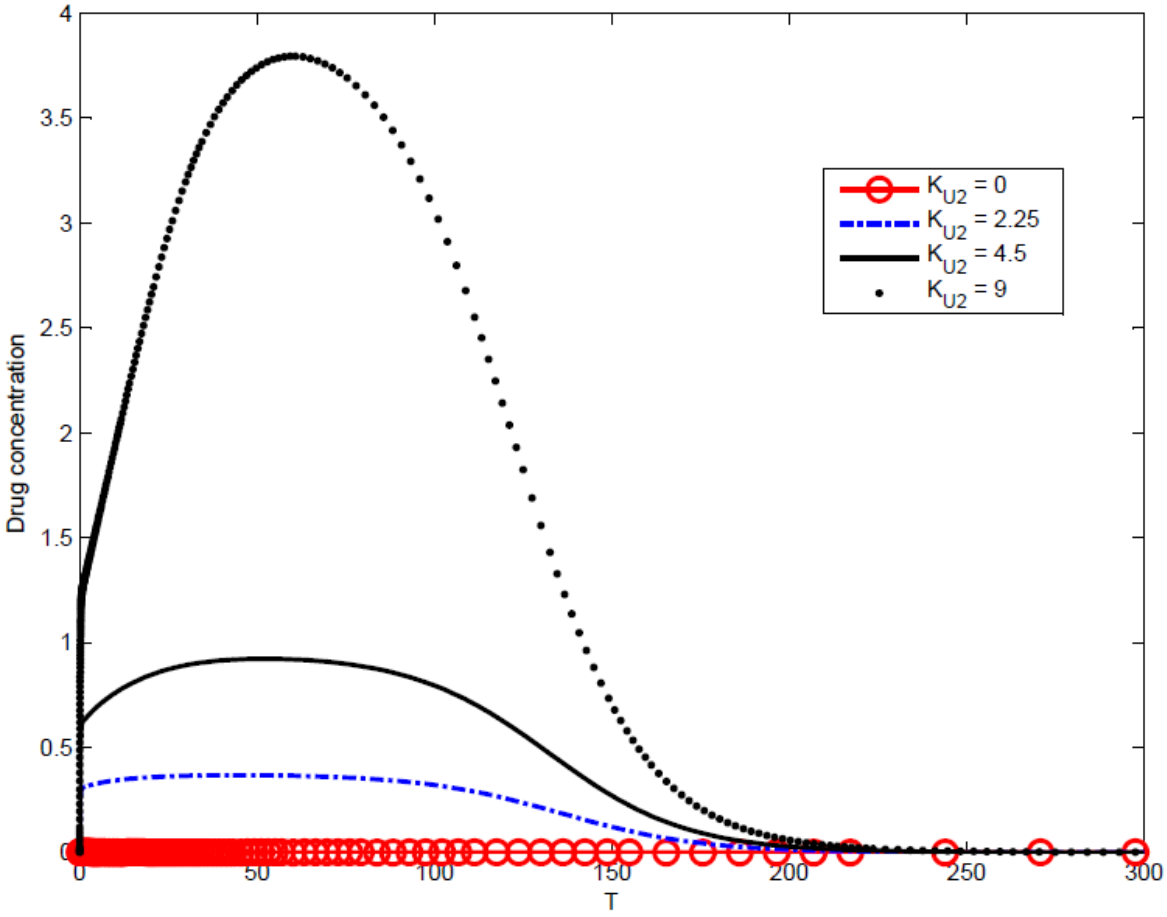

Figure 5.2: Time course of drug concentration in the presynaptic neurons at different drug feed rates

Figure 5.3 shows β- amyloid dynamics in the presynaptic neurons of the brain. It is observed that β- amyloid aggregates concentrations are inversely proportional to drug concentrations as indicated in Figure 5.2. Figure 5.3 shows that after treatment with drug at feed rate of K_{U2} = 2.25, the level of β- amyloid aggregates drops to 9.89 (corresponding to 197.8 nM) to the value 8.2 (corresponding to 164 nM) after passing time of 63 (corresponding to 6.3 hours) where absorbed drug concentration increases in the same period at the same feed rate of K_{U2}. In the latter period, the drug is helpful to increase the degradation rate of β- amyloid aggregates and inhibits the polymerization of β- amyloid. As the β- amyloid concentration drops from 9.89 to 8.2, β- amyloid aggregates undergoes a transient rise and then returns to the pretreatment levels

in the period (63-250) corresponding to (6.3-25 hr) indicating that β-amyloid aggregates production takes place in the same period that drug concentration is eliminated from the neural tissues.

As drug is exposed to clearance where its levels in brain tissues decrease, β- amyloid aggregates concentration increases monotonically to pretreatment levels. As the feed drug rates increase where K_{U2} = 4.5, β- amyloid aggregates decreases very fast from 9.98 to 6.5 corresponding to (197.8- 130 nM) after passing 75 corresponding to 7.5 (hr) from administering drug as shown in Figure 5.2 where drug is absorbed in the same period as explained previously in Figure 5.1. It is observed that β- amyloid aggregates returns to the pretreatment state as drug is eliminated completely in the same period. While the feed drug rate increases to K_{U2} = 9, β-amyloid aggregates levels drop to the lowest level which is 3 (corresponding to 60 nM) after passing 6.3 hr where drug content increases due to absorbance. Then, the drug starts to be eliminated allowing levels of β- amyloid aggregates to return to the pretreatment level due to increasing the production of β- amyloid aggregates where drug content decreases significantly as shown in Figure 5.2.

The potency and efficacy for lowering β-amyloid aggregates can be defined by the function % X_s which measures the average of β-amyloid aggregates reduction after treatment. It defines the intrinsic PK/PD relationship for the drug. This intrinsic PK/PD relationship is equivalent to the relationship between an exposure and time-weighted-average of β-amyloid aggregates lowering after treatment.

In addition, the impact of drug feed rate on the percent of β-amyloid aggregates removal is investigated as shown in Figure 5.4 to confirm β-amyloid aggregates levels illustrated in Figure 5.3. In Figure 5.4, β- amyloid profiles with changing drug input rates are compared with that at the pretreatment case (K_{U2} = 0). It is observed that the maximum β- amyloid aggregates removal levels increase from 15 % to 34%, and 69.5 % as K_{U2} increases from 2.25 to 4.5 and 9 respectively. Our results are compatible with the experimental findings obtained by Craft et al., (2002) that developed mathematical models for β-amyloid aggregates fertilization and plaque growth. Craft e al., (2002) showed that vaccines help to inhibit accumulating β-amyloid large molecules (polymers) more than monomers and by the end of the period, β-amyloid aggregates

return to the pretreatment steady state due to the equlibrium between a zero-order generation rate (K_{in}) and a first-order clearance rate (K_{out}).

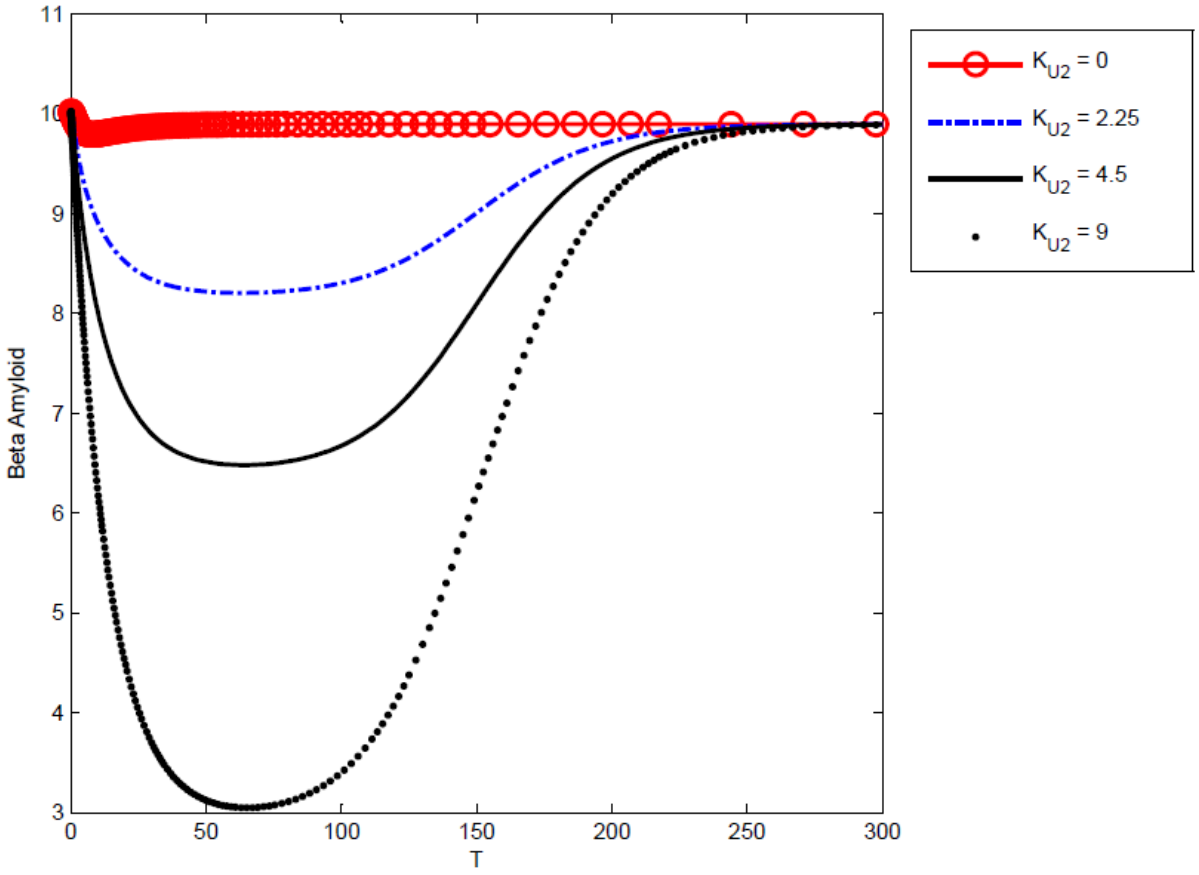

Figure 5.3: Time course of β- amyloid aggregates concentration at different drug feed rates

It is observed from pharmacodynamics aspects that the minimum peaks of β-amyloid aggregates concentrations of the presynaptic neurons are achieved in the range from 6-7 h after drug administration as shown in Figure 5.3. Furthermore, these minimum peaks in β- amyloid aggregates levels are lowered with increasing K_{U2} indicating the effective impact of AD therapeutics on the content of β- amyloid aggregates inside compartment 1. It is observed that the time required to attain the minimum β-amyloid levels differs based on the value of administered drug input rates. Furthermore, greater input drug rates are accompanied with higher percent of

decrease in levels of β- amyloid aggregates. These results are compatible with those obtained by Gopu et al., (2013) and Engelhardt et al., (1995).

The increase of β- amyloid aggregates during drug elimination could be explained by the increase of the activities of γ- and β-secretase relative to that of α secretase which might lead to disturbances in APP proteolysis. Consequently, β- amyloid aggregates increase and become uncontrolled by the drug (Liu and Murphy, 2006). The latter observation shows that more research is needed on the level of the interaction between β- amyloid aggregates growth and the drug in order to enhance the PK/PD modeling and develop more effective therapeutic strategies for AD.

Figure 5.5 (a) shows the time course of rate of ACh synthesis catalyzed by ChAT at different feed rates of drug. It is observed that at $K_{U2} = 0$, the synthesis rate (Rate 1) drops to the minimum steady state value which is around 0.005 where β-amyloid aggregates cause ChAT activity inhibition and there is no drug to inhibit the effect of β- amyloid aggregates. As K_{U2} increases to 2.25, Rate 1 increases. It is observed that Rate 1 drops fast after passing 12 (c.t. 1.2 hr) from the initial value of 0.0165. This drop can be illustrated by the fact that in the beginning of drug administration, β- amyloid aggregates have still a great effect. At $K_{U2} = 2.25$, Rate1 drops to reach 0.0062, then it rises to reach 0.0068 after passing around 60 (c.t. 6 hr), then it drops to reach 0.0051 at the end of the period 300 (c.t. 30 hr) where the drug at inlet rate of $K_{U2} = 2.25$ in the last period is eliminated allowing to increase β-amyloid aggregates and leading to formation of pathways in the presynaptic membranes and then choline is leaked out of the presynaptic neuron.

When the feed rate of the drug increases to $K_{U2} = 4.5$, it is noticed that the synthesis rate takes the same behavior as at $K_{U2} = 2.25$ but the level at the middle period is higher where it reaches 0.0085 then it decreases to reach the steady state value at the end of the administration period. It is observed at $K_{U2} = 9$, Rate 1 in the middle stage increases to reach the maximum level compared to that at the previous values of K_{U2} where Rate1 reaches 0.0127, then it decreases as usual to reach the steady state value of 0.0052. The dynamic behavior of Rate 1 is expected to affect all state variables in compartment 1 as will be explained later.

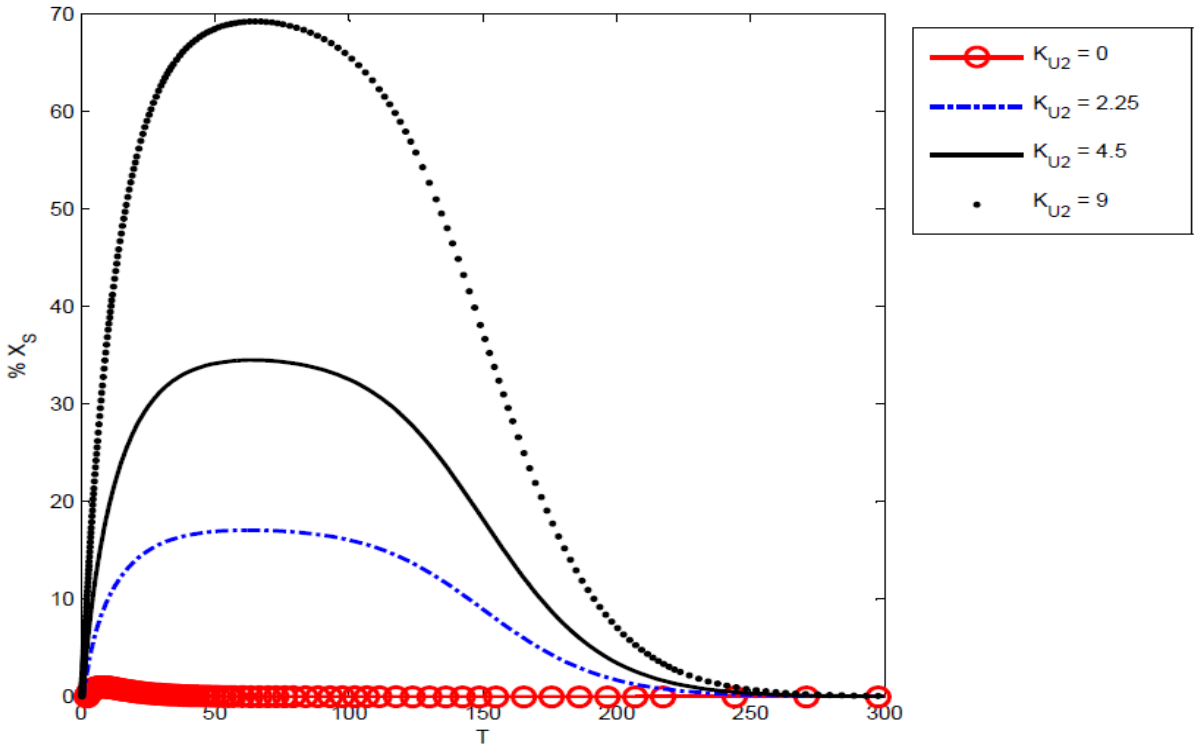

Figure 5.4: Time course of % β- amyloid aggregates removal at different drug feed rates

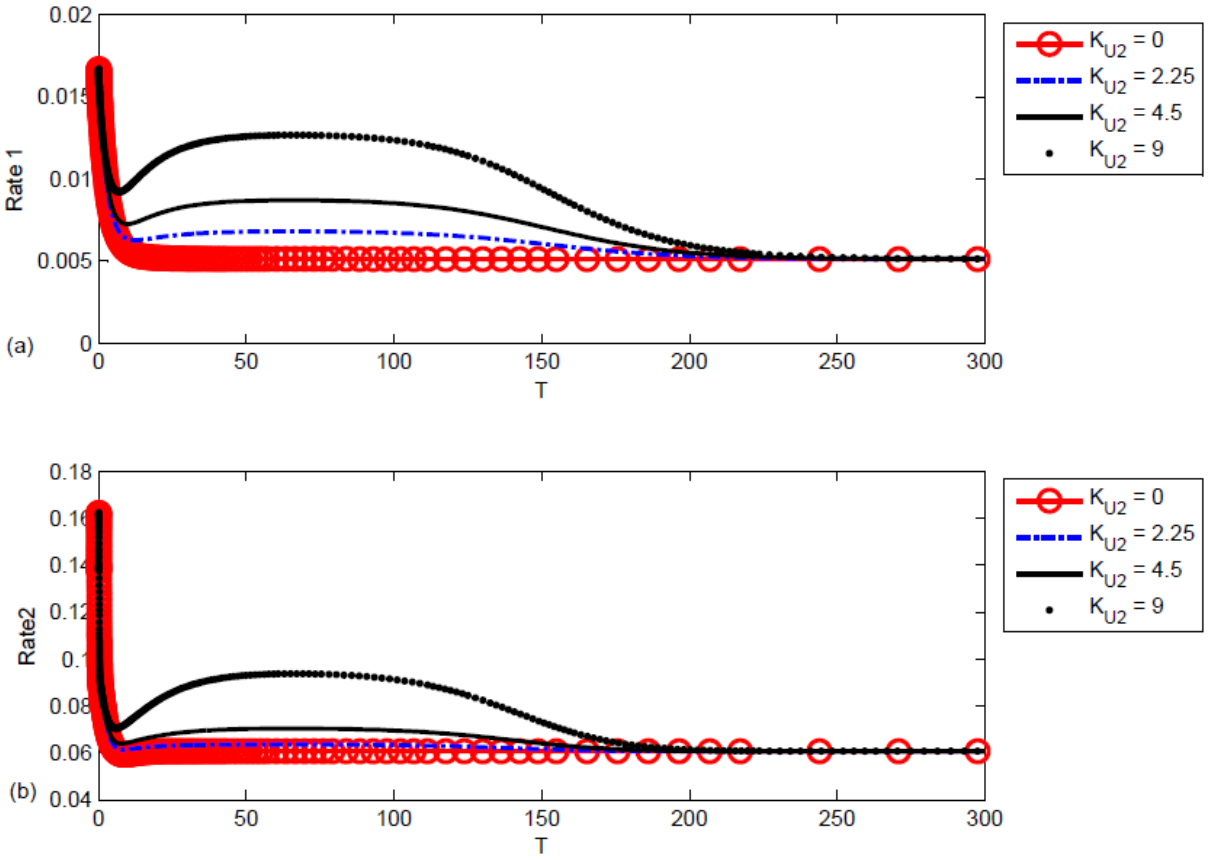

Figure 5.5: Time course of : a) Rate of ACh Synthesis (Rate 1) ,
b) Rate of ACh hydrolysis (Rate 2) at different K_{U2} values

Figure 5.5 (b) shows the dynamic behavior of ACh hydrolysis process by AChE enzyme in compartment 2 at different values of K_{U2}. It is observed that Rate 2 at K_{U2} = 0 is not affected where it decreases monotonically to reach the steady state value of 0.061 due to consumption of ACh in compartment 2. AT K_{U2} = 2.25 and 4.5, Rate 2 takes a similar behavior where Rate2 drops from 0.167 at the beginning to 0.062 and 0.064 after passing 7.5 (c.t 0.75 hr) then Rate 2 increases to reach 0.063 and 0.071 respectively after passing 75 (c.t, 7.5 hr) then Rate 2 decreases gradually due to drug elimination to reach the steady state value by the end of the period. When the feed drug rate increases to K_{U2} = 9, Rate 2 takes the same behavior but it

reaches the maximum level which is Rate 2 = 0.095 then it drops gradually to reach the lowest steady state value at Rate 2 = 0.062 as shown in Figure 5.5 (b).

Figure 5.6 (a) depicts the time course of ACh synthesized in compartment 1 (ACh1) with different feed rates of drugs. At $K_{U2} = 0$, it is observed that ACh1 increases after passing 1.5 (0.15 hr) from drug administration from 3.9 to around 5.5. The increase of ACh1 at early times after administration of doses could be explained as an almost instantaneous increase in the synthesis of ACh1. Then it decreases monotonically to reach the steady state value of 3.7 at the end of administration period of 300 (c.t, 30 hr). When the feed drug rate increases to $K_{U2} = 2.25$, ACh1 drops from 5.5 at time of 1.5 (0.15 hr) to 4.1 at a time of 13 (1.3 hr) to reach the plateau around 3.7 by the end of the administration period of 300 (c.t. 30 hr).

While $K_{U2} = 4.5$, ACh1 takes the same behavior as that at $K_{U2} = 2.25$, but the levels of ACh1 are higher where ACh1 in the middle period of ($7.5 < t < 75$) corresponding to ($0.75 < T <$ 7. 5 hr) increases from 4.1 to 5.1. Then, ACh1 decreases monotonically to 3.7 by the end of drug taking period, where the drug is eliminated completely giving the opportunity to β-amyloid aggregates to generate and cause leakage pathways in the presynaptic membrane and reduce the intracellular choline levels. Moreover, at $K_{U2} = 9$, where the drug concentration increases due to absorbance, the maximum ACh1 level is around 7 and is reached at t = 75 (c.t. 7.5 hr), then it decreases continuously to reach 3.7 where the rate of ACh synthesis decreases in the relevant period due to drug elimination. It is noticed that as K_{U2} increases from 0 to 9, ACh1 increases 2-folds from 3.5 to 7, and the increases of 2 folds of K_{U2} from 4.5 to 9 leads to an increase of ACh1 levels from 4.85 to 5.

Figure 5.6 (b) shows the dynamic behavior of ACh in compartment 2 (ACh2) produced from the hydrolysis of ACh by AChE. It is observed that the dynamic behavior of ACh2 looks like that of Rate 2 explained in Figure 5.5(b). At $K_{U2} = 0$, it is observed that ACh2 decreases moronically from 0.37 at the beginning of drug administration to reach 0.11 at the end of drug administration. While the drug inlet increases from $K_{U2} = 2.25$ to 4.5 and 9, the levels of ACh2 in the middle drug administration period increase to be 0.12, 0.13, and 0.18 respectively. Then ACh2 decreases continuously to reach the minimum level which is 0.118 by the end of the

period where drug in this period is eliminated and β-amyloid aggregates increase leading to reduction of ACh1 levels and thereby Rate2 as well.

It is observed that when the drug reaches the maximum level at $K_{U2} = 9$ where $C_{max} = 3.8$, ACh1 jumps 2-fold from 3.7 at maximum β- amyloid levels when there is no drug administered ($K_{U2} = 0$) to 7 at ($K_{U2} = 9$) while β- amyloid decreases 3-folds from 9.89 at $K_{U2} = 0$ to 3.05 $K_{U2} = 9$. These results are compatible with those obtained by Craft e al., (2002) who developed mathematical models for β- amyloid fertilization and plaque growth and showed that the decrease in drug content reduces the neuronal ACh burden where β- amyloid grows due to accumulating large molecules (polymers) more than monomers (Craft e al., 2002).

Figure 5.7 (a) shows the dynamic response of the intracellular choline concentrations in the presynaptic neurons in compartment 1. It is observed that at $K_{U2} = 0$ where no drug is administered, choline content (Ch1) decreases continuously from 3.23 (corresponding to 323 μM) to the steady state value of 0.99 (corresponding to 99 μM) due to the choline leakage caused by β- amyloid aggregates. As the drug is administered with the rate of $K_{U2} = 2.25$, the drug level decreases from 3.23 at the beginning of administration to t = 7.5 (c.t. 0.75 hr), then it increases as drug is absorbed until it reaches the maximum 1.313 after passing 45 (c.t. 4.5 hr) then as drug is eliminated after the latter period, β- amyloid polymer is reproduced to cause pathways in the presynaptic neuron membrane to permit choline substrate to get out of the presynaptic neuron and reduces gradually to reach the value 1(corresponding to 100 μM). When the drug input increases to $K_{U2} = 4.5$, the drug content takes a similar behavior where it decreases in the first period of t = 7.5 (0.75 hr) to reach 1.37 then it increases as drug is absorbed to reach 1.682 at t = 52.51 (c.t. 5.251 hr) then it decreases to reach the minimum level where Ch1 = 0.99 (corresponding to 99 μM) at the end of drug administration.

In addition, at $K_{U2} = 9$, Ch1 takes the same behavior while it takes higher levels than that at low K_{U2}. Where the maximum level of choline is attained at the maximum concentration of drug reached at t = 60.87 (c.t. 6.087) where Ch1 = 2.45 (corresponding to 245 μM), it decreases gradually as drug is eliminated and β- amyloid polymer is regenerated until the end of the drug administration. It is observed that the maximum content of choline in compartment 1 is reached

at the maximum K_{U2} = 9 where the high content of drug inhibits the capability of β- amyloid aggregates to form pathways in the membranes of compartment 1 and prevent choline leakage.

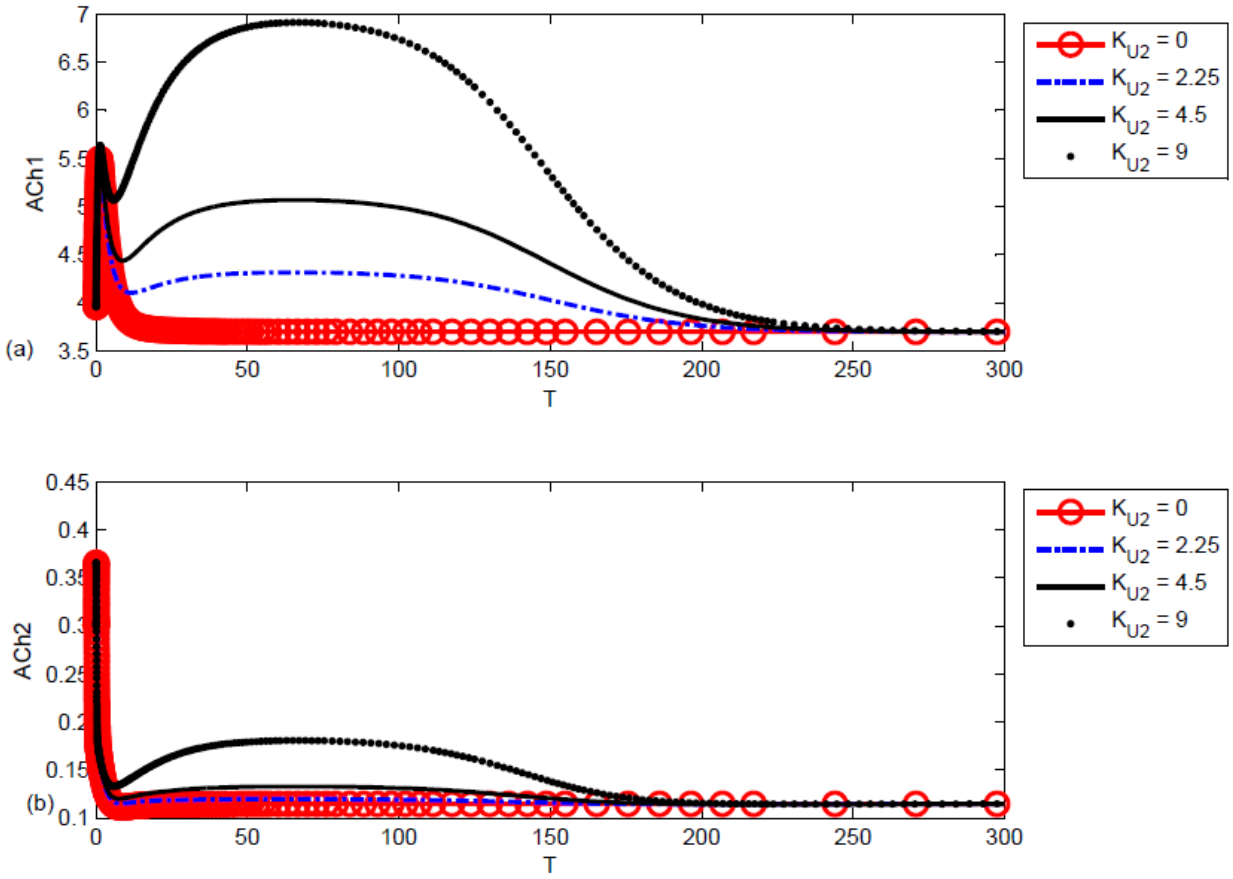

Figure 5.6:Time course of : a) ACh concentration in compartment 1 (ACh_1),

b) ACh concentration in compartment 2 (ACh_2) at different K_{U2} values

Figure 5.7 (b) illustrates the time course of choline level in compartment 2 (Ch2). The minimum level of Ch2 is attained at K_{U2} = 0 where β- amyloid aggregates cause the maximum effect on Ch1. The low levels of Ch1 result in lowering levels of Ch2 due to the low transport Ch rate from compartment 1 to compartment 2. It is observed that in the time period of (7.5 < t < 75) corresponding to (0.75 < T < 7. 5 hr) the maxim levels of Ch2 jumps from 0.41(corresponding to 41 µM) at K_{U2} = 0 to 1.021 (corresponding to 102.1 µM) at K_{U2} = 9 as drug concentration

increases because of absorption as K_{U2} increases then Ch2 decreases gradually as drug is eliminated to reach 0.4 as shown in Figure 5.7 (b).

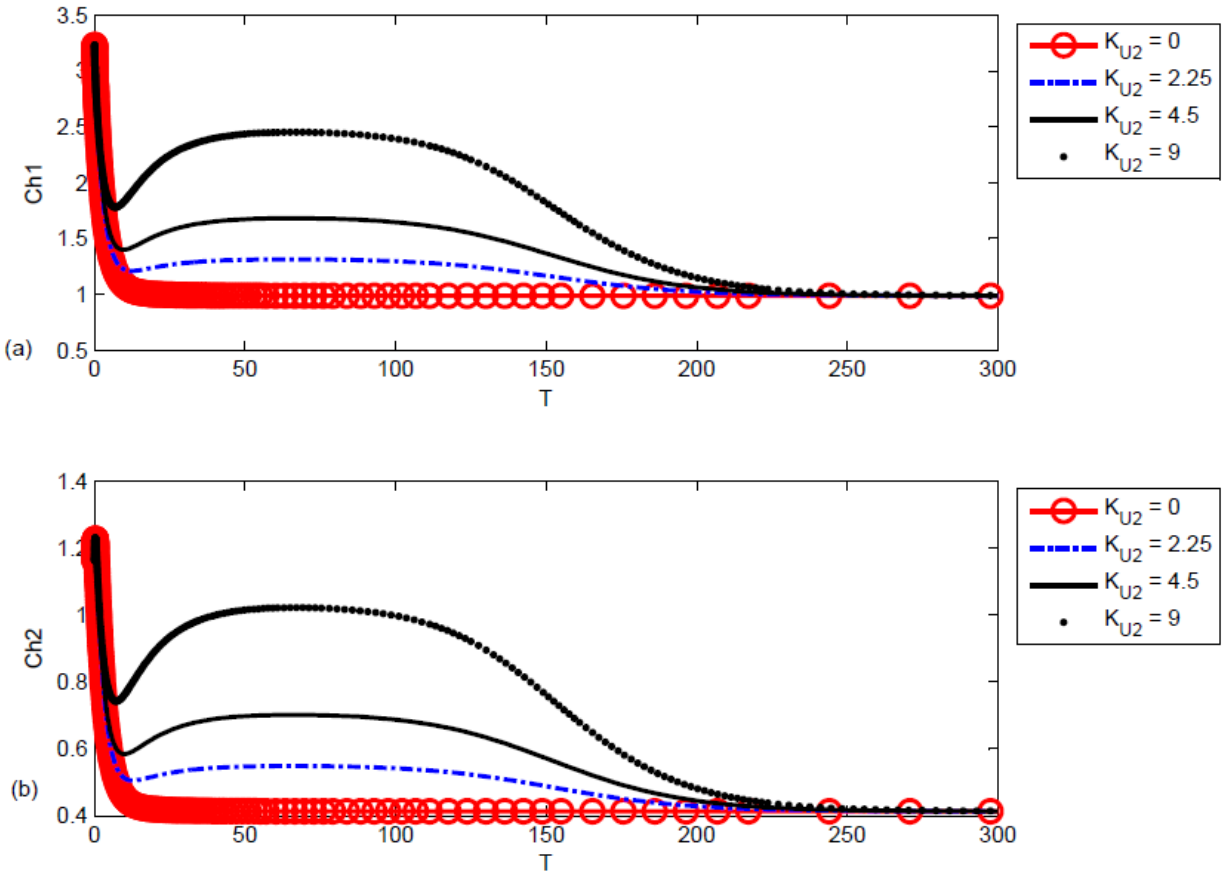

Figure 5.7: a) Choline concentration in compartment 1 (Ch 1),

b) Choline concentration in compartment 2 (Ch_2) at different K_{U2} values

Figure 5.8(a) shows the dynamic response of the acetate concentrations in compartment 1. It is observed that the levels of acetate are the maximum at K_{U2} = 0 where no drug is administered, and β- amyloid aggregates cause the maximum effect and form channels in the membranes of compartment 1 and allow choline leakage to be out of compartment 1. Therefore, acetate is accumulated in the presynaptic neurons. It is observed that the final steady state of Acetate 1 is around 7.863 (corresponding to 7.863 µM). It is observed in the beginning of the administration period that Acetate 1 decreases fast from 8.3 (corresponding to 8.3 µM) to 6.5

(corresponding to 6.5 µM) at t = 7.5 (c.t. 0.75 hr) where acetate is consumed with choline towards production of ACh. Then, acetate 1 increases from 6.5 to settle down around 7.863 by the end of the t = 300 (c.t. 30 hr), where the synthesis reaction of ACh is reversible as shown in Figure 5.8(c).

At K_{U2} = 2.25, it is observed that Acetate 1, in the period 0 < t < 10, decreases first to reach 6.4 (corresponding to 6.4 µM) at t = 2.5 (c.t. 0.25 hr) then it increases to reach 7.5 (corresponding to 7.5 µM) at t = 15 (c.t. 1.5 hr) then it decreases slightly to reach 7.4 due to its consumption with available choline where drug reaches the maximum absorption, however, it is observed that Acetate 1 increases to reach the final steady state of the pretreatment state which is 7.863. At K_{U2} = 4.5, Acetate 1 takes a similar behavior as that at K_{U2} = 2.25, however, it is observed that Acetate 1 is consumed more where the minimum level of Acetate1 = 7.062 is attained at t = 52.51 (c.t. 5.5251) then it increases again to reach the final steady state obtained at the end of the period: t = 300 (c.t. 310 hr). The level of acetate 1 at K_{U2} = 4.5 which is lower than that of K_{U2} = 2.25 and K_{U2} = 0 is attributed to the inhibition of β-amyloid aggregates and its incapability to form channels through the membranes and to the efficacy of the drug through the relevant period of absorbance and the abundance of choline to react with acetate to form ACh. While the drug input rate increases to reach K_{U2} = 9, more choline becomes available in compartment 1 to react with acetate leading to consumption of acetate to give lower levels of Acetate 1 to reach 6.34 (corresponding to 6.34 µM) than that at K_{U2} = 4.5, 2.25 , and 0.

Figure 5.8(b) shows acetate concentrations in compartment 2 (Acetate 2). It is observed that Acetate2 is produced in the period (0 < t < 2.5) to increase from 4.95 to 5.4 (corresponding to 4.95 and 5.4 µM) respectively. Then, at K_{U2} = 0, it decreases to reach 4.95 at t = 5 (c.t. 0.5 hr) then it increases to reach 5.22 at t = 20 (c.t. 0.2 hr). When the inlet drug rate increases to K_{U2} = 2.25, 4.5, and 9, acetate 2 increases in the period (20 < t < 75) to reach 5.28, 5.35, and 5.7 respectively (corresponding to 5.28, 5.35, and 5.7 µM) respectively due to its consumption with the available choline prevented from leakage because of the drug inhibition of β- amyloid aggregates.

Figure 5.9(a) shows the dynamic response of the intracellular pH in compartment 1 (pH_1) at different input drug rates. It is observed that pH_1 decreases from 8.5 to 6 in the first small

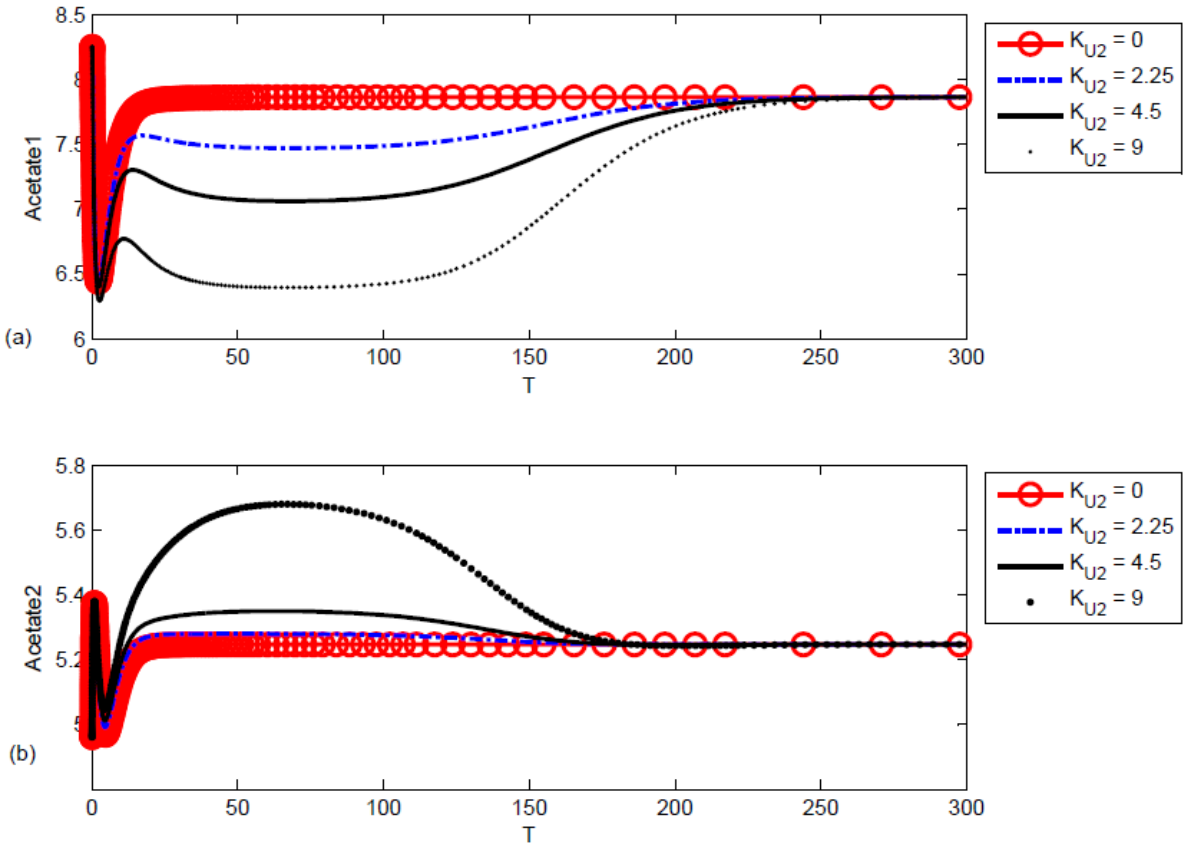

Figure 5.8: Time course of: a) Acetate concentration in compartment 1 (Ac_1),
b) Acetate concentration in compartment 2 (Ac_2) at different K_{U2} values

period ($0 < t < 5$). Then, at $K_{U2} = 0$, pH_1 increases to 6.5 and settles down around the latter value until the end of period. The behavior of pH_1 looks like that of Acetate 1. At $K_{U2} = 2.25$, more choline will be available to consume acetate 1 and allows to pH_1 to decrease to be 6.25 until t = 44.74 (c.t. 4.474 hr) then it increases to 6.25 and stabilizes around this value. It is observed that at $K_{U2} = 4.5$ and 9, pH_1 decreases in the same period to 5.85 and 5.55, then it increases again and

settles down around 6.25 until the end of the period where through the last period of drug administration the drug is eliminated allowing choline channels in the membrane to be formed and giving the opportunity to choline to get out of compartment 1. Figure 5.9(b) shows the time course of pH_2. It is observed that the behavior of pH_2 looks like that of pH_1. However, the levels of pH_2 are lower than those of pH_1. At K_{U2} = 2.25, 4.5 and 9, pH_2 decreases to reach 5.85, 5.75, and 5.45 respectively in the period of (40 < t < 100) c.t. (4 < t < 10) hrs. Then pH_2 increases to return to the pretreatment state which is 5.99. Table 5.3 shows the typical PK and PD parameters and their values. From the results and Table 5.3, it is observed that t ($_{max}$), at which the maximum absorbed drug concentration in the presynaptic neuron (C_{max}) is achieved, is in the range from 10 to 20 h. The results show that longer periods are needed for high drug input rates to achieve C_{max} as shown from the high AUC values.

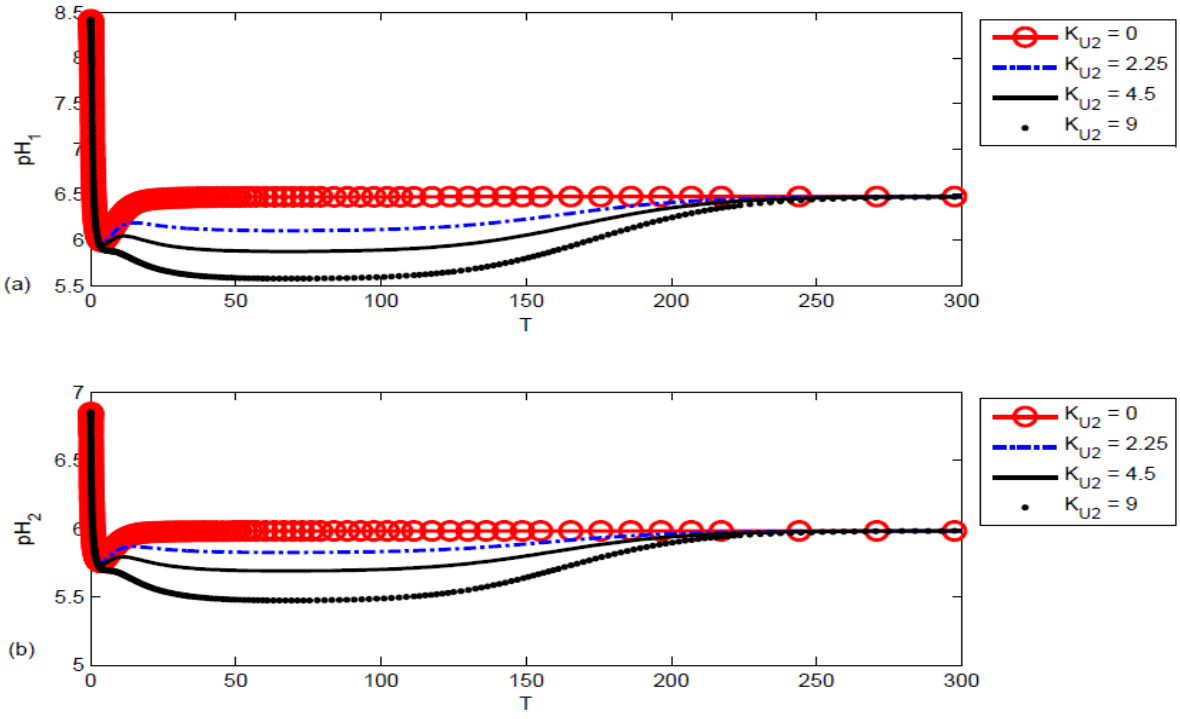

Figure 5.9: Time course of : a) pH in compartment 1 (pH_1),
b) pH in compartment 2 (pH_2) at different K_{U2} values

Table 5.3: PK/PD parameters

Drug input rate (K_{U2}) (mg)	0	225	450	900
C_{max} (µM)	0	37	92.3	379.35
t_{max} (h)	0	4.474	5.251	6.8655
β-amyloid min. (nM)	198	164	129.6	60.94
ACh1 max. (µM)	188	215.5	255	350
ACh2 max. (µM)	5.5	6	7	10
Ch1max. (µM)	99	131.3	168.2	245
Ch2 max. (µM)	41	54	70	102.1
AUC (µMh)	0	498.2	1199	4252.2

These results are compatible with theoretical and experimental results obtained by Gopu et al., (2013). It is observed that as the drug input rate increases, the peak of the drug increases and the minimum concentration of β-amyloid decreases, and the peaks of ACh and choline concentrations in compartments 1 and 2 increase. It is not easy to compare PK parameters with other different theoretical or experimental study of rats or rabbits models due to the wide range of drug administration doses and experimental conditions.

5.4) Summary and Conclusions

In this chapter, a tenth-dimension nonlinear pharmacokinetic/pharmacodynamics model was built to evaluate the impact of AD medications on the concentrations of β-amyloid aggregates and levels of ACh, Ch, acetate, pH, rate of ACh synthesis and rate of ACh hydrolysis in both compartments based on the choline leakage hypothesis. The interaction between drug and β-amyloid aggregates is formulated in a one-compartment drug which is the presynaptic compartment based on single doses to investigate the dynamic behavior of cholinergic system before and after treatment. From the profound pharmacodynamics results through high drug doses administration, modeling and simulation of PK/PD is a useful tool for predicting the dynamic behavior of the effect of therapeutics on cholinergic and β- amyloid aggregates and

could be helpful for selecting the appropriate dosing of AD inhibitors not just in the specific targets of the neurons. It is found that modeling of drugs that stop the β-amyloid aggregation is the main approach for developing AD diseases where β-amyloid aggregates cause channels in the membranes of the presynaptic neurons leading to choline leakage and disturbances in the neurocycle of ACh. A one-compartment PK/PD model is developed to describe the impact of therapeutics on complexities in the interaction between β-amyloid aggregates, drug PK/PD, and ACh neurocycle. The model could predict the reduction in β-amyloid aggregates levels and the increase of choline and ACh, in both compartments as well as both rates of ACh synthesis activated by ChAT enzyme in compartment 1, and ACh hydrolysis catalyzed by AChE enzyme in compartment 2.

Our study shows that drugs or agents that inhibit β- amyloid aggregation in the brain are likely to cause significant reduction in β-amyloid aggregates concentrations and increase in the levels of ACh and choline in both compartments. The results of the PK-PD models are compatible with the experimental findings obtained by Craft et al., (2002), and Walsh et al., (2000) who suggested that β- amyloid aggregates are mainly the reasons of lowering levels of ACh and even the destruction of the neurons. Although some of the model parameters are not known accurately, the incorporation of β- amyloid aggregates and drug equations into 2E2C model enabled us to understand the interaction between β- amyloid aggregates, drug, and ACh neurocycle and could be a guide to perform clinical and physiological experiments to achieve the optimal drug effect and could give systematic highlights to develop future trials for AD medications.

Chapter 6
Conclusions and Future Work

The work described in this thesis has concentrated on the effect of β-amyloid peptide aggregates on the cholinergic neurocycle. Although many researchers focused on β-amyloid interactions, the mechanisms that β-amyloid aggregates affect cholinergic neurons and reduction in ACh levels are still unclear. The effect of β-amyloid was investigated through proposing two hypotheses into two-enzyme /two compartment model (2E2C): the first is choline leakage hypothesis, and the other is the loss of ChAT activity hypothesis. The dynamic behavior for all states of the ACh neurocycle was investigated in a wide range of β- amyloid aggregate concentrations and was compared with healthy neurons where there is no β- amyloid aggregates in order to explain the physiological and dynamic phenomena occurring in brains with Alzheimer's disease. In addition, the interactions between β-amyloid aggregates and a drug orally administered were investigated through proposing one-compartment pharmacokinetics/pharmacodynamics (PK/PD) model. The main outcomes of this dissertation are summarized below.

6.1 Conclusions

In Chapter 3, the effect of β-amyloid aggregates on ACh neurocycle is studied through the hypothesis of choline leakage. It is suggested that β-amyloid aggregates create pathways in membranes of the presynaptic neurons leading to choline loss outside of the cholinergic neurocycle. A novel nine-dimensional nonlinear mathematical model of 2E2C of the neuron terminals is built where the presynaptic neuron is considered as compartment 1 and both synaptic cleft and the postsynaptic neuron are considered as compartment 2. It is noticed that the increase of the production rate of β-amyloid aggregates (K_{L2}) leads to an increase in the amount of leaked choline from compartment 1 resulting in a decrease in choline levels in both compartments. In addition, it is observed that as K_{L2} increases, the intracellular concentration of β- amyloid aggregates increases thereby the loss of choline from compartment 1 increases. Furthermore, the rate of ACh synthesis

catalyzed by the enzyme ChAT in compartment 1 and the rate of ACh hydrolysis activated by AChE decrease with the increase in K_{L2}.

The concentrations of ACh in both compartments 1 and 2 decrease significantly with the increase of K_{L2}. However, the acetate level in compartment 1 increases in parallel with the increase in K_{L2} but the acetate level in compartment 2 decreases. It is concluded that the choline leakage hypothesis gives a reasonable explanation for the reduction of levels of the neurotransmitter and choline in the neurocycle of ACh which are the main hallmarks in brains with AD. The results of the mathematical model are compatible with the theoretical results obtained by Ehrenstein et al., (1997) and the experimental results obtained by Kar et al., (1998, 2004), Galdzicki et al., (1994), and Allen et al., (1997) on PC 12 cells. The results are also compatible with those reported by Allen et al., (1994) who showed that β-amyloid aggregates could lead to increase in choline loss from neurons and negatively affected generated ACh levels. Therefore, a therapeutic strategy based on blocking choline leakage channels caused by β- amyloid aggregates is a promising strategy for curing AD and could achieve the physiological levels of intracellular choline and ACh.

In Chapter 4, three different kinetic mechanisms explaining the interaction between β-amyloid aggregates and ChAT activity are suggested and tested through the incorporation of the rate of ACh synthesis where ChAT activity is inhibited by β-amyloid into the 2E2C model. The reduction in ChAT activity is one of the symptoms of brains with AD. In the first kinetic mechanism, β- amyloid aggregates attack activated enzyme complex E_2H. It is found that the increase in K_{L2} to the presynaptic neuron leads to increase in β-amyloid aggregates concentrations inside the presynaptic neurons and reduction of ACh synthesis rate compartment 1 and ACh levels in both compartments. However, it is observed that all choline levels in both compartments, the rate of ACh hydrolysis in compartment 2, ACh levels in compartment 2, and pH_2 are not affected.

The results obtained from the second kinetic mechanism where a competitive inhibition of β-amyloid aggregates occurs with enzyme intermediate complex X_2 are similar to those achieved from the first kinetic mechanism where the effects of β-amyloid interaction in both kinetic mechanisms are similar. In the third kinetic mechanism, β- amyloid aggregates attack all species in ChAT enzyme; it is found that at very high input rate of β- amyloid aggregates, there is an observed new phenomenon which is the oscillatory behavior for all components of the neurocycle of ACh. The

disturbance observed in ACh levels in both compartments reflects the harmful effect of the fully attack of β-amyloid aggregates to all species of ChAT. The latter disturbances in ACh neurocycle are the symptoms of brains with AD and indicate that the fully inhibition of ChAT caused by β-amyloid aggregates could be a possible kinetic mechanism explaining the loss in ChAT activity due to the interaction with β-amyloid aggregates in ACh neurocycle. The latter results show that protecting the enzyme ChAT from β-amyloid aggregates inhibition is a reasonable therapeutic approach for brains with AD. In comparison to the effect of β- amyloid aggregates via choline leakage hypothesis, it is observed that ChAT activity to be reduced significantly needs a high concentration of inlet β-amyloid aggregates. These results are consistent with the experimental results got by Kar et al., (1998) who showed that the exposure for small concentrations of β-amyloid aggregates has no impact on ChAT activity in cortex tissues and indicated that when neurons tissues exposed to low concentrations of β-amyloid aggregates for a while, choline uptake reduced significantly.

In Chapter 5, the effects of AD therapeutics are investigated through building a new PK/PD model by incorporating a one-compartment drug model into the two-enzyme/two-compartment model to give a ten-dimensional model. The drug is suggested to interact with the tissues of the presynaptic neurons where β- amyloid aggregate is located. The PK/PD model is built based on the effect of β-amyloid aggregates via choline leakage hypothesis where the maximum generation rate of β-amyloid aggregates ($K_{L2} = 1$) is considered. The dynamic behavior of all concentrations of β-amyloid aggregates, choline, ACh, acetate, and pH in both compartments in addition to the rate of ACh synthesis in compartment 1 and ACh hydrolysis is investigated through observing the impacts of drug on β-amyloid aggregates and cholinergic neurocycle in a wide range for the input rate of drug (K_{U2}). The PK/PD model could predict the reduction of β-amyloid aggregates levels and the increase of choline and ACh, in both compartments as well as both ACh synthesis rate activated by the enzyme ChAT in compartment 1, and ACh hydrolysis rate catalyzed by the enzyme AChE in compartment 2.

The outcomes of PK/PD drug model such as C_{max}, T_{max} , AUC, and E_{max} are in agreement with that obtained by Craft et al., (2002) who showed that concentration of β-amyloid aggregates after adding a therapeutic agents in the brain experiences a rapid reduction in levels of β-amyloid aggregates then addresses a rise then returns to the pre-treatment state where at steady state there is

no change in the levels of β-amyloid aggregates. Our study shows that drugs or agents that inhibit β-amyloid aggregation in the brain are likely to be a successful therapeutic approach to give systematic highlights to develop future trials, new diagnostic techniques, and medications for AD.

6.2 Future Work

The development of the present work can be extended as follows:

1) For the effect of β-amyloid aggregates, we considered two hypotheses in the presynaptic neurons for the impacts of the interaction with β-amyloid aggregates. The model can be extended to consider the interaction between β-amyloid aggregates and acetyl co-A. The experimental review showed that β-amyloid aggregates could affect the synthesis of acetyl CoA. In addition, the effect of β-amyloid aggregates on the internal diffusion for ACh vesicles and the effusion of theses vesicle with the presynaptic membrane to release ACh into synaptic cleft. Furthermore, the model can be extended to take into account the effect of β-amyloid aggregates on the activity of AChE and the postsynaptic receptors. In these cases, the outcomes of the effects of β-amyloid aggregates on compartment 2 could help understand the nature of the interaction between β-amyloid aggregates and cholinergic neurocycle and the central nervous system.
2) Considering the polymerization (aggregation) of β-amyloid peptides from soluble monomers to produce aggregates accumulating in brains with AD could help understand the toxicity nature of β- amyloid aggregates. The rates of association, initiation and elongation of β-amyloid and their kinetics could enrich our model and describe accurately the impacts of β-amyloid aggregates on ACh neurocycle and could be useful for designing therapeutic agents that inhibit β-amyloid aggregation and toxicity.
3) The incorporation of β-amyloid aggregates into two-enzyme/two-compartment model combined with experimental and clinical data could be helpful for understanding β-amyloid aggregates interaction and developing therapeutic agents that inhibit the agglomeration of β-amyloid peptides or increase the rate of defragmentation of oligomers.
4) The pharmacokinetic/pharmacodynamics model could be developed to be a two-compartment or a multi-compartment based models in order to take into consideration the

drug blood and plasma concentrations and compare between different types of drug administration either orally, intravenously, or intramuscularly.

5) Investigate the optimal drug control strategy using the developed the pharmacokinetic and pharmacodynamics models in order to identify the optimal drug dose giving the maximum efficiency and minimize the toxic effect for the drug and β- amyloid aggregates. Optimal control could be used to test such hypotheses. It can be performed through multi-compartment model in order to properly model the actions of the drugs. Both discrete and continuous nonlinear optimal controls for drug doses could be employed in order to investigate the optimal scheduling drug doses for AD and compare the effects of different processes.

References

1) Arispe, N., E. Rojas, and H. B. Pollard. 1993. Alzheimer disease amyloid beta protein forms calcium channels in bilayer membranes: blockade by tromethamine and aluminum. Proc. Natl. Acad. Sci. USA. 90:567-571
2) Allen DD, Galdzicki Z, Brining SK, Fukuyama R, Rapport SI, Smith QR. B--amyloid induced increase in choline flux across PC12 cell membranes. Neurosci Lett 1997; 234:71-3.
3) Ansell, G.B.; Spanner, S. Studies on the Origin of Choline in the Brain of the Rat. Biochem. J. 1971, 122 (5), 741.
4) Benet, Zia-Amirhosseini, (1995); Basic principles of pharmacokinetics; Toxicol Pathol. 1995 Mar-Apr; 23(2):115-23.
5) Billingsley ML, Kincaid RL. Regulated phosphorylation and dephosphorylation of tau protein: effects on microtubule interaction, intracellular trafficking and neurodegeneraion. Biochem J 1997; 323: 577-91.
6) Buxbaum, J. D., A. A. Ruefli, C. A. Parker, A. M. Cypess, and P. Greengard. 1994. Calcium regulates processing of the Alzheimer amyloid protein precursor in a protein kinase C-independent manner. Proc. Natl. Acad. Sci. USA. 91:4489-93.
7) Craft D., (2002), A Mathematical Model of the Impact of Novel Treatments on the A_ Burden in the Alzheimer's Brain, CSF and Plasma; Bulletin of Mathematical Biology (2002) 00, 1–21
8) Davis, K. L., J. Y.-K. Hsieh, M. I. Levy, T. B. Horvath, B. M. Davis, and R. C. Mohs. 1982. Cerebrospinal fluid acetylcholine, choline, and senile dementia of the Alzheimer's type. Psychopharmacol Bull. 18:193-195
9) Dobransky T, Brewer D, Lajoie G, Rylett RJ. Phosphorylation of 69-kDa choline acetyltransferase at threonine 456 in response to amyloid-beta peptide 1-42. J Biol Chem 2003;278: 5883-93.
10) Duff K, Suleman F., (2004), Transgenic mouse models of Alzheimer's disease: how useful have they been for therapeutic development?, Brief Funct Genomic Proteomic. 2004 Apr;3(1):47-59

11) Elble, R., E. Giacobini, and C. Higgins. 1989. Choline levels are increased in cerebrospinal fluid of Alzheimer patients. Neurobiol. Aging. 10: 45-50.
12) Elnashaie, S.S.E.H.; Ibrahim, G.; Teymour, F. A (1995). Chaotic behavior of an acetyl cholinesterase enzyme system. Chaos, Solitons & Fractals 5, 933.
13) Estradal.D.etal,Curr.ToicsMed.Chem.2007,7,115-126
14) Elnashaie, S.S.E.H.; El-Rifai, M.A.; Ibrahim, G. (1983). The effect of hydrogen ion production on the steady-state multiplicity of substrate inhibited enzymatic reactions. II. Transient behavior. Applied Biochemistry and Biotechnology 8, 467-479.
15) Elnashaie S. S.E., Uhlig F., and Affane C.b , 2007, Numerical techniques for chemical and biological engineers using MATLAB: a simple bifurcation approach, Springer., New York.
16) Elble, R., Giacobini, E. and Higgins, C., Choline levels are increased in cerebrospinal fluid of Alzheimer's patients, Neurobiol. Aging, 10(1989) 45-50
17) Galdzicki, Z., R. Fukuyama, K. C. Wadhwani, S. I. Rapoport, and G. Ehrenstein, 1994. Beta-Amyloid increases choline conductance of PC12 cells: possible mechanism of toxicity in Alzheimer's disease. Brain Research, 646:332-336
18) Hung, A. Y., C. Haass, R. M. Nitsch, W. Q. Qiu, M. Citron, R. J. Wurtman, J. H. Growdon, and D. J. Selkoe. 1993. Activation of protein kinase C inhibits cellular production of the amyloid beta-protein. J. Biol. Chem.268:22959-22962
19) Holmes C. Genotype and phenotype in Alzheimer's disease. Br J Psychiatry 2002;180:131-4
20) Harkany T, Lengyel Z, Soos K, Penke B, Luiten PG, Gulya K.Cholinotoxic effects of β-myloid1-42 peptide on cortical projections of the rat nucleus basalis magnocellularis. Brain Research 1995;695:71-5
21) Kandimalla, curran, Holasek, Gilles, Wengenack, and Poduslo, (2005) pharmacokinetic Analysis of the Blood- brain Barrier Transport of 1-Amloid β Protein 40 in Wild-Type and Alzheimer's Disease Transgenic mice(APP, ps1) and its Implications for Amyloid plaque formation. The journal of Pharmacology and Experimental Therapeutics, 313:1370-1378
22) Iqbal K, Alonso AC, Gong CX, Khatoon S, Pei JJ, Wang JZ, et al. Mechanisms of neurofibrillary degeneration and the formation of neurofibrillary tangles. J Neural Transm Suppl 1998;53: 169-80

23) Gopu D, Gomathi P2 and Harish Kaushik, (2013), Pharmacokinetic/Pharmacodynamic (PK/PD) modeling of antipyretic effect of meloxicam: A preferential cyclooxygenase inhibitor in rat, African Journal of Pharmacy and Pharmacology Vol. 7(9), pp. 488-494,

24) Kar, A.M.Issa, D. Seto, D.s. Auld, B. Auld, B. collier, and R. Quirion, (1998). Amylod β-peptide Inhibits High- Affinity Choline Uptake and Acetylcholine release in Rat Hippocampal Slices. The journal neurochemistry 70, 2179-2187

25) Kar and Slowikowski, (2004). Interaction between β-amyloid and central cholinergic neurons; implications for Alzheimer's disease. Journal of J psychiatry neurosci 29(6): 427-41

26) Kelly JF, Furukawa K, Barger SW, Rengen MR, Mark RJ, Blanc EM, et al. Amyloid β-peptide disrupts carbachol-induced muscarinic cholinergic signal transduction in cortical neurons. Proc Natl Acad Sci U S A 1996;93:6753-8

27) Knipper, M., M. da Penha, Berzaghi, A. Blochl, H. Breer, H. Thoenen, and D. Lindholm. 1994. Positive feedback between acetylcholine and the neurotrophins nerve growth factor and brain-derived neurotrophic factor in the rat hippocampus. European journal of Neuroscience, 6:668-671

28) Liu L, Murphy RM, (2006), Kinetics of inhibition of β-amyloid aggregation by transthyretin, Biochemistry, 45(51):15702-9

29) Lockman and D.D Allen, (2002). The transport of Choline, The journal of drug development and industrial pharmacy. Vol. 28, No. 7, pp. 749-772

30) Mandelkow, E.M., and Mandelkow, E. (2012). Biochemistry and cell biology of tau protein in neurofibrillary degeneration. Cold Spring Harb Perspect Med 2, a006247.

31) Martel, C. L., J. B. Mackic, J. G. McComb, J. Ghiso and B. V. Zlokovic (1996). Blood brain barrier uptake of the 40 and 42 amino acid sequences of circulating Alzheimer's amyloid in guinea pigs. Neurosciennce Letters, 206, 157–160

32) Moore SA, Huckerby TN, Gibson GL, Fullwood NJ, Turnbull S, Tabner BJ, El-Agnaf OMA & Allsop D. (2004) Both the D-(+) and L-(-) enantiomers of nicotine inhibit Aβ aggregation and cytotoxicity, Biochemistry 43, 819-826

33) Mustafa I H, G. Ibrahim, A. Elkamel, S.S.E.H. Elnashaie, P. Chen, (2009), Non Linear Feedback Modeling and Bifurcation of the Acetylcholine Neurocycle and its Relation to Alzheimer's and Parkinson's Diseases; Journal of chemical engineering science 64(1), 69-90

34) Mustafa I H, G. Ibrahim, A. Elkamel, S.S.E.H. Elnashaie, P. Chen, (2009), Effect of Choline and Acetate Substrates on Bifurcation and Chaotic Behavior of Acetylcholine Neurocycle and Alzheimer's and Parkinson's Diseases; Journal of Chemical Engineering Science, 64(9), 2096-2112

35) Mustafa I. , A. Elkamel, A. Lohi P. Chen, S.S.E.H. Elnashaie, G. Ibrahim, (2012), Application of Continuation Method and Bifurcation for Acetylcholine Neurocycle Considering Partial Dissociation of Acetic Acid, Computers an Chemical Engineering 46 (2012) 78-93

36) Mustafa I H, G. Ibrahim, A. Elkamel, S.S.E.H. Elnashaie, P. Chen, (2012), Effect of Cholineacetyltransferase Activity and Choline Recycle Ratio on Modelling, Bifurcation and Chaotic Behavior of Acetylcholine Neurocycle and Their Relation to Alzheimer's and Parkinson's Diseases; Journal of Chemical Engineering Science, 68(1), 19-35

37) Muller-Spahn F, Hock C. Risk factors and differential diagnosisof Alzheimer's disease. Eurpean Archives of Psychiatry and Clinical Neuroscience, 1999;249(Suppl 3):37-42

38) Nitsch, R. M., J. K. Blusztajn, A. G. Pittas, B. E. Slack, J. H. Growdon, and R. J. Wurtman. 1992. Evidence for a membrane defect in Alzheimer disease brain. Proceeding of the National Academy of Science of the United States of America. 1992; 89:1671-1675

39) Olesen OF, Dago L, Mikkelsen JD , (1998), Amyloid β neurotoxicity in the cholinergic but not in the serotonergic phenotype of RN46A cells. Molecular brain Research. 1998; 57: 266-74.

40) Oliver, B. Nikolau, V. Wurtele, (2009, Acetyl_CoA- Life at the metabolic nexus. Journal of Plant science 176: 597-601

41) Pedersen WA, Blusztajn JK. Characterization of the acetylcholine reducing effect of the amyloid-β- peptide in mouse SN56 cells. Neuroscience letter, 1997; 239:77-80.

42) Poirier J, Davingnon J, Bouthillier D, Kogan S, Bertrand P,Gauthier S. Apolipoprotein E polymorphism and Alzheimer's disease. Lancet 1993;342:697-9

43) Pollack SJ, Lewis H. Secretase inhibitors for Alzheimer's dis-ease: challenges of a promiscuous protease. Current Opinion in investigational Drugs. 2005; 6 (1): 35-47.

44) Schuberth, J.; Sparf, B.; Sundwall, A. A Technique for the Study of Acetylcholine Turnover inMouse Brain In Vivo. Journal of Neurochemistry, 1969, 16 (5), 695–700

45) Schuberth, J.; Sparf, B.; Sundwall, A. On the Turnover of Acetylcholine in Nerve Endings of Mouse Brain In Vivo. Journal of Neurochemistry, 1970, 17 (4), 461–468

46) Slotkin, T. A., F. J. Seidler, B. J. Crain, J. M. Bell, G. Bissette, and C. B.Nemeroff. 1990. Regulatory changes in presynaptic cholinergic function assessed in rapid autopsy material from patients with Alzheimer disease: implications for etiology and therapy. Proc. Natl. Acad. Sci. USA. 87:2452-2455

47) Slotkin, T.A., Seidler, F. j., Crain, B.J., Bell, J. M., Bissette, G. and nemeroff, C.D. regulatory changes in presynaptic cholinergic function assessed in rapid autopsy material from patients with Alzheimer disease: implications for etiology and therapy proc. Proceedings of the National Academy of Science of the United States of America. 1990; 2452-2455

48) Spuch C., Ortolano S., and Navarro C., (2012), Review Article: New Insights in the Amyloid-Beta Interaction withMitochondria, Hindawi Publishing Corporation, Journal of Aging Research, Volume 2012, Article ID 324968, 9 pages doi:10.1155/2012/324968

49) Stepanov, Kuznetsova, Klement'ev, and Sapronov; (2007), Effects of Intracerebroventricular Administration of Beta-Amyloid on the Dynamics of Learning in Purebred and Mongrel Rats; Neuroscience and Behavioral Physiology, Vol. 37, No. 6

50) Strittmatter WJ, Saunders AM, Schmeckel D, Pericak-Vance M,Enghild J, Salvesen GS, et al. Apolipoprotein E: high-avidity binding to β-amyloid and increased frequency of type 4 allele in late-onset familial Alzheimer disease. Proceedings of the National Academy of Science of the United States of America. 1993; 90:1977-81

51) Tang L., Su J., Huang D., Lee D., Li K,1 and Zhou X., (2012), Research Article An Integrated Multiscale Mechanistic Model for Cancer Drug Therapy, International Scholarly

Research Network, ISRN Biomathematics, Volume 2012, Article ID 818492, 12 pagesdoi:10.5402/2012/818492

52) Tucek, S., (1978). Acetylcholine Synthesis in Neurons; Champan &hall, London. 1978.

53) Tucek S. (1983), The synthesis of acetylcholine, in Handbook of Neurochemistry, 2nd ed., Vol. 4 (Lajtha A., ed), pp. 219- 249. Plenum Press, New York.

54) Tucek, S. (1985). Regulation of acetylcholine synthesis in the brain. The Journal of Neurochemistry 44:11-24

55) Tucek S. (1988) Choline acetyltransferase and the synthesis of acetylcholine, in Handbook of Experimental Pharmacology, vol. 86. Springer, Berlin 125-165

56) Tucek S (1990), The synthesis of acetylcholine: twenty years of progress. Progress in Brain Research 84: 467-477

57) Tohgi, H., T. Abe, K. Hashiguchi, M. Saheki, and S. Takahashi. 1994. Remarkable reduction in acetylcholine concentration in the cerebrospinal fluid from patients with Alzheimer type dementia. Neuroscience letters. 177:139-142

58) Verdier, Zarandi, and Penke.,(2004). Amyloid β-Peptide Interactions with Neuronal and Glial Cell Plasma Membrane: Binding Sites and Implications for Alzheimer's Disease. Journal of peptide science 10: 229-248

59) Villaca, filgueiras, and manhaes, (2011). Developmental aspects of the cholinergic system. Journal of behavioural, brain research 221. 367-378

60) Wakelkamp M, Alván G, Scheinin H, and Gabrielsson, (1998), The influence of drug input rate on the development of tolerance to frusemide, British Journal of Clinical Pharmacology, 1998; 46: 479–87

61) Wakelkamp M, Alván G, and Paontaud G, (1997), Natriuretic efficiency of frusemide as a consequence of drug input rate, British Journal of Clinical Pharmacology, 19987 43: 481–91

62) Wecker L. The synthesis and release of acetylcholine by depolarized hippocampal slices is increased by increased choline available in vitro prior to stimulation. Journal of neurochemistry 1991;57: 119-49.

63) Wurtman, R. J. 1992. Choline metabolism as a basis for the selective vulnerability of cholinergic neurons. Trends Neurosci. 15:117-122

64) Wurtman, R. J. 1994. The return of the cholinergic hypothesis, Journal of Clinical Investigation. 1994; 94(2): 470.

65) Yasong Lu , (2012), Integrating Experimentation and Quantitative Modeling to Enhance Discovery of B- Amyloid Lowering Therapeutics for Alzheimer's Disease, Frontiers Pharmacology, 2012; 3: 177.

66) Zambrzycka A, Alberghina M, Strosznajder JB (2002) Effects of aging and amyloid-beta peptides on choline acetyltransferase activity in rat brain. Neurochemical Research 27:277–281.

67) Zheng WH, Bastianetto S, Mennicken F, Ma W, Kar S, Amyloid β-peptide induces tau phosphorylation and neuronal degeneration in rat primary septal cultured neurons. Neuroscience 2002;115:201-11.

68) Zlokovic, B. V., J. Ghiso, J. B. Mackic, J. G. McComb, M. H. Weiss and B. Frangione (1993). Blood brain barrier transport of circulating Alzheimer's amyloid, Biochem. Biophys. Res. Commun. 197, 1034–1040